

08475

W.P.

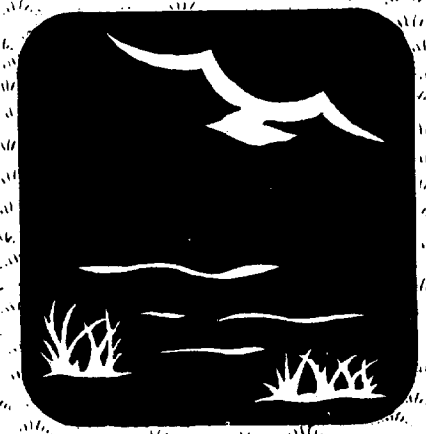
Coastal Zone  
Information  
Center

OCT 27 1976

# CURRENTS AND CIRCULATION IN THE COASTAL WATERS OF LOUISIANA

Louisiana State Planning Office, Coastal Resources Prog.

COASTAL ZONE  
INFORMATION CENTER



Louisiana  
Coastal  
Resources  
Program

GC  
281  
.M4  
M87  
1976  
c.2

STATE PLANNING OFFICE  
OPERATION WITH  
LOUISIANA WILDLIFE AND FISHERIES COMMISSION  
LOUISIANA COASTAL COMMISSION  
LOUISIANA SEA GRANT PROGRAM

GC 281, MY M87 1976 CID

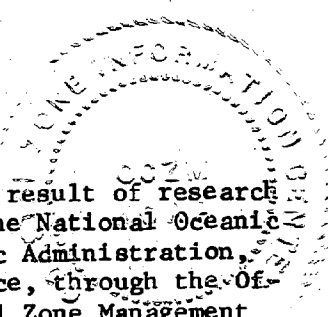
CURRENTS AND CIRCULATION IN THE  
COASTAL WATERS OF LOUISIANA

S. P. Murray

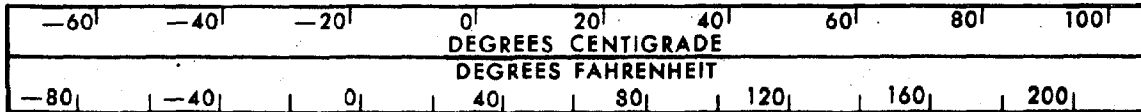
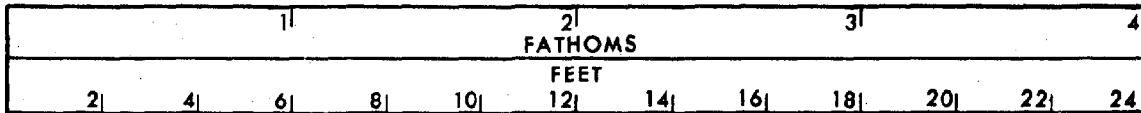
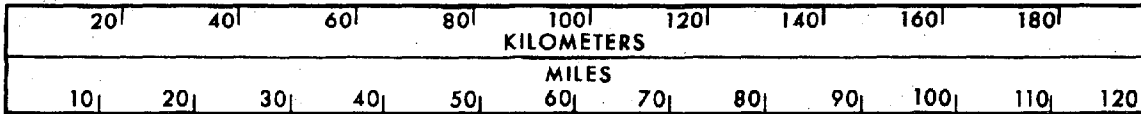
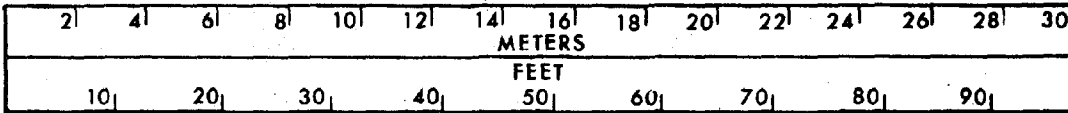
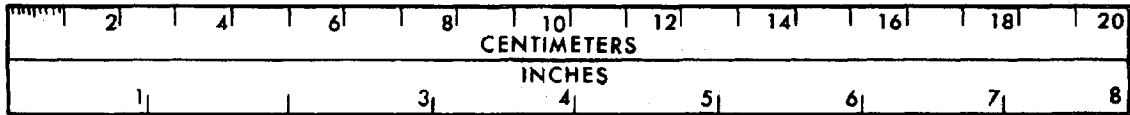
CENTER FOR WETLAND RESOURCES  
LOUISIANA STATE UNIVERSITY  
BATON ROUGE, LOUISIANA 70803

Sea Grant Publication No.  
LSU-T-76-003

CSI Publication No. 204

  
This work is a result of research sponsored by the National Oceanic and Atmospheric Administration, US Dep. Commerce, through the Office of Coastal Zone Management and the Office of Sea Grant; and it is a by-product of research conducted over a period of years under the auspices of the Geography Programs, Office of Naval Research, and the Center for Wetland Resources.

SPRING 1976



## CONVERSION FACTORS

### LENGTH

1 inch	= 2.54 centimeters	1 centimeter	= 0.40 inch
1 inch	= 25.40 millimeters	1 millimeter	= 0.04 inch
1 foot	= 0.30 meter	1 meter	= 3.28 feet
1 yard	= 0.91 meter	1 meter	= 1.09 yards
1 fathom	= 1.83 meters	1 meter	= 0.55 fathom
1 fathom	= 6.00 feet	1 meter	= 39.37 inches
1 foot	= 0.17 fathom	1 meter	= 100 centimeters
1 mile	= 1.61 kilometers	1 kilometer	= 0.62 mile
1 mile	= 1609.34 meters	1 kilometer	= 1000 meters
1 mile	= 5280 feet	1 kilometer	= 3280.84 feet

### AREA

1 foot <sup>2</sup>	= 0.09 meter <sup>2</sup>	1 meter <sup>2</sup>	= 10.76 feet <sup>2</sup>
1 yard <sup>2</sup>	= 0.84 meter <sup>2</sup>	1 meter <sup>2</sup>	= 1.20 yards <sup>2</sup>
1 mile <sup>2</sup>	= 2.59 kilometers <sup>2</sup>	1 kilometer <sup>2</sup>	= 0.39 mile <sup>2</sup>
1 acre	= 0.40 hectare	1 hectare	= 2.47 acres

### VOLUME AND CAPACITY

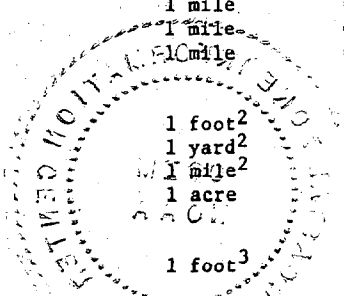
1 foot <sup>3</sup>	= 0.03 meter <sup>3</sup>	1 meter <sup>3</sup>	= 35.31 feet <sup>3</sup>
		1 meter <sup>3</sup>	= 264.17 gallons (US)

### VELOCITY

1 foot/second	= 0.68 mile/hour	1 meter/second	= 3.60 kilometers/hour
1 foot/second	= 1.10 kilometers/hour	1 meter/second	= 2.24 miles/hour
1 foot <sup>3</sup> /second	= 0.03 meter <sup>3</sup> /second	1 meter <sup>3</sup> /second	= 35.31 feet <sup>3</sup> /second
1 mile/hour	= 1.47 feet/second	1 kilometer/hour	= 0.91 foot/second
1 mile/hour	= 0.45 meter/second	1 kilometer/hour	= 0.28 meter/second

### TEMPERATURE

°Fahrenheit	= 9/5 (°C + 32)	°Centigrade	= 5/9 (°F - 32)
-------------	-----------------	-------------	-----------------



CONTENTS

List of Figures	iv
Acknowledgments	vii
Abstract	ix
Introduction	1
The Major River Mouths	2
Open Coastal Waters	5
Nearshore Currents	12
Coastal Bays and Lakes	13
Chandeleur-Breton Sound	16
Tidal Passes, Minor Rivers, and Wetland Circulation	17
Summary and Recommendations	20
Literature Cited	22
Figures, <u>after page</u>	26

## LIST OF FIGURES

1	Location map of Louisiana coastal waters.	28
2	Bivariate frequency distributions of wind speed vs. wind direction for two offshore areas.	29
3	Distribution of current speed and salinity across a channel cross section.	30
4	Cross section of density and velocity fields along the South Pass effluent plume	30
5	Three-dimensional model of geometry of velocity field in the South Pass effluent plume	31
6	Surface salinities in bight west of the Mississippi delta.	32
7	Cross section of salinity field near west end of LOOP study area	33
8	Temperature-salinity diagram of hydrographic data collected in bight west of Mississippi delta.	34
9	Observed and residual currents at various times during anchor station.	35
10	Tidal current hodographs at four depths.	36
11	Tidal current velocity field before high water at Barataria Pass.	37
12	Tidal current velocity field after high water at Barataria Pass.	38
13	Distribution of tidal current amplitudes and co-phase line of tide before high water at Barataria Pass.	39
14	A comparison of current velocity with wind velocity at Boothville station on the Mississippi River.	40
15	Tidal current hodographs at the 6-m depth	41
16	Tracks of drogues drifting at 1-m depth showing probable water entrainment into Barataria-Caminada Bay complex.	42
17	Basic geometry of trapped vortex west of Mississippi delta.	43
18	Tidal current hodograph from GURC-OEI meter.	44

19	Long-term drift current.	45
20	Summer northeasterly drift along central Texas coast.	46
21	Surface salinity pattern along Louisiana coast during high river season.	47
22	Surface salinity pattern along Louisiana coast during low river season.	48
23	Time series plot of isopycnals showing effects of strong onshore winds and their sudden dropoff on local density field.	49
24	Vertical profiles of currents in same time series as in Fig. 23.	50
25	Conceptual model of coastal air circulation system of Gulf in summer.	51
26	Nearshore currents driven by light winds along Florida Panhandle coast.	52
27	Profile of alongshore current speed showing effect of density gradient in damping out downward transfer of momentum needed to generate currents at low levels.	53
28	Power spectrum of nearshore wave field under light coastal winds.	54
29	Wave-driven currents in breaker zone showing onshore flow on both flanks of a strong seaward-directed "rip" current.	55
30	Observations of direction and magnitude of water surface slopes in Caminada Bay.	56
31	Simulation of direction and magnitude of water surface slopes in Caminada Bay.	57
32	Vertical cross-section of salinity distribution in Barataria Bay.	58
33	Distribution of isohalines in Barataria Bay predicted by numerical model.	59
34	Distribution of isohalines in Barataria Bay after drop in salinity in passes.	60
35	Surface circulation in Lake Pontchartrain under influence of southerly wind.	61
36	Bathymetry of Chandeleur-Breton Sound.	62
37	Currents after low tide at entrances predicted by numerical model.	63
38	Currents after high water at entrances predicted by numerical model.	64

39	Co-range lines predicted by model.	65
40	Co-phase lines predicted by model.	66
41	Sequential profiles of current speed in Caminada Pass.	67
42	Sequential profiles of salinity in Caminada Pass.	68
43	Vertical averages of speed and salinity as a function of time in Caminada Pass.	69
44	Current at various levels in Barataria Pass in 1934.	70
45	Isohalines and values of time-averaged net discharge in wetland west of Caminada Bay.	71

#### ACKNOWLEDGMENTS

This work is a result of research sponsored by the National Oceanic and Atmospheric Administration, U.S. Department of Commerce, through the Office of Coastal Zone Management and the Office of Sea Grant. The activity is coordinated through the Louisiana State Planning Office.

The nature of this study required assistance and information from a relatively large number of individuals and agencies. Work primarily involved collection, analysis, and interpretation of existing data located at a number of sources. The authors are particularly indebted to the individuals, departments, and agencies listed below:

The Study Management Team of the Louisiana Coastal Zone Management Program: Patrick Ryan, Director, State Planning Office; Lyle St. Amant, Assistant Director, Louisiana Wildlife and Fisheries Commission; Vernon Behrhorst, Director, Louisiana Coastal Commission; and Jack R. Van Lopik, Director, Center for Wetland Resources, Louisiana State University, Baton Rouge Campus.

Louisiana State University, Baton Rouge Campus: Robert Chabreck, Associate Professor, Forestry and Wildlife Management.

Louisiana State Planning Office: Patrick W. Ryan, Director; Paul R. Mayer, Jr., Assistant Director; Coastal Resources Program: Paul H. Templet, Program Coordinator; Lynne Hair, Assistant Program Coordinator; John M. Bordelon, Chief Planner; Jim Renner, Economic Planner.

Louisiana Wildlife and Fisheries Commission: Alan B. Ensminger, Chief, Refuge Division; Robert A. Beter, District VIII Supervisor, Game Division; Barney Barrett, Geologist.

The large number of local, state, and federal agencies whose foresight in sponsoring such basic research as this report before the "coastal crisis" emerged upon us should be applauded. The insight provided by my colleagues in the Coastal Studies Institute is sprinkled liberally throughout. The author's personal knowledge of Louisiana coastal waters has been made possible through the support of both the Geography Programs of the Office of Naval Research, under Contract N00014-75-C-0192, Project NR 388 002, and the Center for Wetland Resources of Louisiana State University.



#### ABSTRACT

A review of our knowledge of circulation and currents in the coastal water of Louisiana indicates that, despite notable progress in a few specific areas, we lack a rudimentary knowledge of the mechanics of water motion along most of the coastline. The Mississippi River salt wedge and the mixing of its effluent plume into the open water of the Gulf of Mexico are generally understood, but detailed salt balance and turbulent mixing studies should now be undertaken. The portion of the Louisiana shelf within the area 80 km west of the Mississippi has been studied in detail with regard to tidal currents, long-term drift, hydrography, and local wind drift. Outside of this area, apparent ignorance prevails except for seasonal salinity patterns and the occasional isolated study. Summer current reversals toward the east and high tidal ranges in the vicinity of Calcasieu Lake, for example, remain unexplained. Detailed knowledge of the dynamics of our prolific coastal bays and estuaries is embarrassingly poor. Numerical modeling perhaps offers a shortcut to overcoming this disadvantage, but realistically this technique will only be effective after the controlling forces are better defined and understood by dynamically oriented field studies. Existing numerical models of Barataria Bay and Chandeleur-Breton Sound are cases in point. Tidal passes, minor river mouths, and the circulation within the wetlands proper have been subject to sporadic, short-term measurement programs, but definitive studies of the flux of mass, heat, salt, and other important scalars have yet to be performed. A list of research priorities to eventually allow better utilization of our coastal waters is presented at the end of this report.

## INTRODUCTION

From the point of view of the physical oceanographer, Louisiana is endowed with a fascinating variety of dynamical environments. The more than 450 km of coast from the Mississippi state border westward to the Sabine Lake boundary with Texas (see Fig. 1) are studded with great rivers of continental scale, a sound of impressive dimensions, and a series of brackish bays and estuaries that are unrivaled for biological productivity anywhere in the contiguous United States. The usual oceanographic driving forces of wind, tide, atmospheric pressure gradients, and semipermanent water surface slopes keep Louisiana coastal waters constantly in motion. These movements, however, are affected to an unusual degree by the huge volume of fresh water injected into the coastal waters by two great rivers, the Mississippi and the Atchafalaya, plus abundant rainfall along most of the coast. The density gradients and buoyancy effects brought on by the mixing of these fresh and brackish waters drained from the land with the saline waters of the Gulf of Mexico must always be considered in understanding the mechanics controlling circulation and diffusion along the Louisiana coast. In the immediate nearshore zone, wave-driven currents will control the circulation and beach drift, while buoyancy spreading and gravitational convection will assume important roles at tidal passes and estuary mouths.

The large-scale geometry of the coast is not only of geomorphic interest but also of importance in determining large-scale flow patterns. The 80-km protrusion of the Mississippi delta into the Gulf of Mexico is exceeded perhaps only by Cape Cod in its ability to alter and affect the current, tidal, and wave fields operating in the local coastal waters. Large-scale topographic controls on the flow field can be expected to be exerted by these three zones: the shallow sound and shelf east of the delta, the severe bathymetric curvature characteristic of the delta proper, and the long, regular coast and shelf extending west to the Texas boundary.

Winds are quite consistent along the length of the Louisiana coast from the Mississippi delta westward to Sabine Lake. Figure 2 illustrates with bivariate wind speed and direction plots the changes between seasons and between the two offshore areas, Bayou Lafourche and Sabine Pass, which are separated by 280 km. As the season progresses from summer to fall, winds generally increase in speed and shift to a more easterly and northeasterly direction. Winter brings only slightly higher wind speeds, but the directions are the most variable of the year. Spring is a transition back to the summer direction distribution but with slightly higher wind speeds. The notable lack of westerly wind components is apparent at both stations throughout the year. We then might expect local wind-driven currents to be predominantly toward the west.

Considering the thousands of observations (replotted from Brower et al. 1972) making up the distribution plots, the similarities between these two locations near the extremities of the Louisiana coast are remarkable. Long-term statistics, however, can be quite misleading when it comes to the nonlinear response of water to wind. Murray (1972b, 1975b) has clearly shown the dominant role that intense winds associated with specific sectors of migrating high and low pressure cells play in determining three-dimensional circulation on the eastern Louisiana shelf.

The objective of this compendium report is to systematically review the major areas of research involved in the understanding of Louisiana's coastal waters, pointing out progress where it is present, ignorance where appropriate, and finally ranking what are felt to be the most urgent needs for knowledge in order to wisely utilize our coastal waters.

#### THE MAJOR RIVER MOUTHS

If one had to identify the one most dominant influence on Louisiana's coastal waters it certainly would be the discharge of the Mississippi River. It is a phenomenon so conspicuous that it is readily seen on numerous satellite photographs because of its unusually high levels of turbidity and its temperature contrasts to normal Gulf waters, which are apparent on the infrared scanners.

The seaward ends of the Mississippi passes

are classical examples of what estuarine oceanographers refer to as salt wedge estuaries (Pritchard 1952, 1955). Figure 3 is a typical example of the processes operating inside the channels. Despite the high volume of flow from the Mississippi, weakly diluted Gulf water is actually flowing upstream in the lower half of the channel. In the upper half of the channel, river water, which has entrained small quantities of salt water from beneath, flows gulfward at speeds in excess of 3 ft/sec. It is the greater density of the Gulf salt water that sets up the horizontal pressure gradient favorable for the Gulf water to intrude up the river channel. Low tide ranges inhibit the intense mixing between the river and the seawater normally seen in the estuaries of the Atlantic coastal plain, but salt does apparently move vertically up into the upper layer. The exact mechanism, although long conjectured to be the breaking of interfacial waves, remains unproven. Flooding tides increase the upstream flow in the bottom layer and at times can even temporarily halt the river flow in the upper layer. On the other hand, it is common for the salt wedge to be completely swept out of the passes during the flood stage of the river in the spring.

A definitive series of papers on Mississippi River mouth processes have been published in recent years by Wright and his colleagues at Louisiana State University (Wright 1970, 1971; Wright and Coleman 1971; Wright et al. 1973) and most notably in the definitive review by Wright and Coleman (1974). Wright's work shows that buoyancy forces rather than turbulence are usually the most important at natural stratified river mouths. A controlling parameter expressing the ratio of inertial forces to buoyancy forces is the densimetric Froude number  $F'$ , given by

$$F' = \frac{\bar{u}}{(\gamma h')^{1/2}}$$

where

$\bar{u}$  is the average speed in the upper layer

$$\gamma = 1 - (\rho_f/\rho_s)$$

where

$\rho_f$  is the density of the effluent water and

$\rho_s$  is the density of the lower intruding water,

$g$  is the acceleration of gravity, and

$h'$  is the depth to the density interface

According to Stommel and Farmer (1952), during salt wedge intrusion the average speed of the

freshwater effluent and the depth to the density interface will mutually readjust so as to keep the densimetric Froude number near unity. Monthly observations over a 2-year period at South Pass confirmed this relationship (Wright 1970). Landward of the edge of the channel the densimetric Froude number will decrease as the salt wedge thins out upstream. As shown in Fig. 4, however,  $F'$  will increase sharply over the bar, achieving supercritical values over the bar crest, apparent breaking of internal waves, and rapid vertical entrainment of salt water into the upper layer. According to Wright's division by regions, in region I the effluent plume displays a rapid lateral expansion following the buoyant plume mechanics of Bondar (1970). In response to the vertical thinning of the surface freshwater layer, the isopycnals (lines of equal density) rise sharply, creating a supercritical Froude number and internal wave breaking. Maximum thinning occurs in region II, a distance of four to eight channel widths seaward of the mouth. Farther offshore, in region III, as Fig. 4 shows, the interfacial depth increases with the internal hydraulic jump suggested by Wright. In region IV the buoyant lateral expansion mechanism is still operative, but it is here that wave-, wind-, and tide-induced mixing of the river effluent causes the formation of the characteristic low-salinity Louisiana coastal water.

During high river stage the increased river discharge can drive the salt wedge from the channel, causing the densimetric Froude number to go to infinity at the channel entrance. Figure 5 shows the effluent boundary is highly irregular under these conditions because of the increased role of turbulent diffusion in shaping the plume geometry. While the flow inside the channel and in region III is completely downstream, below a depth of 2 m in region III the slightly diluted Gulf water moves directly toward the bar, to be vigorously mixed upward in region II. The cross-plume secondary circulation cells shown in Fig. 5 are predicted by a numerical simulation model of stratified water mouths (Waldrop and Farmer 1974) and have important morphological implications on seaward levee expansion.

It is clear that significant progress has been made both on the geometry and the behavior of the salt wedge and on the processes controlling effluent mixing and expansion at Mississippi River mouths. The role of interfacial waves,

although widely discussed, remains conjectural, although Wiseman et al. (1975a) tentatively report a positive role for this phenomenon. What is really needed, however, is a detailed study of the entire salt balance in order to evaluate the relative importance of diffusive and advective terms both vertically and longitudinally in this type of estuarine channel. Interfacial wave breaking is only one possible mode of vertical advection contributing to the three-dimensional salt balance. Time-dependent shear flux and flux associated with time-dependent cross-sectional areas might be significant (although previously ignored) terms to be considered.

Compared to the Mississippi, the other major river mouth in Louisiana, the Atchafalaya, is essentially unknown. The Atchafalaya debouches directly into the largely enclosed Atchafalaya Bay, and the information available (Barrett 1971) indicates that this bay and much of adjoining Cote Blanche Bay are fresh during most of the year. If there is a salt wedge in the channel of the Lower Atchafalaya River, its existence is not widely known. Tidal induced mixing of these fresh waters throughout the adjacent bays and coastal water is probably the dominant dispersion mechanism, but these questions sorely need scientific attention. Satellite imagery does clearly point out, however, its significant intrusion of fresh turbid water from the Atchafalaya into the coastal current stream. This recharging of coastal waters with more fresh water 160 km west of the Mississippi mouths keeps the coastal water diluted all the way to the Texas border.

#### OPEN COASTAL WATERS

The coastal waters immediately to the west of the Mississippi delta have recently been the subject of intense examination with regard to the location of the Louisiana Offshore Oil Port (LOOP) in that vicinity. Wiseman et al. (1975b) presented a detailed summary of new data on tides, current, and hydrography taken during a 1-year field study covering the offshore area from Southwest Pass to the east end of Timbalier Bay and generally enclosed by the 36-m depth contour. Figure 6 shows a characteristic distribution of surface salinity in this area with a band of very low salinity waters (<12 ppt) hugging the coast.

These brackish waters are the result of fresh-water discharge from the bays to the north and crevasses along the river channel to the northeast as well as recirculated Mississippi River effluent. The track of the Mississippi effluent plume is readily apparent in Fig. 6 as an intrusive tongue of low-salinity water pointing toward Caminada Bay. An example of the vertical structure of the salinity field is shown in Fig. 7, a vertical section along  $90^{\circ}03'W$  longitude or about 54 km west of Southwest Pass. A distinct halocline is seen at the 10-m depth level where the layer of coastal brackish water overlies the high-salinity Gulf water. The thin lens of fresher water (15-16 ppt) near the coast is probably the low-tide effluent plumes from Barataria and Caminada bays. Clearly the water mass structure here is a quite complicated mixture of water types varying both spatially and temporally. Careful sampling, however, allowed Wiseman et al. (1975b) to construct the salinity-temperature diagram in Fig. 8 from several thousand data points. The well-defined L-shaped configuration of the points strongly suggests that three different water types contribute to the coastal waters: a warm saline type, a cold saline type, and a freshwater type whose temperature varies as a function of time.

These types of water are moved and mixed along the coast by tidal currents, local wind effects, and other semipermanent currents. In order to isolate the tidal currents from the other driving mechanisms, ten anchor stations of 50 hours' duration (2 tidal days) were occupied in consecutive months at the time of tropic tide when tidal currents are expected to be at a maximum. Figure 9 gives an example of six of the fifty hourly profiles of the observed currents at the July 1973 station near the western boundary of the study area. Note the significant shear of current speed and direction with depth. The tidal currents oscillate with an amplitude comparable to the magnitude of the longer term steady currents, a situation that causes the observed currents to present a rather confused picture. Simple averaging, however, over the 50 hours produces a very well-behaved residual current profile (inset, Fig. 9) whose orderly clockwise rotation with depth suggests a steady wind-driven current to the northeast. Hourly analysis of the same two tidal days of observation yields good estimates of the tidal currents (see Fig. 10), which in general rotate clockwise

due to the Coriolis force with amplitude of 10-15 cm/sec. The tidal ellipse near the 4-m level is deformed due to the interference of vertical momentum transfer by a sharp pycnocline in the area. The 14-m tidal ellipse also shows deformed and reduced currents, likely due to a density step just above the isohaline Gulf water.

The spatial distribution of the tidal current stations allowed hourly maps to be made of the tidal current field in the water mass below the main pycnocline. Figure 11 shows that the tidal currents 0.5 hour before high water at Barataria Pass have a circulatory pattern apparently controlled by the bottom bathymetry. Nearer shore, currents move northeastward along the coast, while seaward of about the 25-m contour currents are actually reversed with a 12-hour phase lag. One half a tidal day later (Fig. 12) the current field has essentially reversed itself except that the southwest corner of the study area shows a tendency for seaward-directed flow. Contrary to common beliefs, the tidal current field along the coast is well organized and of sufficient strength to significantly affect the movement and mixing of the coastal waters. The strengths of the tidal currents appear to be distributed in three zones that roughly follow the depth contours (see Fig. 13). It may be significant that the strongest currents occur near Southwest Pass where the severe bottom curvature has produced a complex pattern of co-phase lines, also shown in Fig. 13. These lines of equal tidal phase indicate, for example, that high tide arrives 3 hours earlier at Southwest Pass than at Barataria Pass.

Temporal variability of the currents in the LOOP study area was also examined by means of continuously recording current meters moored in the southwest corner of the study region at the location of the black square shown in Fig. 12, where the water depth is 30 m. Figure 14 compares the currents at a depth of 6 m below the surface to the wind velocity observed at Boothville on the Mississippi River (29°0.5'N, 89°25'W) during the interval 30 January through 6 February 1974. The current record shown in this figure is the low-pass output from the 39-point Doodson-Warburg tidal filter (Groves 1955), which means that the tidal (diurnal) and higher frequency currents have been removed from the signal, leaving only the long-term mean drift currents for comparison. Drift currents remained steadily westward flowing at about 10 cm/sec up



through 2 February, despite the fact that the wind shifted through more than  $360^\circ$  during this interval. Only when the wind steadies down from the south at speeds in excess of 5 m/sec at about 0400 2 February does the current at the 6-m level respond by shifting toward a south-southeasterly direction against the wind. It appears that the south wind is driving the surface layers above 6 m northward toward the coast and the waters at the level of the current meter (probably below the pycnocline) are flowing seaward as a return flow to satisfy continuity. When the wind speed stopped abruptly at about 1800 hours on 5 February, the shoreward-directed density gradient vector, set up by the onshore wind, drives the water at the 6-m level back toward the north, as seen in the current direction shift late in the evening of 4 February. Identical processes have been reported in detail from the stratified waters east of the Mississippi delta by Murray (1972b). Thus the coastal waters this far from shore (32 km) respond only to steady trends in the wind decidedly in excess of 5 m/sec, such as associated with migrating pressure systems and frontal passages.

During intervals of low wind speeds the waters at this same location (6-m level) are strongly influenced by the temporal changes of the tidal currents. The tidal current hodographs in Fig. 15 are obtained as the tidal band pass signal using the same Doodson-Warburg filtering process described above. On 2 February a 36-cm tide produced a well-behaved clockwise-rotating current of a 20 cm/sec amplitude (Fig. 15), not inconsiderable for the open coastal waters of Louisiana. As the lunar declination grew larger on 3 February the tide height increased to 45 cm, but surprisingly the tidal current hodograph is severely distorted and damped to an amplitude of only about 10 cm/sec. This behavior is very likely the result of the pycnocline migrating vertically across the current meter level and damping out vertical momentum exchange. On 4 February trophic tides occur, the highest tides of the month. Currents, apparently again free from the hinderance of the pycnocline, amplify dramatically, reaching amplitudes of over 40 cm/sec. As tide ranges drop off in the following days, tidal currents follow suit, exhibiting their temporal dependence on the tropic-equatorial cycle of lunar declination.

The salinity (hydrographic) data discussed earlier suggested a repetitive but intermittent

northward intrusive flow in the surface waters at the western edge of the study area. Several experiments were conducted during the LOOP study using free-drifting drogues set at 1-m depth. Figure 16 shows a good example of the interaction between clockwise-rotating tidal currents and a northward mean drift. Two drogues released offshore simultaneously execute a tidal loop while tracking directly toward the Caminada Bay shoreline. Although the data is lacking, the drogues are probably entrained in Mississippi River effluent and will be carried into the Caminada-Barataria complex by the next flooding tidal current, thus illustrating a mechanism for introducing river water into the coastal bays via the tidal passes.

Collective consideration of hydrographic data, drogue data, drift card data, and current meter data, strongly reinforced by ERTS and DMSP satellite imageries, brought Wiseman et al. (1975b) to conclude the existence of a mean flow pattern in the form of a trapped vortex along the western flank of the Mississippi River delta. This type of current pattern, shown in Fig. 17, still allows for a westerly drift in the low-salinity, highly turbid coastal boundary layer that is probably driven by and closely coupled to the local wind field with its dominant component from the east.

Immediately to the west of the LOOP study area, in the waters south of Timbalier Bay, a hydrographic study by Oetking et al. (1974a) sponsored by the Gulf Universities Research Corporation (GURC) has shed some light on the coastal circulation. Figures 18 and 19 are a tidal current hodograph and a segment of a low-frequency long-term drift current obtained by analyzing basic data presented by Oetking et al. with the Doodson-Warburg tidal bank pass technique. The tidal current record taken from a bottom current meter at 28°50'N, 90°23'W, is quite similar to those obtained in the LOOP study area, showing clockwise rotation with an 8 cm/sec amplitude. The bottom current is perhaps better developed here due to increased distance from the Mississippi River and the smoother vertical density gradients. The drift current shown in Fig. 19 is from the same bottom current meter installation and shows a sudden change in current direction from east-northeasterly flow to westerly flow. Inspection of the daily weather maps provides no suggestion as to what may have caused this reversal. The answer may lie as far away as

the Texas coast, where strong southerly winds in the summer months are known to drive the coastal currents northward and northeastward along the coastal bend. A recent example of this situation determined from drifter studies is shown in Fig. 20, from the work of Hill et al. (1976). Several days after the intense southerly winds relax off south Texas we may find the typical westerly drift along the Louisiana coast reasserting itself as in Fig. 19. The summer easterly drift off Louisiana was first reported by Kimsey and Temple (1962, 1963) and verified by Oetking et al. (1974a). The hydrography reported by the GURC study (Oetking et al. 1974b) showed the same variations in salinity and temperature as observed in the LOOP study, that is, a low-salinity surface layer extends out at least 30 km from the coast and a fresh-brackish band of highly turbid water, probably recycled bay water, about 10 km wide hugs the coast. It is somewhat surprising that the tidal currents have not brought about more mixing of the Mississippi effluent at this distance along the coast.

Detailed studies along the coast west of Timbalier Bay are as yet lacking. Among the meager information we do have concerning the western Louisiana coastal waters are the salinity distributions. For example, Gagliano et al. (1969) present data taken by the Bureau of Commercial Fisheries on seasonal changes in salinity patterns. Figures 21 and 22 show the salinity fields in 1963 during a typical flood month--April--and a typical low-stage month--December. During the flood season estuarine levels of salinity actually exist along most of the open coast. While direct measurements are unavailable, such a salinity pattern suggests slow shoreward movement of water in the lower saline layer and a circulation dominated by local wind effects in the upper brackish layer. The wind distribution discussed earlier would then suggest a westerly net drift. Definitive studies of the forces controlling the momentum and the fluxes controlling the salt balance in the brackish coastal waters of western Louisiana have yet to be performed.

For want of further information, it is also instructive to examine the distribution of co-phase lines and co-tide lines along the coast (see Fig. 1), which can be extrapolated from data available in the Tide Table (NOAA 1975). The co-tide lines, which are drawn to represent the arrival time of high water along the coast, are

in hours before high water at Barataria Pass. East of the delta the tide arrives with no lead or lag along the Chandeleur Island chain but leads Barataria Pass by 2-3 hours around the circumference of the delta proper. To the west of the delta, Fig. 1 also shows, the tide arrives increasingly earlier as you move from east to west, reaching a 7-hour lead time near Calcasieu Lake. This gradient of equal tidal phase along the coast implies a similar gradient in tidal currents to remain important along the western shelf. The co-range lines, also plotted on Fig. 1, show a distinct pattern of their own. Tides along the western shelf, especially in the Sabine Lake-Calcasieu Lake area, are considerably amplified over the values in the east around the Mississippi delta. Ranges reaching as high as 2.5 feet, as these do, should produce significantly greater tidal currents than previously expected. The reasons for the tidal amplification in the west, which probably are related to the bottom slope or coastal curvature, are not known but should be the subject of future research.

In the open waters east of the Mississippi delta Murray (1972a, 1972b, 1975b) and Murray et al. (1970) gained considerable insight into the mechanics governing the movement of the coastal waters during the well-known Chevron oil spill off Main Pass in 1970. Density stratification appeared to be quite common in this eastern area also. Figure 23 shows a 5-day time series record of water density  $\sigma_t$  taken from the CGC Dependable, anchored near 29°23'N, 88°58'W, about 15 km east of the Mississippi delta. The primary features to note in Fig. 23 are (a) the sharply plunging isopycnals beginning around noon of 16 March and continuing until about 0300 the following morning, (b) the stability of the isopycnals until noon of 17 March, followed by (c) their sharp rise back up to their early level. In this type of plot, plunging isopycnals indicate that fresher, less dense water has moved across the observation profile and rising isopycnals indicate the opposite. The companion figure, Fig. 24, shows simultaneous vertical current profiles and surface wind stress separated into wind episodes at the same location. Episodes no. 2 and 3 correspond to the time of plunging isopycnals, strong easterly and southeasterly winds blow the brackish surface water toward the coast, driving the saline bottom water offshore. Thus the coastal water prisms are enabled to fill completely

with the lighter water characteristic of the surface layer. The sudden drop in wind stress in episode no. 4 in Fig. 24 reflects the same process, with surface currents streaming back offshore due to the suddenly unbalanced pressure gradient. Bottom currents are similarly reversed. This redistribution of mass by strong onshore winds associated with migrating atmospheric pressure systems and its sudden readjustment when wind stress drops appears to be a fundamental process in stratified coastal waters.

#### NEARSHORE CURRENTS

Very little is known about currents inside the 10-m depth contour along the Louisiana coast. Harper (1974) did make two tidal observation stations in about 6 m of water along the coast off Grand Isle and found weak but well-behaved tidal currents and residual or mean currents directed westerly in response to local winds as he was inside the brackish water coastal boundary layer. The meteorological driving forces have not been studied in detail off Louisiana. A good example of a meteorological system that is probably of great importance here is the coastal air circulation system shown in Fig. 25, synthesized from a study in Texas (Hsu 1970). Varying horizontal pressure gradients because of relative heating and cooling of the land and sea surfaces generate onshore winds in the day and offshore winds in the early morning hours. Note how the winds aloft are reversed from the surface and that distinct scales of wind motion (10-20 km) might be expected to affect inshore water movements. Of particular interest to Louisiana is the damping and lagging effects produced by the two bays depicted schematically in the figure. Currents near the coast can in fact be influenced strongly by this sea breeze wind system, as shown in Fig. 26, where currents of 25 cm/sec are driven along the coast by a southwesterly sea breeze on the Florida Panhandle Gulf of Mexico shore. Murray (1975a), in a detailed study, has demonstrated that theoretical considerations involving wind stress, wind angle to the coast, and eddy viscosity explain the subtle three-dimensional structure he observed in wind-driven currents close to the coastline. The importance of density stratification is again emphasized where Murray (1975a) showed with a numerical solution to the differential equations of motion

that the absence of movement below 6 m in Fig. 27 is due to the density gradient damping out the wind-induced vertical momentum transfer.

These diurnally varying winds, although of modest strength, can have an important effect on the nearshore wave field, as shown by Suhayda in Fig. 28 (from Sonu et al. 1973). Note the introduction of wind waves with a period of 1.5 seconds at 1000 hours by the sea breeze and the subsequent increase in period to 3 seconds by 1800 hours, when this component of the wave spectrum begins to decline as the baroclinic pressure field driving the sea breeze diminishes.

Inside the wave-breaking zone momentum is transferred from the shoaling and breaking waves to what are usually referred to as longshore or littoral currents. This type of wave-driven current is of great importance to beach erosion, beach nourishment, and recreational use. It has been studied widely around the world but virtually ignored in Louisiana. The type of wave-driven circulation cell observed along the Florida Gulf coast (Sonu 1972) is shown in Fig. 29. Currents move onshore on the flanks of a troughlike depression referred to as a rip channel. In the channel seaward flow extends through the breaker line and may reach speeds of 1 m/sec or more. These "rips" are a common cause of drowning for unwary swimmers.

Most of our knowledge of nearshore currents discussed above is based on observations from adjacent but nonetheless sandy type coasts, quite different from the mud and marsh dominated coasts of Louisiana. Significant differences will no doubt emerge as our ignorance of local inshore phenomena is cleared away.

#### COASTAL BAYS AND LAKES

Eight distinct coastal lakes and bay units dominate the coastal wetlands of Louisiana (see Fig. 1). Five of these, (1) the Barataria-Caminada Bay complex, (2) the Terrebonne-Timbalier Bay complex, (3) the Vermilion/Cote Blanche/Atchafalaya Bay complex, (4) Calcasieu Lake, and (5) Sabine Lake, have sufficient salinity concentrations to be considered estuarine in character. The Lake Borgne portion of (6) the Lake Borgne-Pontchartrain complex is also estuarine, while Lake Pontchartrain proper is probably best grouped with (7) Grand Lake and (8) White Lake as characteristically fresh water or nonestuarine.

Broad, shallow estuarine bays with narrow entrances and relatively low interior tide ranges are usually referred to as bar-built estuaries in the literature (Pritchard 1952) because of the presence of long barrier bars frequently separating them from the sea. Sabine Lake, Calcasieu Lake, the Terrebonne-Timbalier and Barataria Bay complexes are clearly of this type, while Atchafalaya Bay will probably evolve into this configuration in the future. Unfortunately, this is the least studied type of estuary from the viewpoint of circulation dynamics. Water levels and salinity distributions are usually the only information available. Wind-driven currents were originally suggested to provide most of the mixing, but recent research suggests that tidal currents, even though of moderate magnitude, may play a significant role in the salt balance except during the period of frontal passage.

Barataria-Caminada Bay is by far the best known scientifically. Kjerfve (1973, 1975) studied water level dynamics in Caminada Bay and related surface slope vectors to tidal waves and to wind stress in fair weather conditions. Kjerfve showed that the instantaneous slope vector either oscillated or rotated in the horizontal plane as a function of time, primarily because of the interaction of tidal input from two major entrances, Caminada Pass to the south and the opening from Barataria Bay to the northeast. A simplified set of equations (assuming a constant depth, neglecting the Coriolis and the nonlinear field accelerations, and the horizontal density gradients, but maintaining a linear bottom friction) were solved analytically for two damped tidal waves entering the bay at right angles and reflecting perfectly at the boundaries. A constant surface wind stress was allowed to act on the model. Figure 30 shows a 63-hour record of the magnitude and direction of the water surface slope in Caminada Bay calculated from three cross-leveled water level instrument stations. The stairstep clockwise rotation of the slope direction and the periodic pulsing of the magnitude of the slope shown in the lower part of the figure are successfully predicted by the analytical model as shown in Fig. 31. Kjerfve shows several other successful predictions of water surface slope under varying wind conditions and concludes that barotropic pressure gradients associated with these complex tidal slopes must play an important role in the momentum balance of this type of bay.

Kjerfve's work did not consider spatial variations in the density field. Barrett (1971), however, shows an outstanding example of the two-dimensional salinity structure in Barataria Bay, reproduced in Fig. 32. The baroclinic pressure gradient term,  $g/\rho \int^z \partial \rho / \partial x dz$ , can be reasonably estimated from<sup>o</sup> this figure at a value of  $3 \times 10^{-6}$ , which is only an order of magnitude smaller than Kjerfve's average surface slopes of  $10^{-5}$ . Thus it appears that the salinity gradient in the estuary undoubtedly will at times make important contributions to the momentum balance.

The technique of mathematical modeling of estuarine tidal flows has recently been applied to Barataria Bay complex by Hacker (1973). Using a Leendertsee (1967) type approach to the solution of the finite difference form of the equations of motion, Hacker predicts velocity and tide height distributions in the bay complex. The reliability of the velocity field maps is difficult to interpret, especially where the many islands and promontories present seem to be ignored. Very interesting predictions are also made of salinity distributions using an average freshwater input of  $1,000 \text{ ft}^3/\text{sec}$ . The magnitude of the salinities (see Fig. 33) simulated in the bay appear to be quite reasonable compared to the data of Barrett (1971). The lateral distributions of salinity, however, do not reflect extreme cross-bay gradients shown in the salinity maps of the area presented by Gagliano et al. (1969). Other simulations presented by Hacker (1973) are (a) high freshwater runoff flow through the system, which simulates conditions that are encountered in an unusually wet year; (b) the effects of a cold front passage; (c) a hurricane surge; and (d) a significant drop in input Gulf salinity due to the migration of Mississippi River effluent into the area. The three-fold increase in freshwater discharge (a) surprisingly did not appreciably affect the location of the isohalines. One wonders if the somewhat arbitrary choice of the constant dispersion coefficient is not governing the model behavior. The cold front passage (b) was somewhat ambiguous, but the surge (c) did push the 15 ppt isohaline 10 km farther inland than normal. The effect of the drop in salinity down to 10 ppt (d) at the passes is shown in Fig. 34. The drop occurred at high tide, 3 hours earlier than the figure, and a high-salinity dome is already evident in the middle of the bay. How long the bay takes to stabilize to the new conditions is not reported.



It is clear that Hacker's work is a significant first step in our understanding of these large, complex systems. Considerably more work needs to be done in understanding the forces acting in the bays so as to increase the reliability of the input functions to the models. For example, the baroclinic pressure gradient term is ignored in the above model and the salt concentration is spread in a passive manner.

The circulation and momentum balance of the coastal lakes is even less well known than the estuaries. Winds, of course, are assumed to be the dominant driving mechanism. Stone et al. (1972), however, have shown through an impressive data collection program using aerial photography the response that the surface circulation may take, depending on wind direction, speed, and basin geometry. This work is apparently the only kinematical study of the large Louisiana coastal lakes and yet it is restricted to Lagrangian tracks of the surface circulation. Stone et al. (1972) reports that in more than 60 percent of the thirty current experiments the current set is controlled directly by the wind direction. It is more than likely that future work will show complex three-dimensional circulation patterns controlling the movement and dispersion of soluble and particulate matter in these lakes. An example of Stone's results showing currents in the southern half of the lake following the wind but meeting south-flowing currents at a convergence line is reinterpreted from the original data in Fig. 35. Such opposing current fields could be caused by a wind shift, density discontinuities, or perhaps even tidal current effects.

#### CHANDELEUR-BRETON SOUND

An integral unit isolated by itself to the east of the Mississippi delta (see Fig. 1), Chandeleur-Breton Sound is an impressive body of water extending 90 km in a northeast-southwest direction and bounded to seaward by the Chandeleur Island-Breton Island chain lying more than 35 km offshore. The U.S. Coast and Geodetic Survey conducted a tide and current survey in the sound along the track of the Mississippi River Gulf Outlet Channel in the early 1960s, but the data from the survey are of good quality only at intermittent times and there is almost no simultaneous data at separate locations. Hence the time-dependent circulation pattern was impossible

to decipher, and a two-dimensional numerical model of the area, based also on the Leendertsee (1967) technique, has been constructed by Hart (1975). Hart's model features tidal inputs from the northern and southern entrances and allows for periodic overflow of the shallow shoals connecting the elements of the island chain. The bottom topography is shown in Fig. 36. Two examples of the tidally driven velocity field are included here as examples. Figure 37 shows the currents 3 hours before input low tide on 12 June 1968. The sound is draining both to the south and to the north, with a divergence zone midway up the axis of the channel. Speeds of 20-30 cm/sec are common near both exits. Eighteen hours later (Fig. 38) the tide is 1 hour after input high water and currents are still filling the sound through the entrances and converging and veering in mid-sound to fill the marsh areas.

Hart has shown that the differences in range at the two entrances can drive significant net circulation through the sound. He also goes a step farther than Hacker (1973) and includes a wind stress in his finite-difference formulation. Winds of 20-knot speed from various quadrants have relatively little effect on the instantaneous circulation but substantially increase the net through flow. The co-range lines for an average tide (Fig. 39) show an interesting pattern. The higher input ranges are apparent at the northern entrances and the range increases to maximum values at the middle of the sound. In a surprising result ranges along the coast can be quite a bit smaller than in mid-sound. Note the steep hydraulic gradient across Chandeleur Island. A co-phase or co-tidal map (Fig. 40) indicates high tide progresses in a fairly well behaved manner across the sound to the coast with a 3-4 hour lag behind the entrances. Hart's model shows considerable detail in the tidal velocity and tidal height distributions that should now be subject to a systematic testing. Comparison between the usable U.S. Coast and Geodetic Survey data and the model was quite favorable.

#### TIDAL PASSES, MINOR RIVERS, AND WETLANDS CIRCULATION

It is discouraging to note that definitive studies of the net flux of momentum, salt, heat, and other biological and chemical scalars through the numerous tidal passes have yet to be reported.

The basic theory and methodology are now well laid out (Dyer 1974; Murray and Siripong 1973) to evaluate the contributions of (a) vertical and lateral shear flux, (b) time-dependent oscillatory shear flux, (c) flux due to time variations in cross-sectional area, and (d) mean freshwater discharge to the balance of these properties. Some limited data are available, however, which will be valuable in designing future experiments. Figure 41 shows about 9 hours of velocity profiles at one station in Caminada Pass. Unfortunately, the data do not extend for a complete tidal cycle, so the vertical distribution of the time-averaged net flow cannot be obtained. Note that at 1530 the tidal current turns earliest near the bottom. This phase priming with depth is due to the presence of frictional forces in the momentum balance. The secondary increase in upchannel speeds after 1530 might be due either to wind effects or a lesser tidal harmonic but does point out the necessity of monitoring the surface wind stress to calculate the eddy stress profile in the channel. Simultaneous salinity profiles are given in Fig. 42. Walters and Hernandez (1971) note that the steepest salinity gradients occur with the largest current amplitudes and that isohaline conditions are approached as the current slackens and moves toward the time of reversal. Hughes (1958) and Murray et al. (1975) report minimum stratification occurring with the maximum current speed in the Mersey Estuary, which is of course to be expected if the energy for vertical mixing is derived from the mean current. With this contradiction in hand the Caminada Pass results deserve further attention. The depth-averaged values of velocity and salinity are plotted against time for the set of observations in Fig. 43. Note that the mean salinity begins to drop very close to the time that the current turns from flood to ebb and, although it is difficult to estimate from less than half a cycle, there does appear to be a considerable net flow of water and salt out of the channel during this period.

An unpublished report by Marmer (1948) gives some data on current measurements in the four major passes of the Barataria Bay complex (Caminada, Barataria, Quatre Bayous, and Abel passes). Figure 44 shows the current speed in knots at a station inside Barataria Pass. Surprisingly there seems to be very little phase shift with depth in the currents and the uniformity of the tidal current speeds with depth lends

support to the two-dimensional model of Hacker (1973). Note the 3-4 hour phase shift between currents and tide height, which means the simple assumption used by Marmer that  $\bar{u} \bar{A} = Q$ , the new discharge, is invalid, as shown by Pritchard (1958), where  $\bar{u}$  is the average current speed and  $\bar{A}$  is the average cross-sectional area. Nonetheless, from the current meter data in the passes Marmer calculates a net discharge over a tidal period of  $449 \times 10^6 \text{ ft}^3$ , which is equivalent to about  $5,000 \text{ ft}^3/\text{sec}$  or five times the value suggested by Gagliano et al. (1969) using hydrologic data. The agreement is actually quite encouraging considering the 20-year difference in the studies and especially since Marmer's results represent only a 2-week interval. The major deficiency in Marmer's study from a modern point of view is his failure to consider the salinity and temperature structure, important not only from the dynamical aspect but also for the mechanics controlling the salt balance and hence biological productivity. Apparently no data is available on the dynamics in the Mermentau River mouth, the Pearl River mouth, or the Sabine and Calcasieu passes, although Barrett's (1971) data (plotted on Fig. 1) indicate very interesting mixing problems exist in the channels and the lower parts of the lakes.

The last topic to be considered in this survey concerns the wetlands circulation; that is, the flow of water and salt through the innumerable interconnecting channels, canals, and small lakes that make up the swamps and marshes. These smaller water conduits are truly the "blood vessels" of the marshlands. In the one such study to my knowledge in Louisiana, Kjerfve (1971) made repeated measurements over 8 days in June 1971 of water velocity, salinity, and local meteorology in the marshlands southwest of Caminada Bay. The time-averaged volume flow and isohalines he found from this period are shown in Fig. 45. It is apparent from the figure that a considerable net flow of water is entering the study area from the north via Bayou Ferblanc. Thus a considerable amount of bayward salt flux must be associated with the new freshwater discharge in order to balance turbulent flux of salt implied by the significant horizontal salinity gradient shown in Fig. 45. Using Pritchard's technique for estimating renewal time, Kjerfve found the water in the study area reaches a 50 percent renewal level in about twelve tidal cycles. Although modest in scale, this study

points out that systematic observations can lead to a reasonable understanding in this complicated regime of interconnecting channels and lakes.

#### SUMMARY AND RECOMMENDATIONS

A review of our knowledge of circulation and currents in the coastal water of Louisiana indicates that, although some notable progress has been made in certain areas, there are considerable segments of the coast for which we lack even the most rudimentary knowledge.

The salt wedge type of estuary in the passes of the Mississippi River is generally understood with regard to wedge geometry and dependence on river stage, but definitive knowledge of the salt balance requires further attention. The effluent plumes from the Mississippi mouths, long considered to be controlled by turbulent mixing, have recently been the subject of intense study and now appear to be heavily dependent on the densimetric Froude number and the principles of buoyant plume expansion. Detailed studies on how steps in temperature and salinity control mixing in this region are now in order.

With respect to the open coastal or shelf waters, recent studies dealing with the Louisiana superport and the Offshore Ecology Investigation of the Gulf Universities Research Corporation have laid a firm basic framework of knowledge of the shelf waters from the Mississippi delta to Timbalier Bay. The roles of tidal currents, density stratification, local wind drift, and regional currents have been identified if not completely understood. There seems to be nearly complete ignorance of the shelf waters west of Timbalier Bay, except that we expect a westerly drift to prevail in all seasons but summer. The reason for the summer reversals remain unclear. High tidal range in the west may have an importance previously unanticipated.

Our detailed knowledge of the dynamics of our prolific coastal bays and estuaries is embarrassingly poor. Salinity distributions and water levels have been examined repeatedly, but details of the momentum, heat, and salt balances have not been ascertained. Numerical modeling perhaps offers a shortcut to achieving this understanding, but such studies will be possible only after the controlling forces are better defined and parameterized by systematic dynamically oriented field studies.

Chandeleur-Breton Sound, which comprises the bulk of Louisiana water east of the Mississippi delta, is poorly known dynamically. A recent numerical study of this area has suggested a number of possibly important aspects of the circulation pattern, such as a net southward flow driven by a differential in the tide ranges at the entrances, and the role of northers in driving a net circulation. Such results need field verification before further extension of this approach to more complicated applications.

The tidal passes and minor river mouths have been subject to a few sporadic measurement campaigns, but definitive studies of salt, heat, and momentum flux in the important channels remain to be performed. In the wetlands proper, one study has suggested a possible approach to understanding the circulation and salinity balance in the tortuous channels and small lakes that make up this complicated but extremely valuable division of the coastal waters.

I would rank the needs for these studies as follows:

- 1) A study to determine the current pattern and mixing characteristics relative to recycling bay waters of the coastal boundary layer, a zone of brackish, highly turbid water. This prism of water extends along the whole coast in a belt about 15 km wide and is usually within the 10-m depth contour.
- 2) A detailed study within a major estuarine bay of the momentum and salt balances designed to contrast winter and summer conditions and input into numerical models.
- 3) A similar study within the confines of one of the important estuarine passes.
- 4) A background study of the hydrography and circulation patterns along the western Louisiana shelf, giving special emphasis to the high-tide zone near Calcasieu Pass.
- 5) A modest field program in Chandeleur-Breton Sound to test the applicability of the existing two-dimensional numerical model.
- 6) Detailed studies of the mechanics of mixing of the Mississippi River effluent with Gulf water that results in the formation of the Louisiana coastal water.
- 7) Detailed studies of the salt and momentum balance in a Mississippi River salt wedge channel.
- 8) An exploratory study to delineate the zone of mixing and the problems associated with the

mixing process of the discharge of the Atchafalaya River.

- 9) A study of the internal tides and tidal currents in stratified waters, unsolved problems typically associated with the Louisiana shelf.

#### LITERATURE CITED

- Barrett, B. 1971. Cooperative Gulf of Mexico estuarine inventory and study, Louisiana. Phase II, Hydrology, and Phase III, Sedimentology. Louisiana Wildlife and Fisheries Commission, New Orleans.
- Bondar, C. 1970. Considerations théoriques sur la dispersion d'un courant liquide de densité reduite et à niveau libre, dans un bassin contenant un liquide d'une plus grande densité. Symposium on the Hydrology of Deltas, UNESCO, vol. 11, pp. 246-256.
- Brower, W., J. Meserve, and R. Quayle. 1972. Environmental guide for the U.S. Gulf coast. National Climatic Center, National Oceanic and Atmospheric Admin., AD 758 455.
- Dyer, K. R. 1974. The salt balance in stratified estuaries. Estuarine and Coastal Marine Science 2(3):273-281.
- Gagliano, S. M., H. Kwon, and J. L. van Beek. 1969. Salinity and temperature atlas of Louisiana estuaries. Prepared for U.S. Army Corps of Engineers, New Orleans District, by Louisiana State University Center for Wetland Resources (unpublished ms.).
- Groves, G. W. 1955. Numerical filtering against tidal periodicities. Trans. Amer. Geophys. Union 36(6):1073-1084.
- Hacker, S. 1973. Transport phenomena in estuaries. Ph.D. diss., Louisiana State University, Baton Rouge.
- Harper, J. R. 1974. Nearshore oceanography, Technical Appendix IV of Environmental Assessment of a Louisiana Offshore Oil Port and Appertinent Pipeline and Storage Facilities, prepared for Louisiana Offshore Oil Port, Inc., by Louisiana State University, Center for Wetland Resources, Baton Rouge (unpublished manuscript).
- Hart, W. E. 1975. A numerical study of current velocities and water levels in Louisiana's Chandeleur-Breton Sound. Preliminary draft, Ph.D. diss., Louisiana State University, Baton Rouge.

- Hill, G. W., L. E. Garrison, and R. F. Hunter. 1976. Drift patterns along the north-central Texas coast, 1973-1974. Preliminary report, U.S. Geol. Survey, Corpus Christi, Texas. Misc. field study.
- Hsu, S. A. 1970. Coastal air-circulation system: observations and empirical model. *Monthly Weather Review* 98(7):487-509.
- Hughes, P. 1958. Tidal mixing in the narrows of the Mersey Estuary. *Geophys. J. Royal Astronomical Soc.* 1(4):271-283.
- Kimsey, J., and R. Temple. 1962. Currents on the continental shelf of the northwestern Gulf of Mexico. Annual Rep. Fiscal Year 1962, Fishery Res. Biol. Lab., Galveston, Tex., pp. 23-27.
- \_\_\_\_\_. 1963. Currents on the continental shelf of the northwestern Gulf of Mexico. Annual Rep. Fiscal Year 1963, Fishery Res. Biol. Lab., Galveston, Tex., pp. 25-27.
- Kjerfve, B. J. 1971. A field study of the physical oceanography of the Airplane Lake, Lake Palourde, and Lake Laurier area of coastal Louisiana. Louisiana State University, Coastal Studies Institute, Baton Rouge, 31 pp. (unpublished manuscript).
- \_\_\_\_\_. 1973. Dynamics of the water surface in a bar-built estuary. Ph.D. diss., Louisiana State University, Baton Rouge. 90 pp.
- \_\_\_\_\_. 1975. Tide and fair-weather wind effects in a bar-built Louisiana estuary. Pages 345-363 in L. E. Cronin, ed., *Estuarine Research. Geology and Engineering*, vol. 2. Academic Press, New York.
- Leendertsee, J. 1967. Aspects of a computational model for long-period wave propagation. Rand Corp., Santa Monica, CA., Memo RM-5294-PR.
- Marmer, H. 1948. The currents in Barataria Bay. Mimeographed. Texas A&M Research Foundation, Proj. 9, College Station.
- Murray, S. P. 1972a. Turbulent diffusion of oil in the ocean. *Limnol. and Oceanog.* 17:651-660.
- \_\_\_\_\_. 1972b. Observations on wind, tidal, and density driven circulation in the vicinity of the Mississippi River delta. Pages 127-142 in D. Swift, D. Duane, and O. Pilkey, eds., *Shelf Sediment Transport*. Dowden, Hutchinson, and Ross, Stroudsburg, Pa.
- \_\_\_\_\_. 1975a. Trajectories and speeds of wind-driven currents near the coast. *J. Phys. Oceanog.* 5(2):347-360.



- Murray, S. P. 1975b. Wind and current effects on large-scale oil slicks. Proc. Seventh Offshore Tech. Conf., Houston, Tex., 1975, Paper No. OTC 2389, pp. 523-535.
- \_\_\_\_\_, D. Conlon, A. Siripong, and J. Santoro. 1975. Circulation and salinity distribution in the Rio Guayas Estuary, Ecuador. Pages 345-363 in Estuarine Research, L. E. Cronin, ed., Geology and Engineering, vol. 2. Academic Press, New York.
- \_\_\_\_\_, and A. Siripong. 1973. Salt flux and velocity sections in the Rio Guayas Estuary, Ecuador (abstract). Trans. Amer. Geophys. Union 54:1123.
- \_\_\_\_\_, W. G. Smith, and C. J. Sonu. 1970. Oceanographic observations and theoretical analysis of oil slicks during the Chevron spill, March 1970. Louisiana State University, Coastal Studies Institute Tech. Rep. 87, 106 pp.
- National Oceanic and Atmospheric Administration. 1975. Tide tables, east coast of North and South America. Ocean Survey, Rockville, MD.
- Oetking, P., P. Back, R. Watson, and C. Merks. 1974a. Currents on the nearshore continental shelf of south-central Louisiana. Final Rep., Southwest Res. Inst., Corpus Christi, Tex.
- \_\_\_\_\_. 1974b. Hydrography of the nearshore continental shelf of south-central Louisiana. Final Rep., Southwest Res. Inst., Corpus Christi, Tex.
- Pritchard, D. W. 1952. Estuarine hydrography. Pages 243-280 in H. E. Landsberg, ed., Advances in Geophysics, vol. 1. Academic Press, New York.
- \_\_\_\_\_. 1955. Estuarine circulation patterns. Proc. Amer. Soc. Civil Engineers 81:1-11, Separate No. 717.
- \_\_\_\_\_. 1958. The equations of mass and salt continuity in estuaries. J. Marine Research 17:412-423.
- Sonu, C. J. 1972. Field observations of near-shore circulation and meandering currents. J. Geophys. Res. 77(18):3232-3247.
- \_\_\_\_\_, S. P. Murray, S. A. Hsu, J. N. Suhayda, and E. Waddell. 1973. Sea breeze and coastal processes. EOS Trans. Amer. Geophys. Union 54(9):820-833.
- Stommel, H., and G. H. Farmer. 1952. Abrupt changes in width in two-layer open channel flow. J. Marine Res. 11:205-214.

- Stone, J. H., W. Subra, and P. J. Minvielle, Jr. 1972. Surface circulation of Lake Pontchartrain: a wind-dominated system. Final Rep., Gulf South Res. Institute, Proj. NS-255, 122 pp.
- U.S. Army Corps of Engineers. 1959. Investigation and data collection for model study of Southwest Pass, Mississippi River. Vols. 1 and 2. U.S. Army Engineer District, New Orleans.
- Waldrop, W. R., and R. C. Farmer. 1974. Three-dimensional computation of buoyant plumes. *J. Geophys. Res.* 79(9):1269-1276.
- Walters, D., and M. Hernandez. 1971. Some physical measurements in the channel of Caminada Pass. *Barataria Gazette* 11:14-24. Louisiana State University, Dep. of Marine Sciences, Baton Rouge, LA, 70803.
- Wiseman, Wm. J., Jr., J. M. Bane, S. P. Murray, and M. W. Tubman. 1975a. Small-scale temperature and salinity structure over the inner shelf west of the Mississippi River delta. *Proc., Seventh Liege Colloquium on Ocean Hydrodynamics*, May 5-9, 1975, Liege, Belgium. (in press)
- \_\_\_\_\_, S. P. Murray, M. W. Tubman, and J. M. Bane. 1975b. Offshore physical oceanography. Technical Appendix III of *Environmental Assessment of a Louisiana Offshore Oil Port and Appertinent Pipeline and Storage Facilities*, vol. 2. Final Rep., prepared for Louisiana Offshore Oil Port, Inc., by Louisiana State University Wetland Resources, Baton Rouge (unpublished manuscript).
- Wright, L. D. 1970. Circulation, effluent diffusion, and sediment transport, mouth of South Pass, Mississippi River delta. Louisiana State University, Coastal Studies Institute Tech. Rep. 84, 56 pp.
- \_\_\_\_\_. 1971. Hydrography of South Pass, Mississippi River delta. *Proc., Amer. Soc. Civil Engineers, J. Waterways, Harbors and Coastal Engineering Div.* 97:491-504.
- \_\_\_\_\_ and J. M. Coleman. 1971. Effluent expansion and interfacial mixing in the presence of a salt wedge, Mississippi River delta. *J. Geophys. Res.* 76:8649-8661.
- \_\_\_\_\_. 1974. Mississippi River mouth processes: effluent dynamics and morphologic development. *J. Geol.* 82:751-778.
- \_\_\_\_\_, J. M. Coleman, and J. N. Suhayda. 1973. Periodicities in interfacial mixing. Louisiana State University, Coastal Studies Institute Bull. 7:127-135.

FIGURES

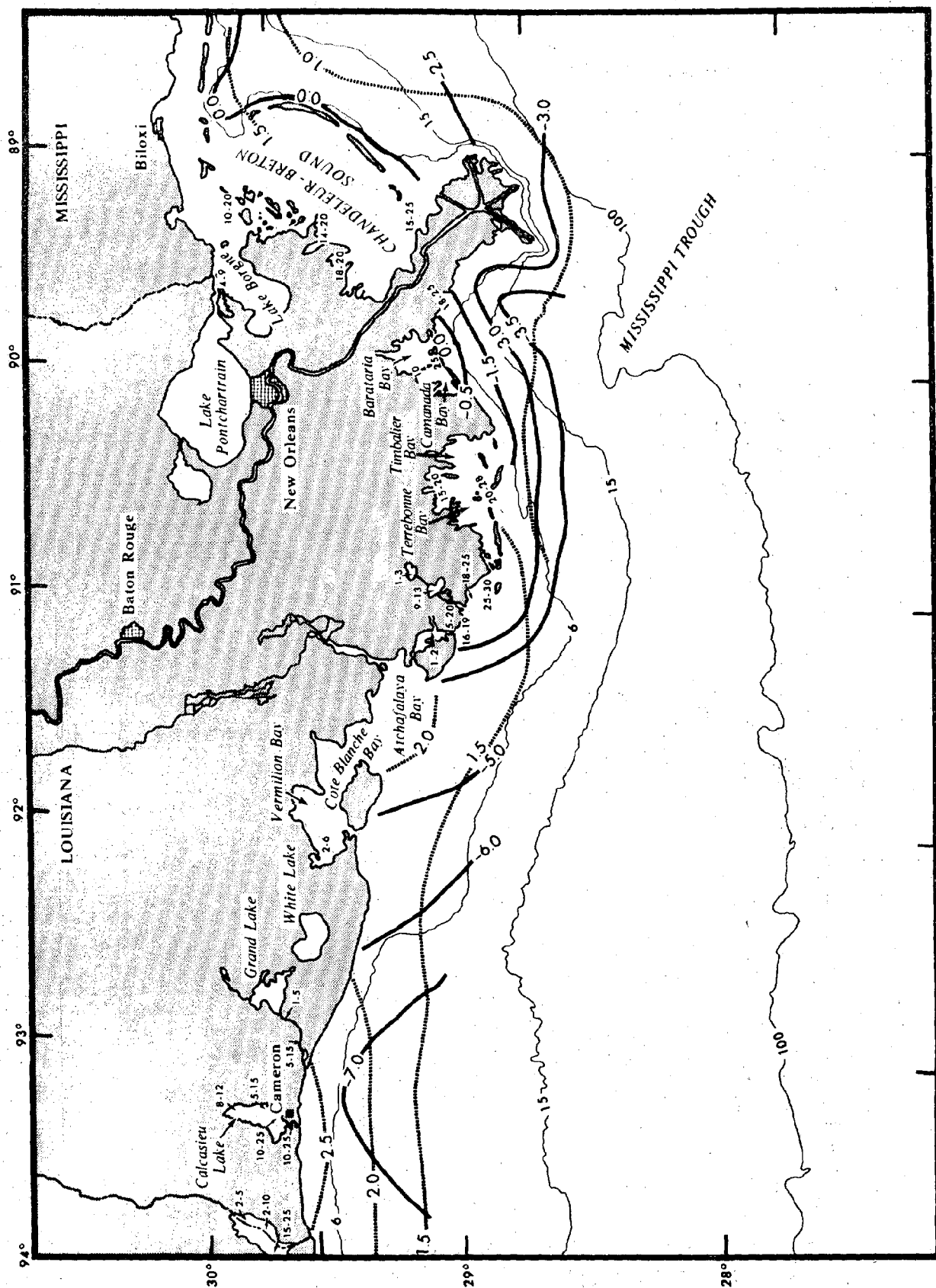
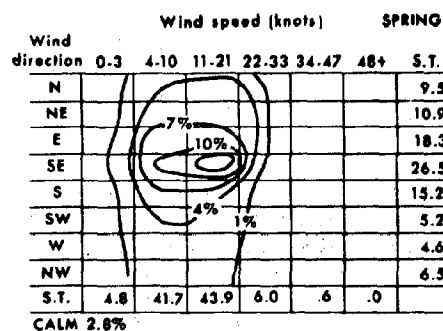
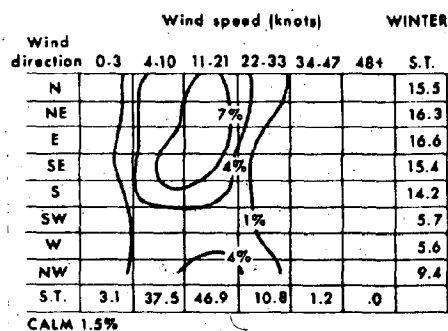
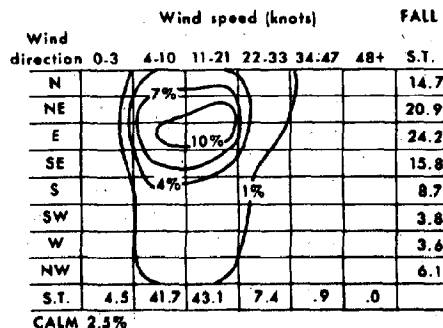
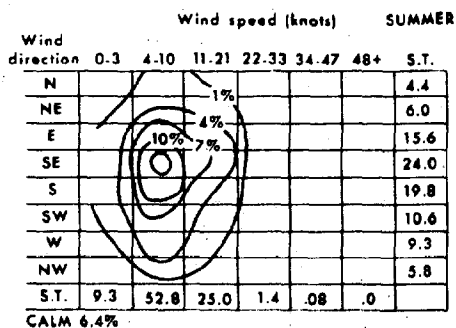


Figure 1. Location map of Louisiana coastal waters. Co-phase lines of the tide in hours before high water at Barataria Pass are shown as heavy solid lines. Co-range lines of the tide in feet are shown as dashed lines. Small numbers indicate observed salinity ranges (ppt) in bays and estuaries.

BAYOU LAFOURCHE



SABINE PASS

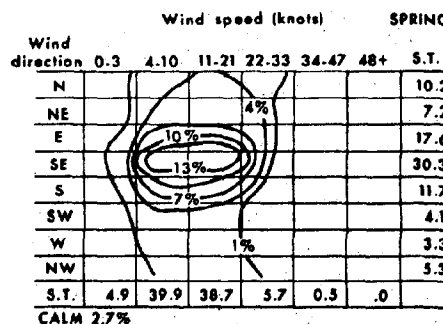
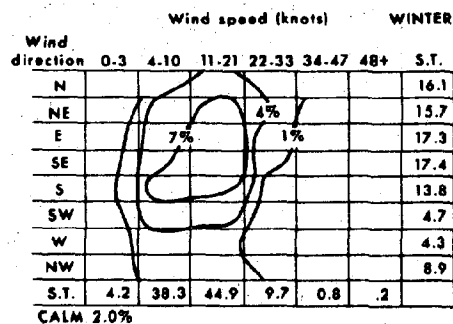
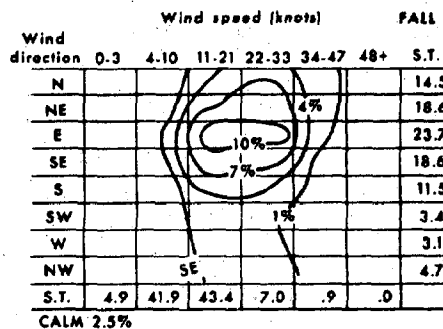
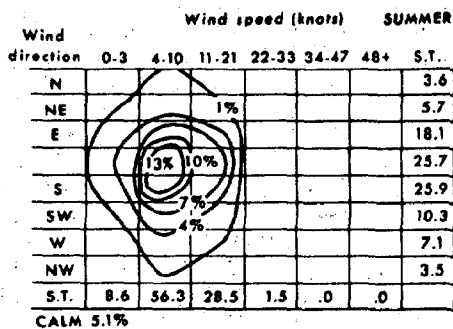


Figure 2. Bivariate frequency distributions of wind speed versus wind direction for the areas offshore from Bayou Lafourche (28°N to 30°N, 89°W to 92°W) and from Sabine Pass (28°N to 30°N, 92°W to 95°W). The percentage subtotals of occurrence are given in the margin.

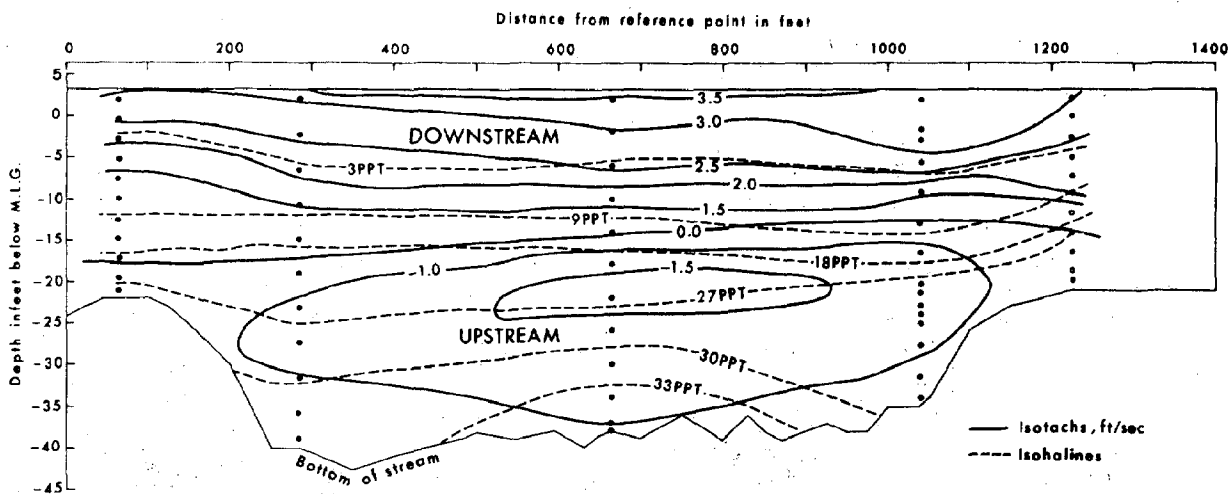


Figure 3. The distribution of current speed and salinity across a channel cross section located about 1,200 feet inside the end of the jetties of Southwest Pass (mile 19.92) on 27 January 1957. The solid dots are the data observation points given in U.S. Corps of Engineers (1959).

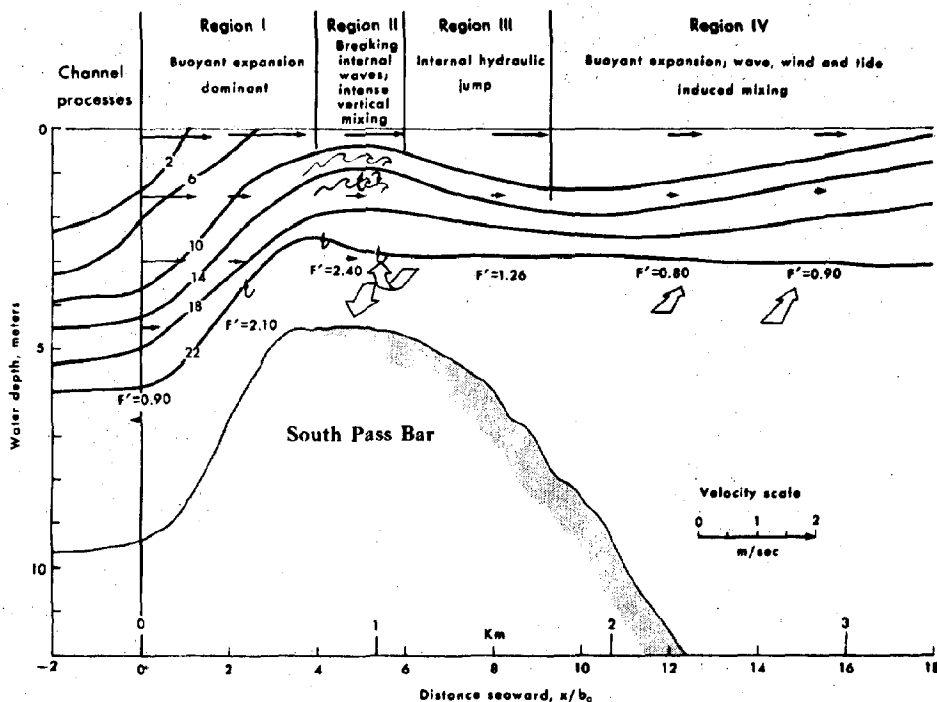


Figure 4. Cross section of the density (in  $\sigma_t$  units) and the velocity fields along the South Pass effluent plume on an ebbing tide during low river stage on 22 October 1969 showing the hydrodynamic regions identified by Wright and Coleman (1974).

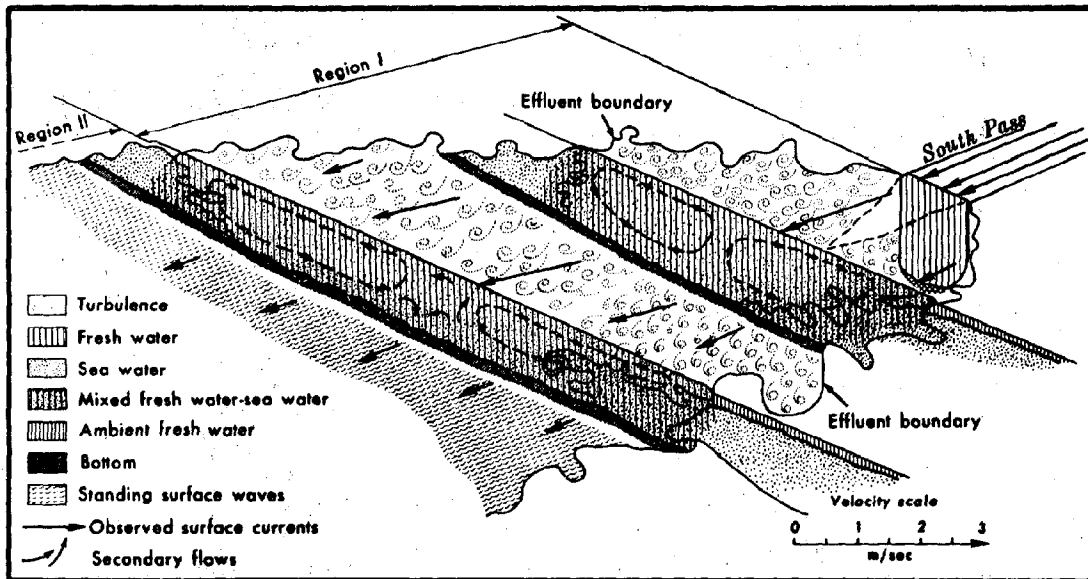


Figure 5. Three-dimensional model of the geometry of the velocity field in the South Pass effluent plume. After Wright and Coleman (1974).

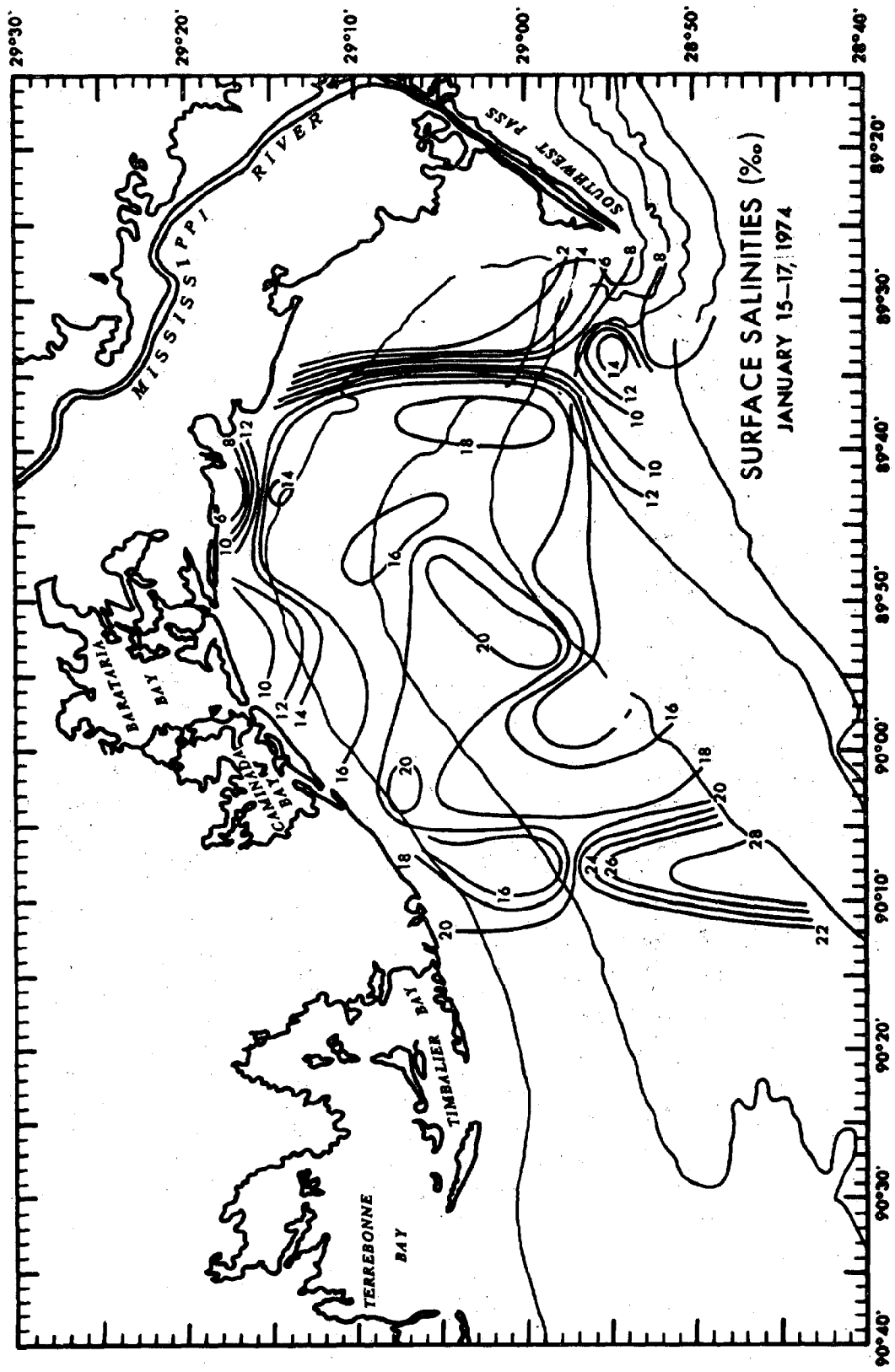


Figure 6. Surface salinities (ppt) in the bight west of the Mississippi delta.



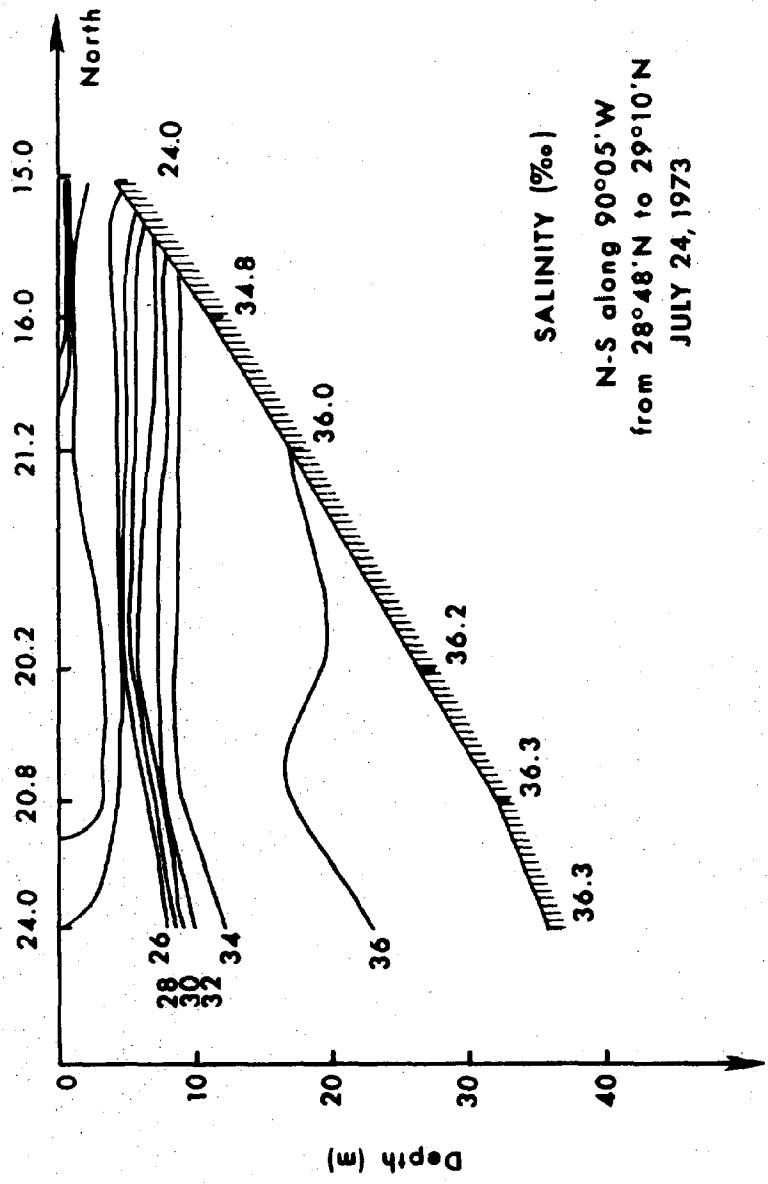


Figure 7. A cross-section of the salinity field near the western extremity of the LOOP study area.

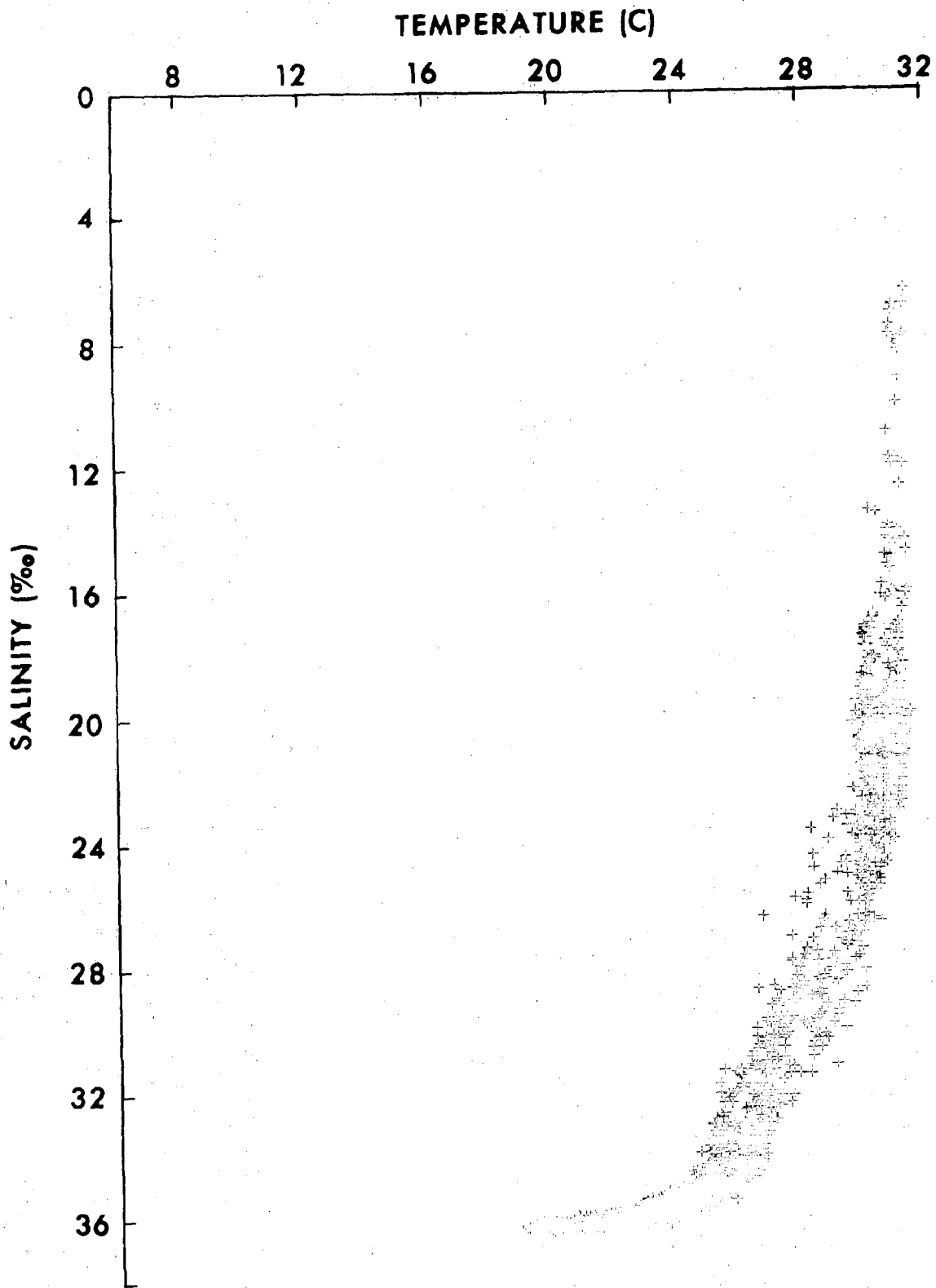


Figure 8. A temperature-salinity (T-S) diagram of the hydrographic data collected in September during the 1-year study in the bight west of the Mississippi delta. Note the continuous mixing of three separate water masses in the area.

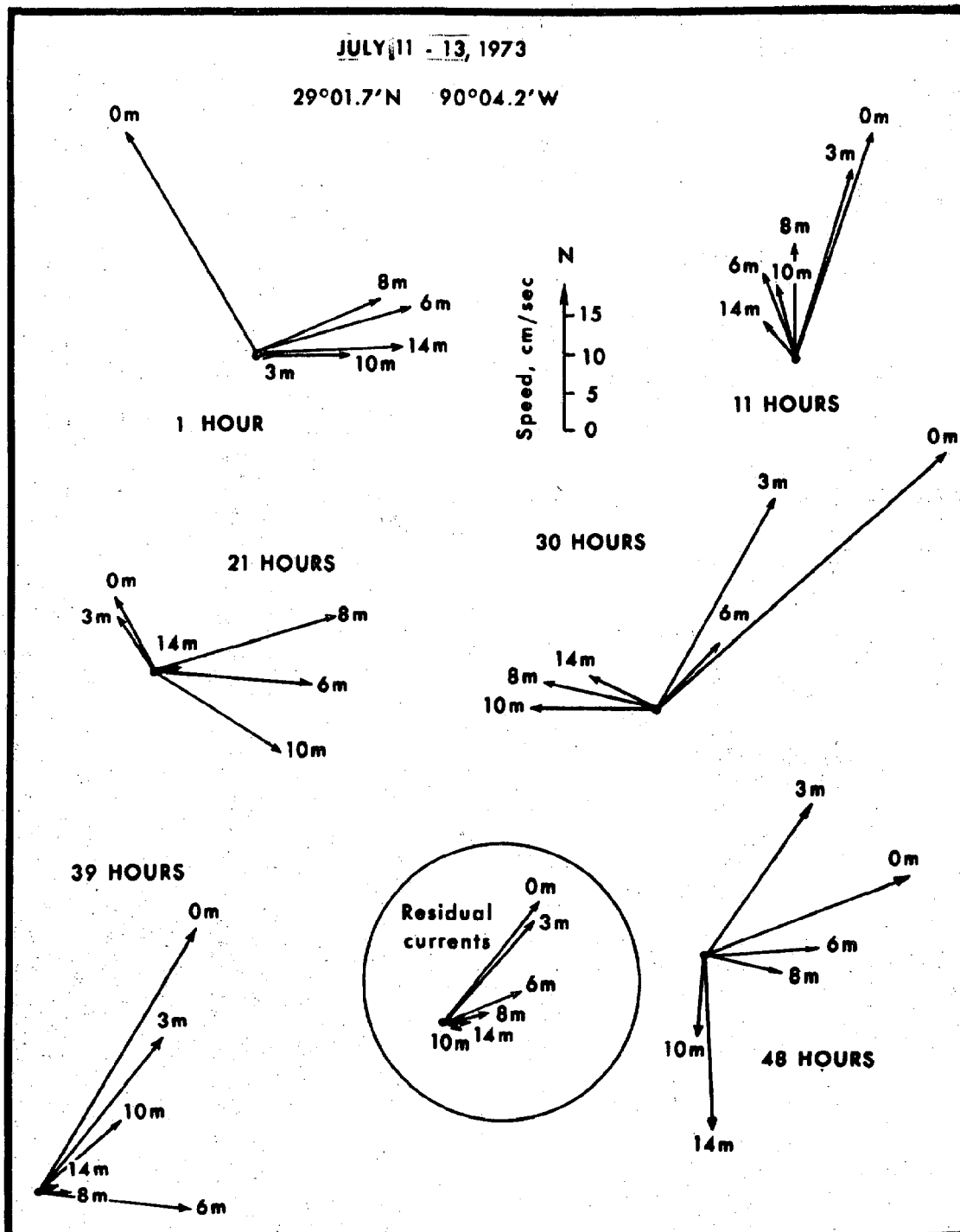


Figure 9. Observed and residual currents at various times during the 2 tidal day anchor station on 11-13 July 1973. The residual currents show the net current profile with tidal currents effectively averaged out.

7/11/73 - 7/13/73  
29° 1.7'N - 90° 4.7'W

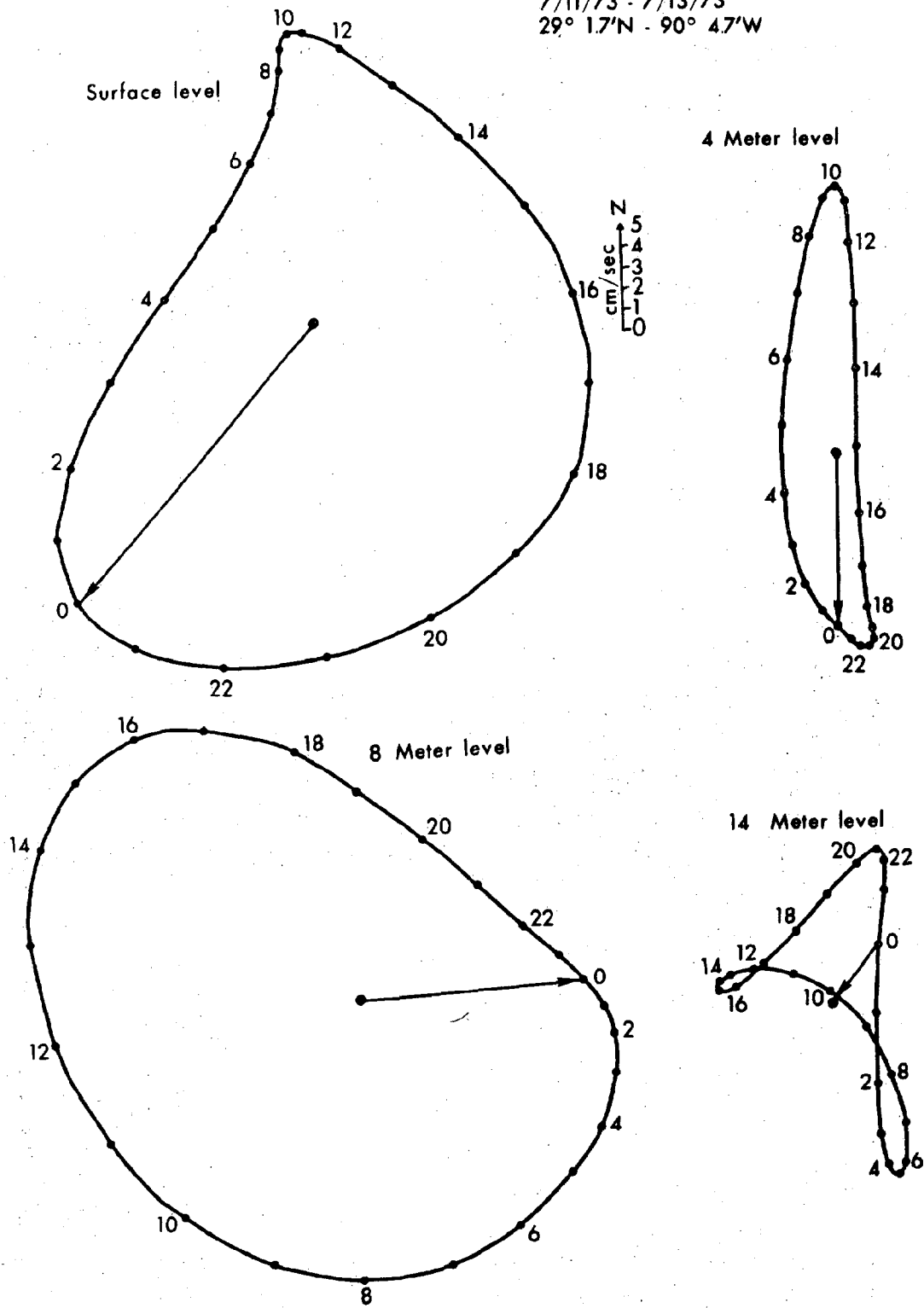


Figure 10. Tidal current hodographs at four depth levels from the anchor station of 11-13 July 1973.

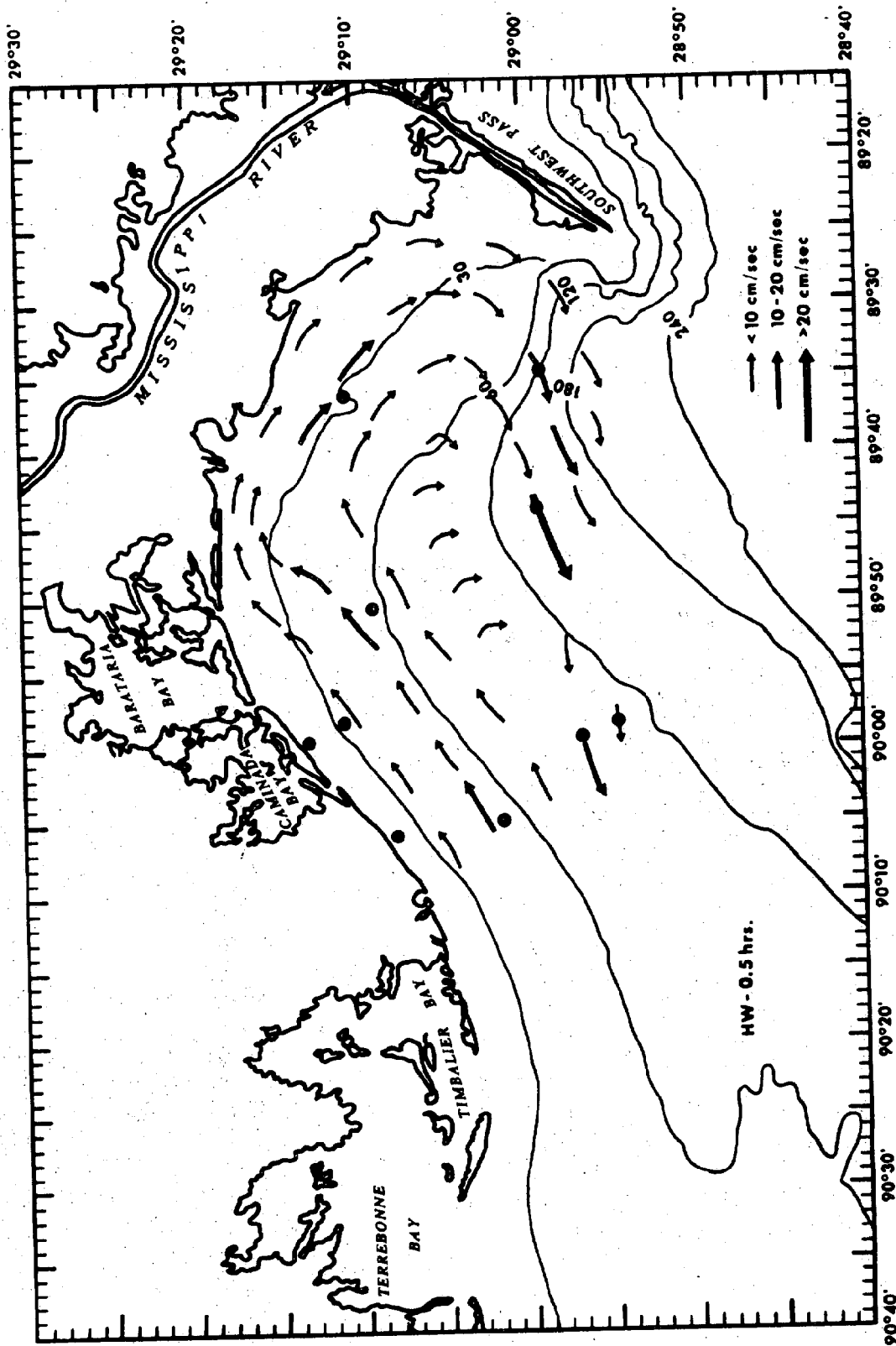


Figure 11. Tidal current velocity field in the waters below the pycnocline 0.5 hour before high water at Barataria Pass.

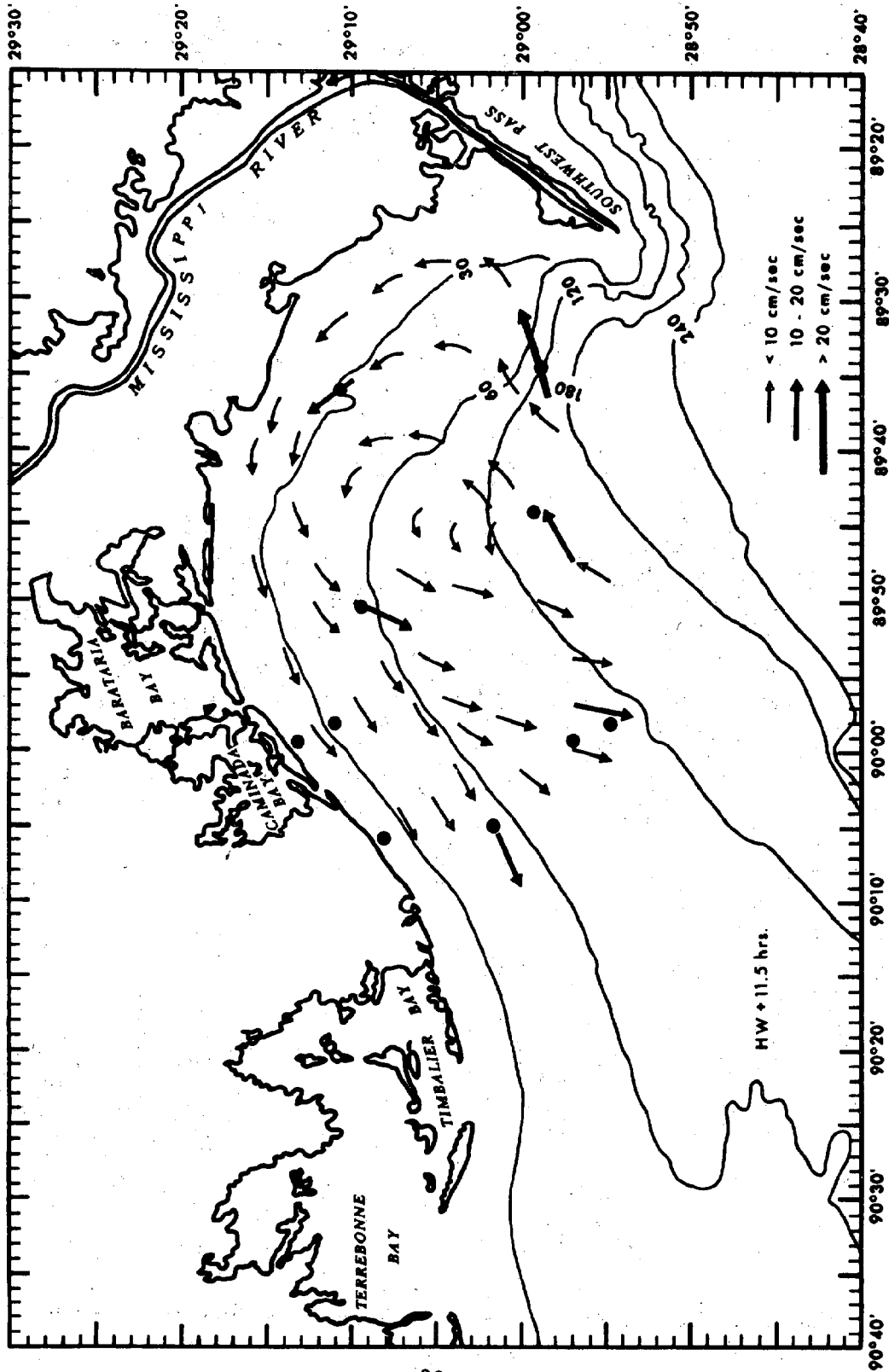


Figure 12. Tidal current velocity field in the waters below the pycnocline 11.5 hours after high water at Barataria Pass.

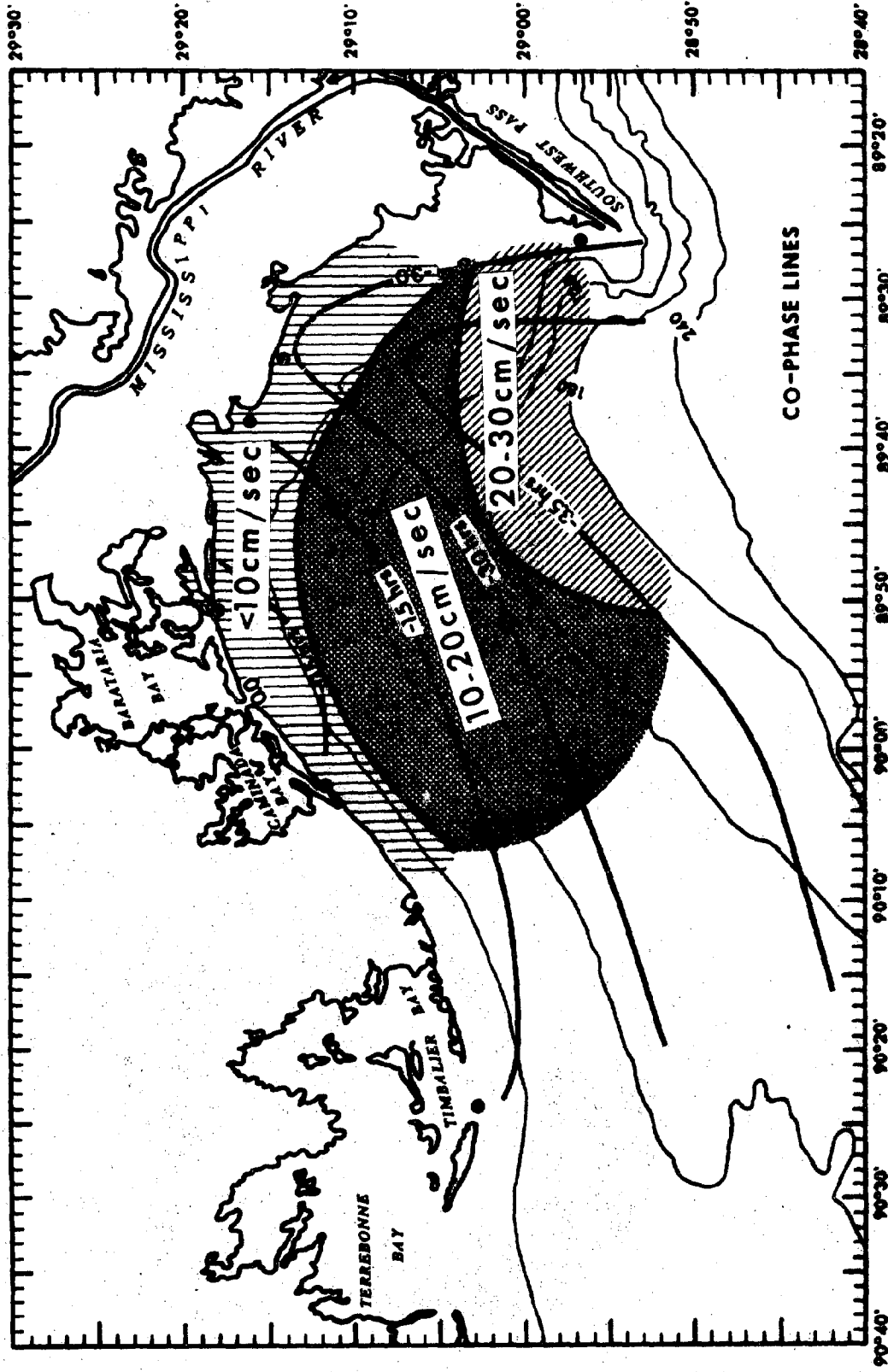


Figure 13. Distribution of tidal current amplitudes and co-phase line of the tide in hours before high water at Barataria Pass.

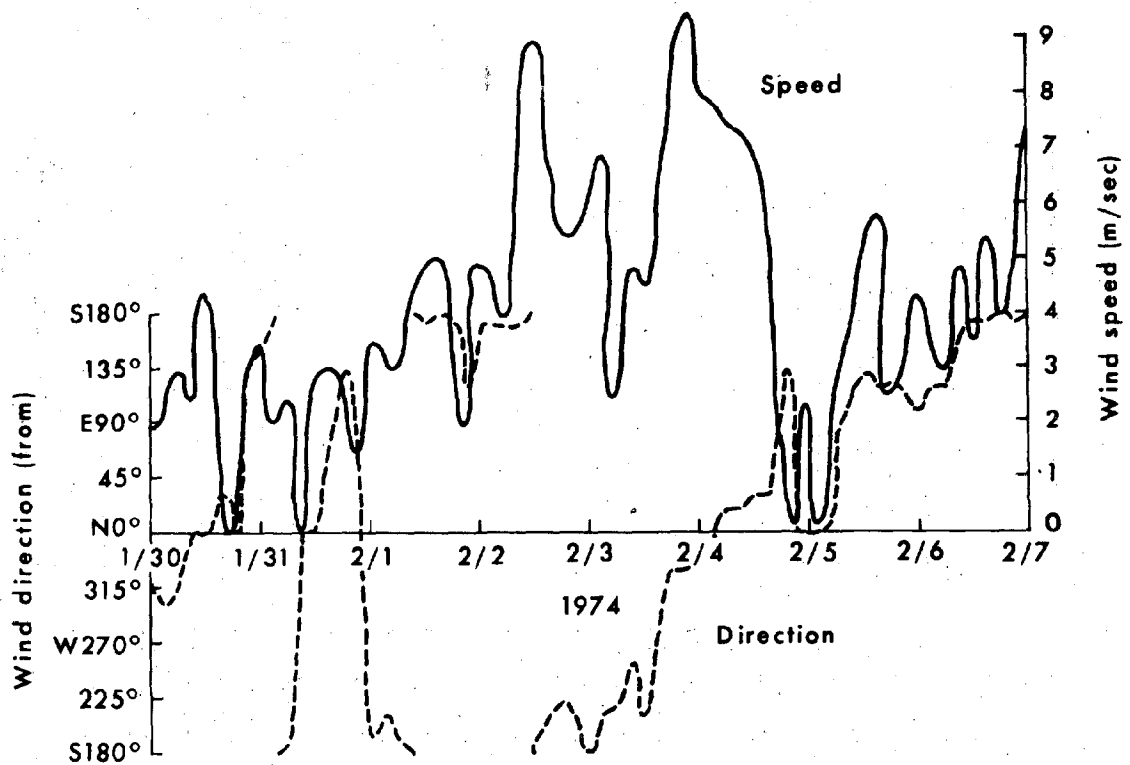
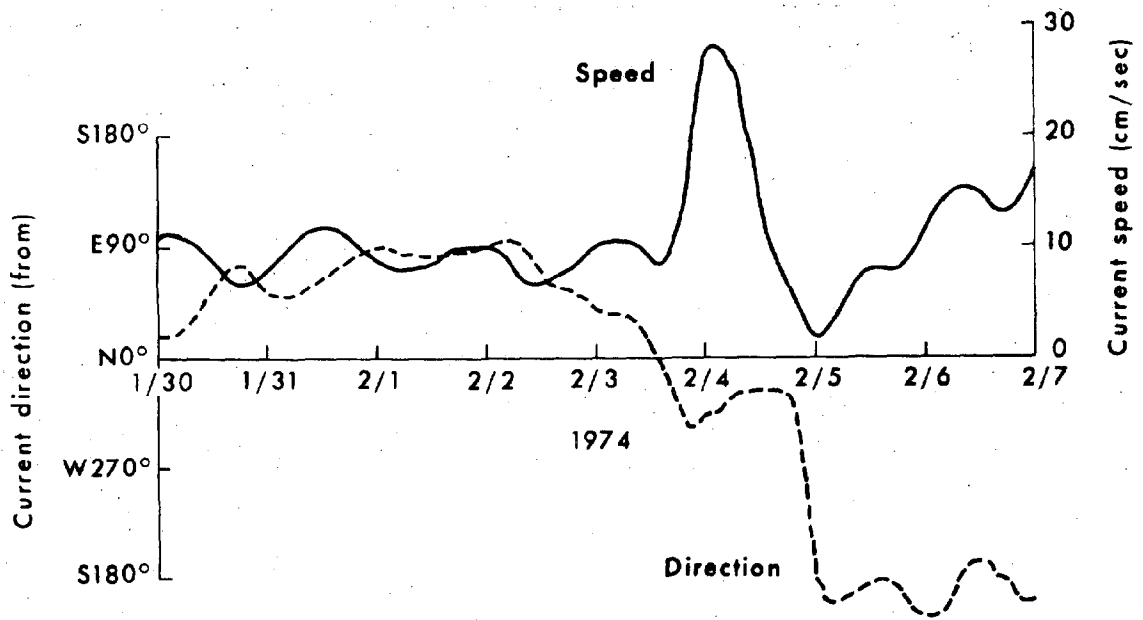


Figure 14. A comparison of current velocity from a current meter moored 6 m below the surface at the location of the black square in Figure 16 with the wind velocity at the Boothville station on the Mississippi River.



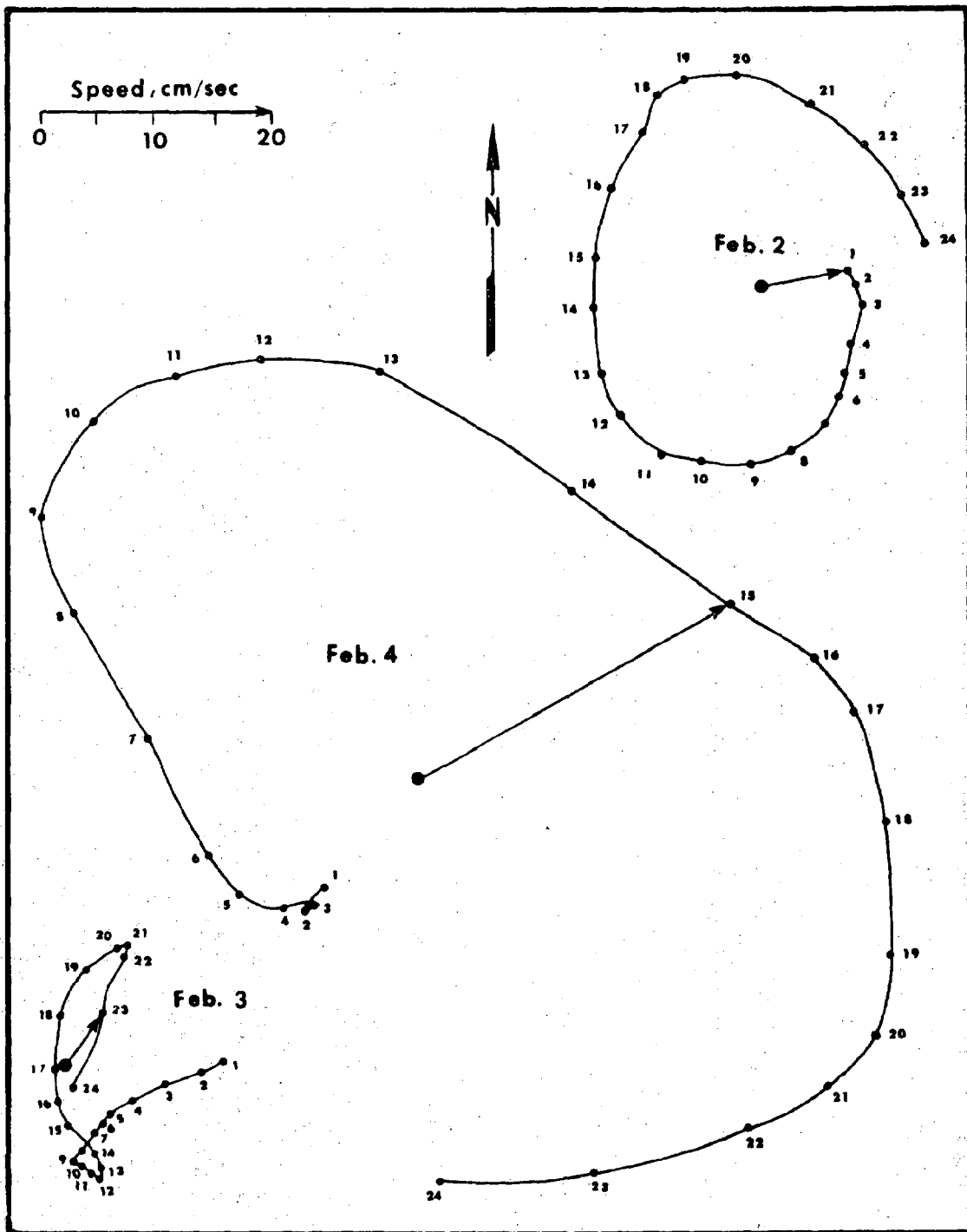


Figure 15. Tidal current hodographs at the 6-m depth level from continuously recording current meter moored at the black square shown in Figure 16.

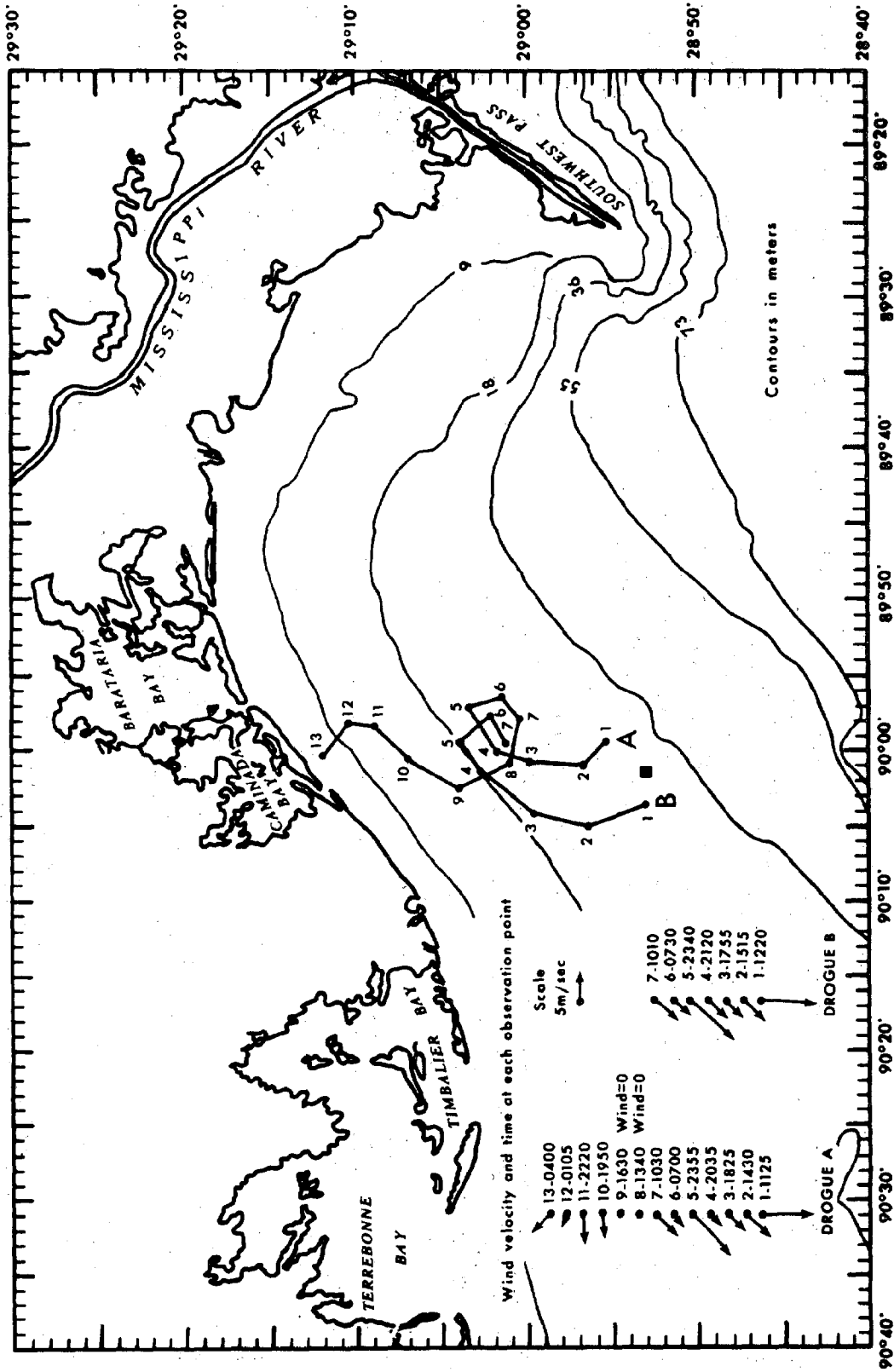


Figure 16. Tracks of drogues drifting at the 1-m depth level showing probable water entrainment into the Barataria-Caminada Bay complex. Drogues were tracked using radio direction-finding techniques during 13-15 March 1974.

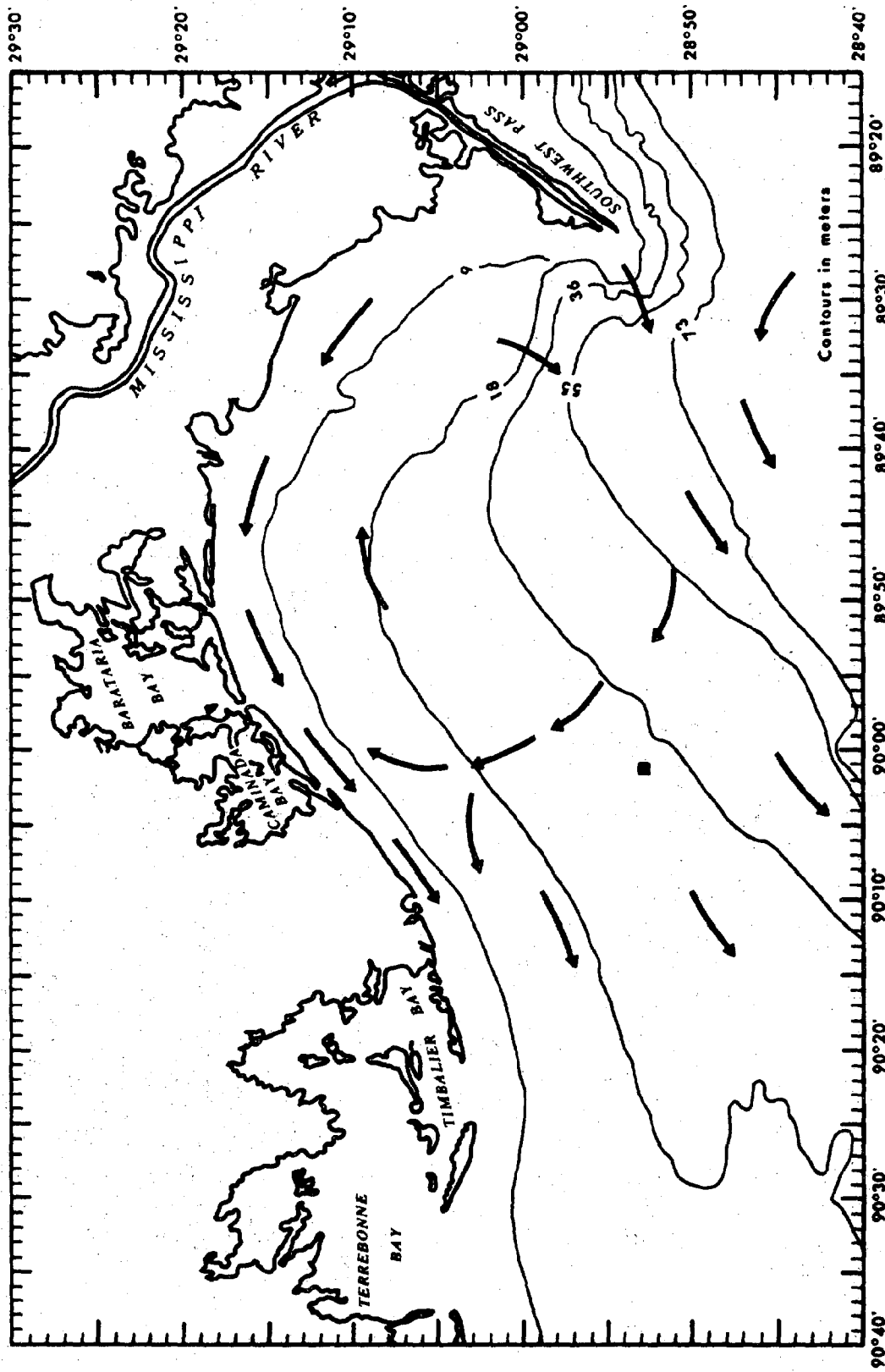


Figure 17. The basic geometry of the trapped vortex west of the Mississippi delta. The generally westward-setting, brackish, highly turbid coastal boundary layer is shown hugging the northern coast.

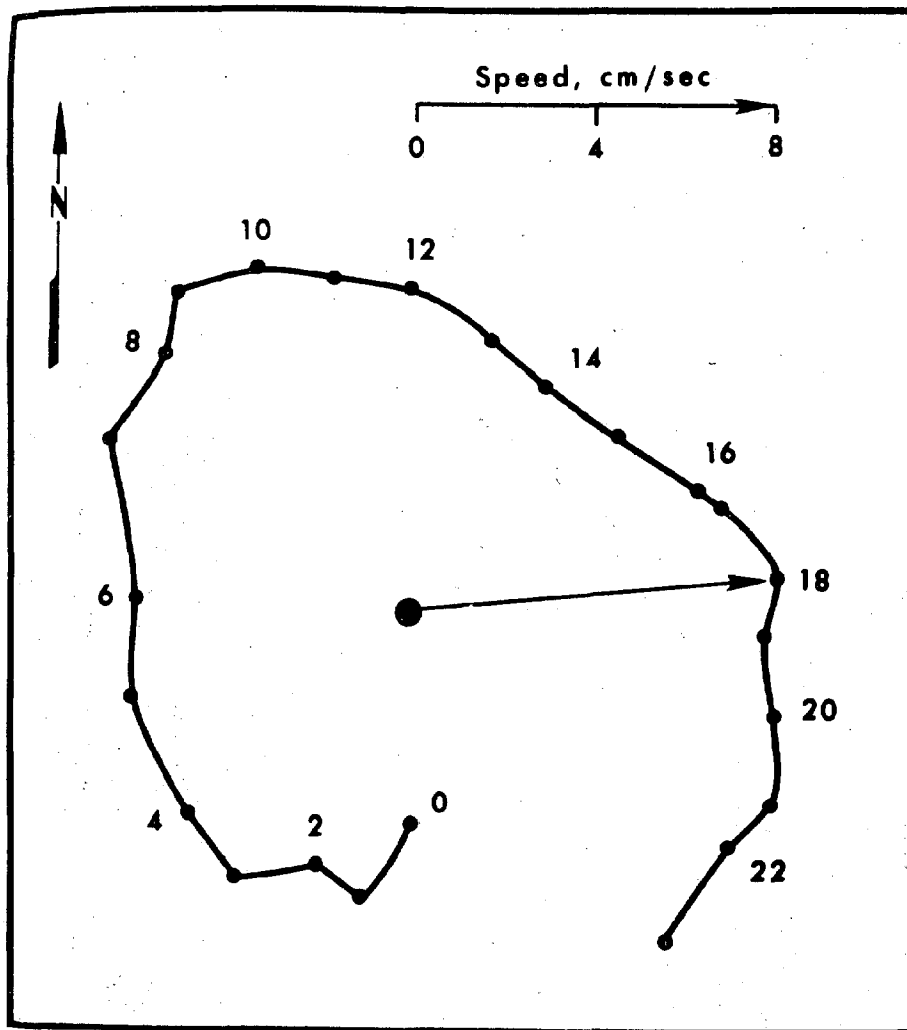


Figure 18. Tidal current hodograph from the GURC-OEI meter at 28°50'N, 90°23'W.

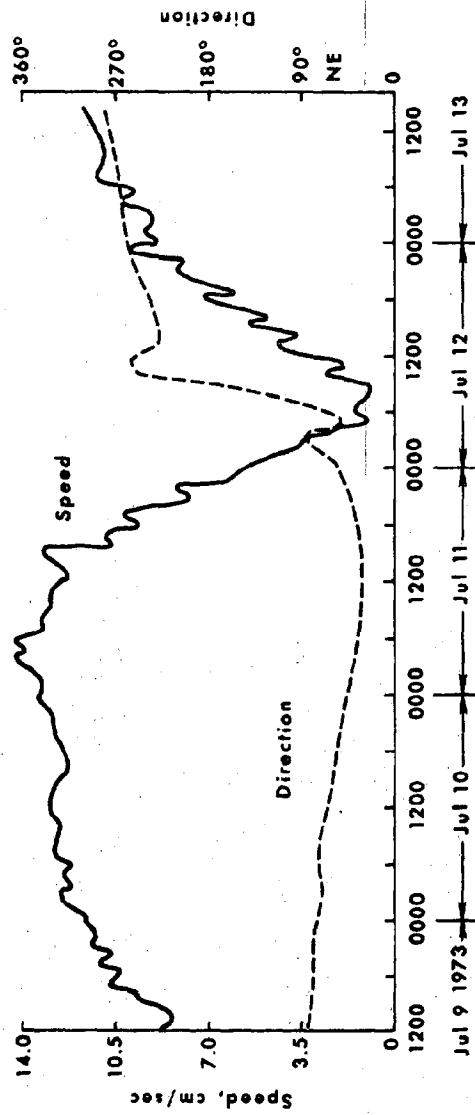


Figure 19. Long-term drift current from Doodson-Marburg filtering of data collected at 28°50'N, 90°23'W, by the Southwest Research Institute.

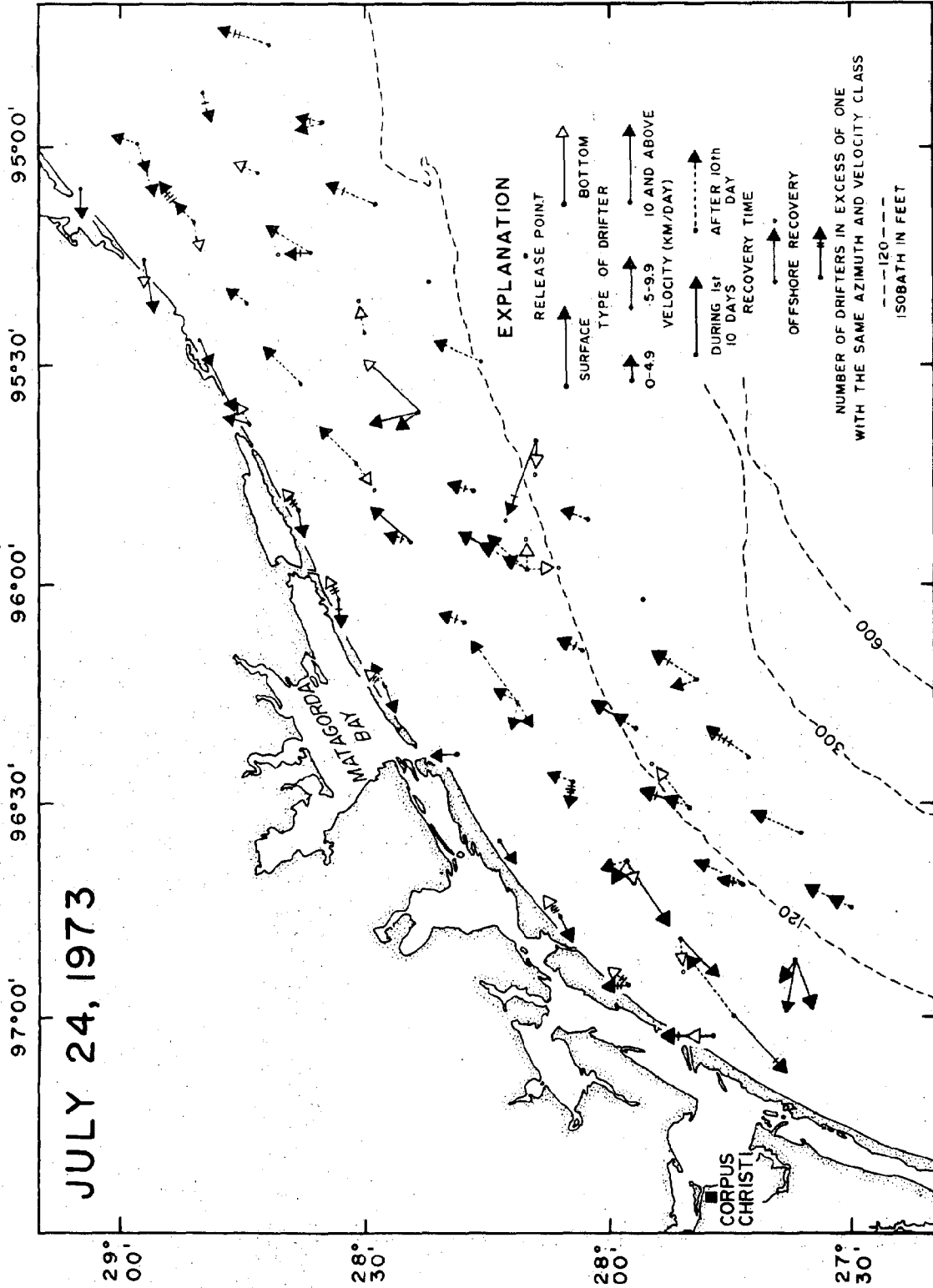


Figure 20. Example of summer northeasterly drift along the central Texas coast. From U.S. Geological Survey field studies.

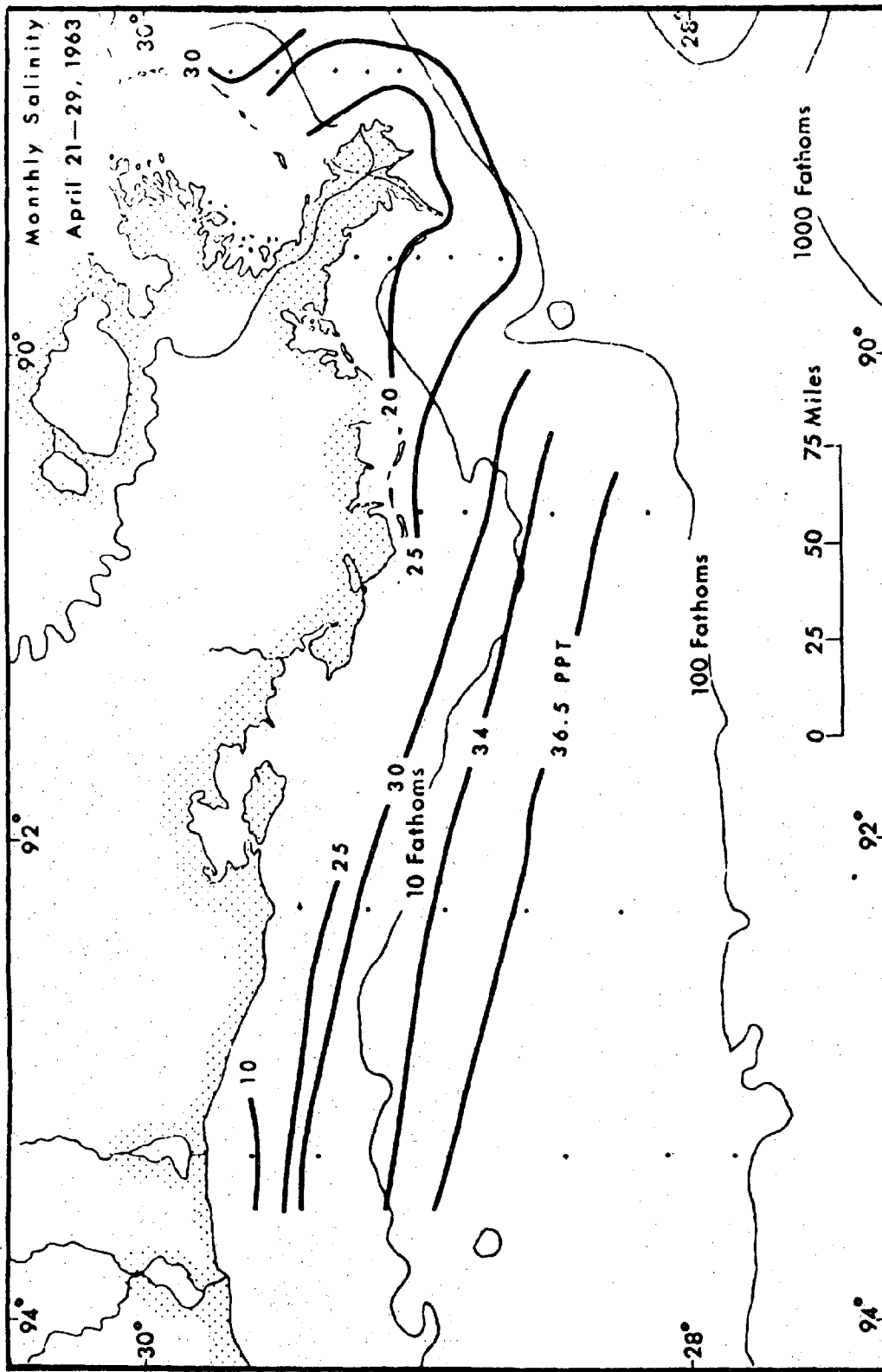


Figure 21. Surface salinity pattern along the Louisiana coast during high river season. From U.S. Bureau of Commercial Fisheries sources.

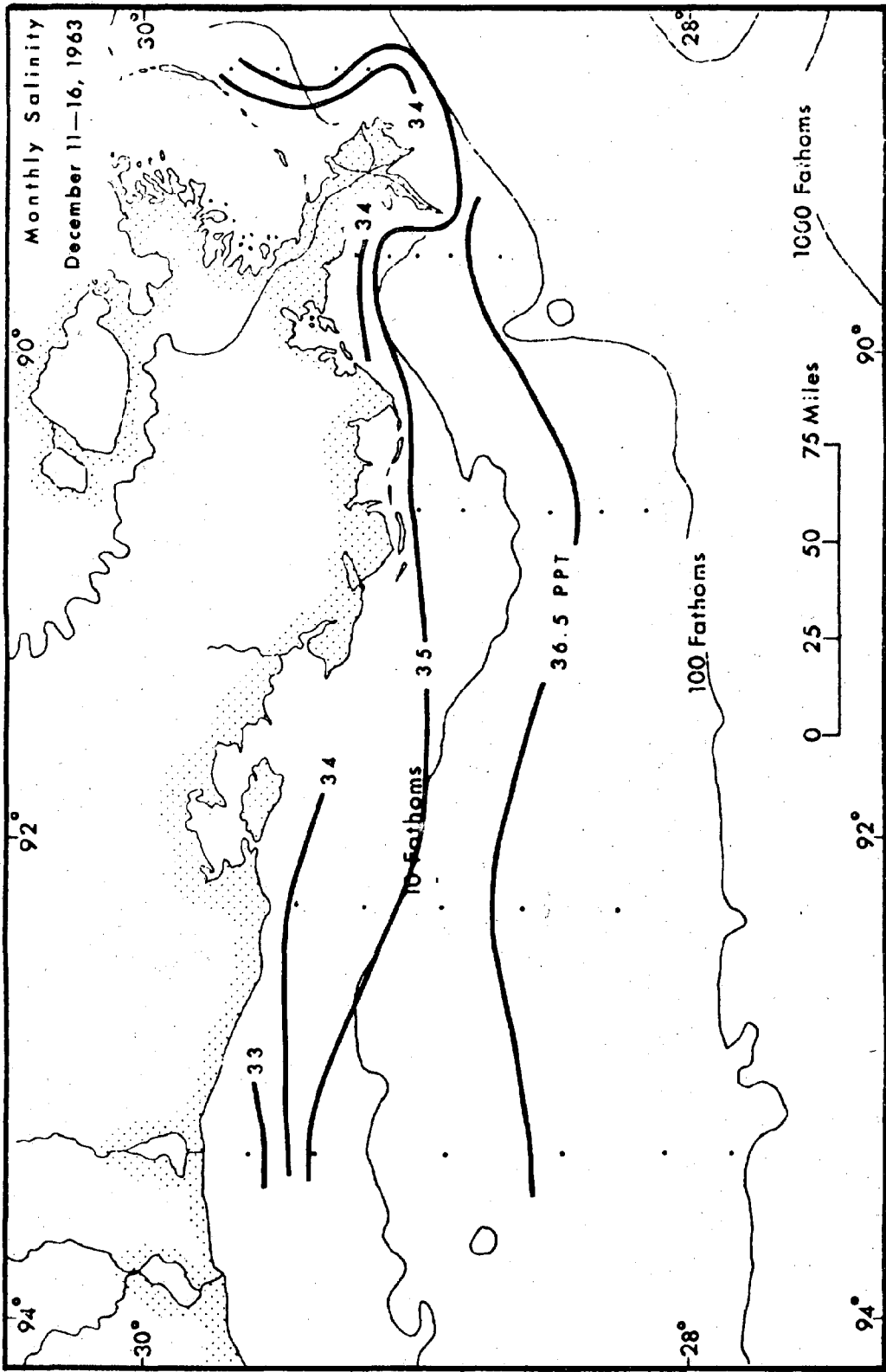


Figure 22. Surface salinity pattern along the Louisiana coast during low river season. From U.S. Bureau of Commercial Fisheries sources.



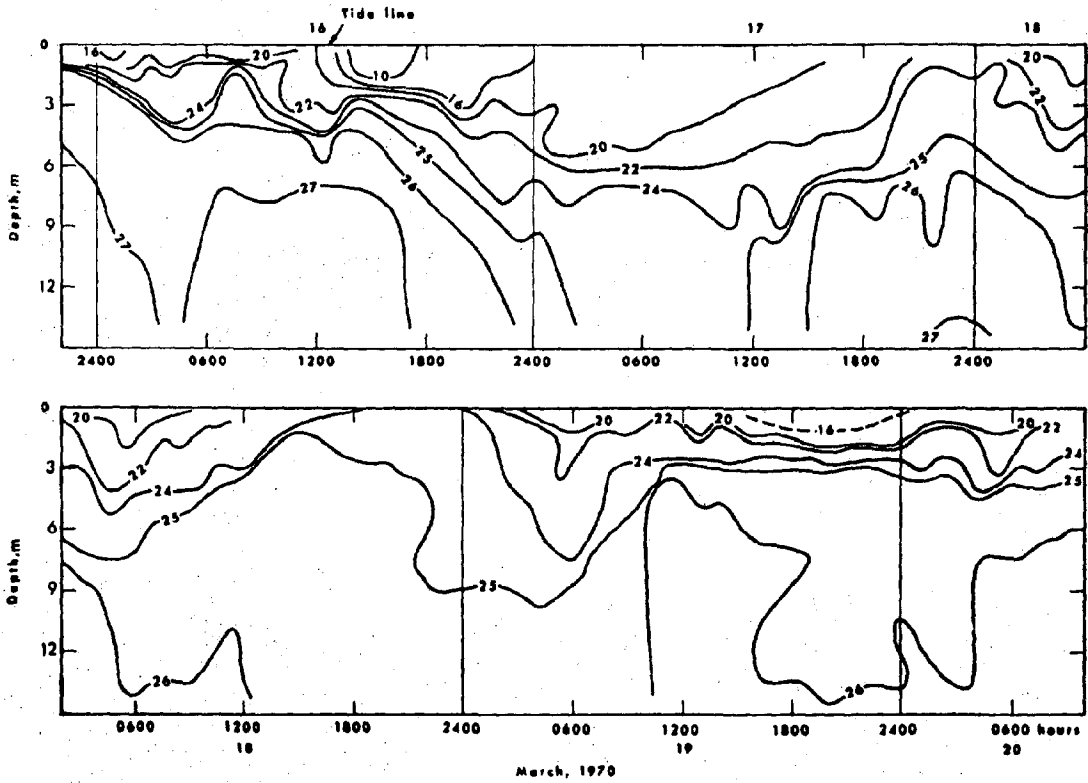


Figure 23. Time series plot of isopycnals (line of equal water density,  $\sigma_t$ ) 15 km east of the Mississippi delta at  $29^{\circ}23'N$ ,  $88^{\circ}58'W$ , showing the effects of strong onshore winds and their sudden dropoff on the local density field.

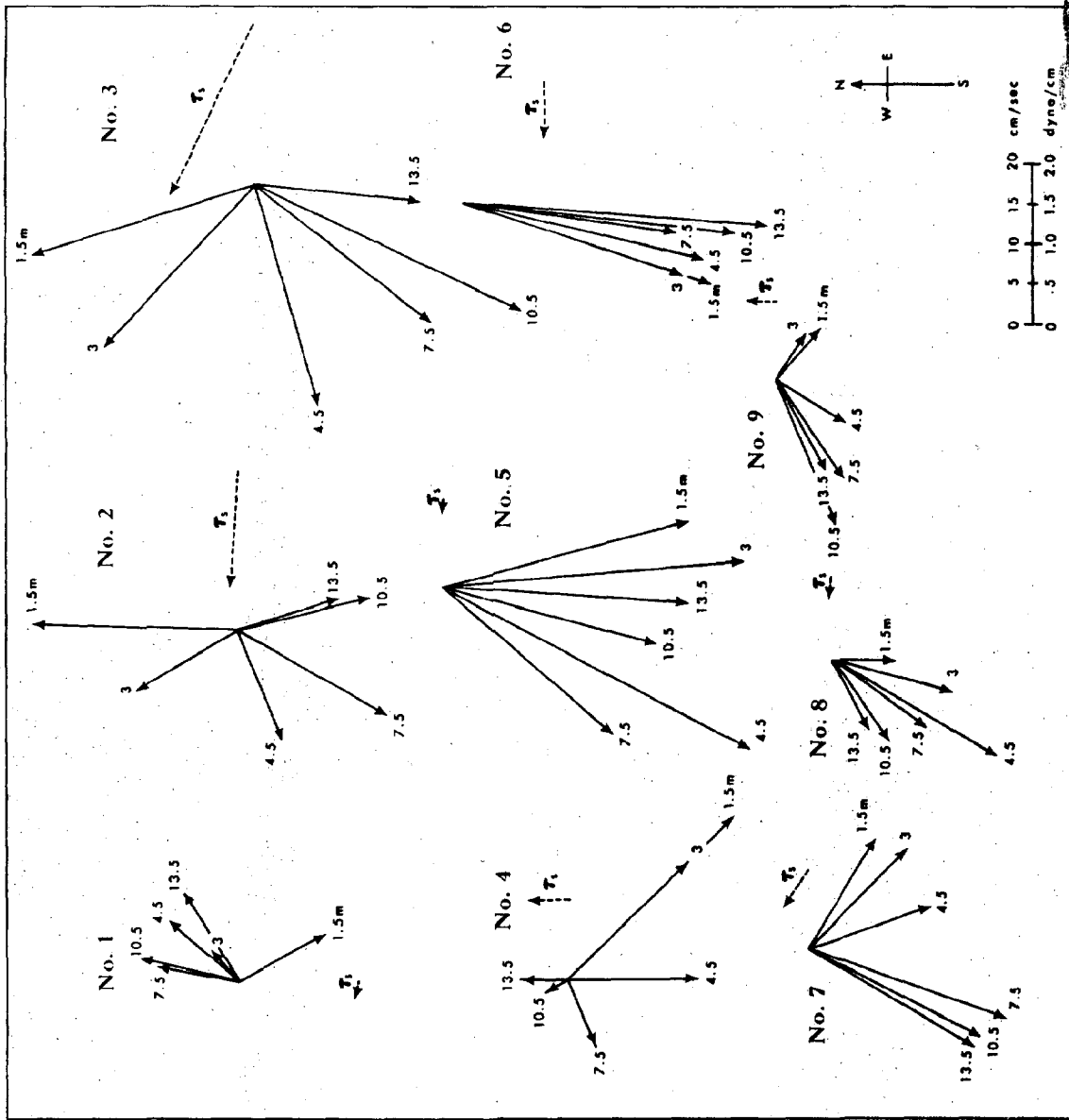


Figure 24. Vertical profiles of currents at the same time and location as the time series plot of density in Figure 23.

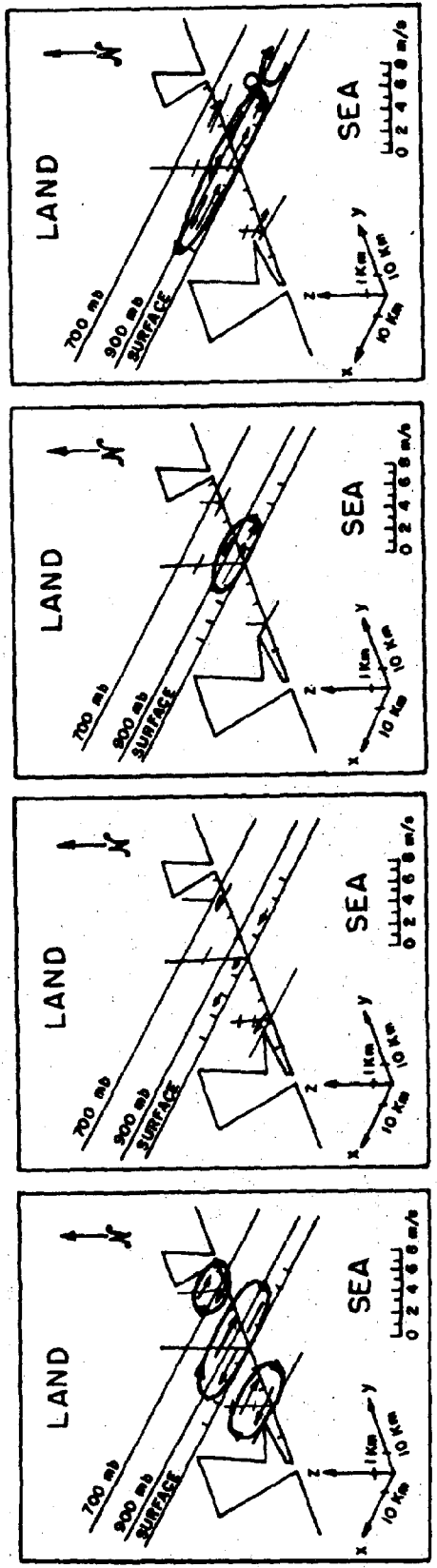
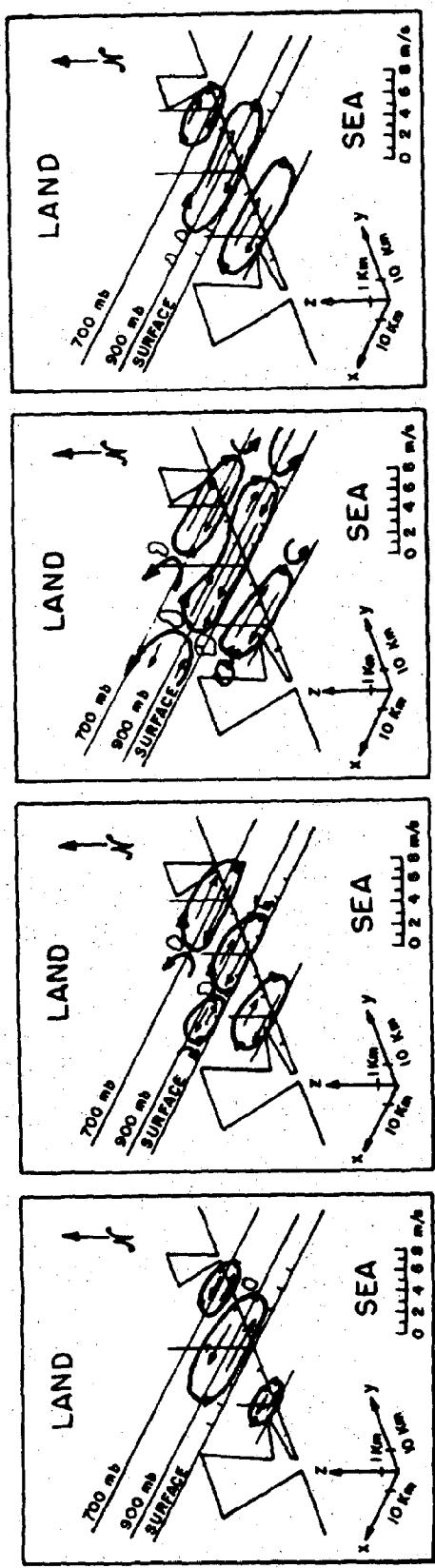


Figure 25. Conceptual model by Hsu (1970) of the coastal air circulation system that develops along the coasts of the Gulf of Mexico in the summer half of the year.

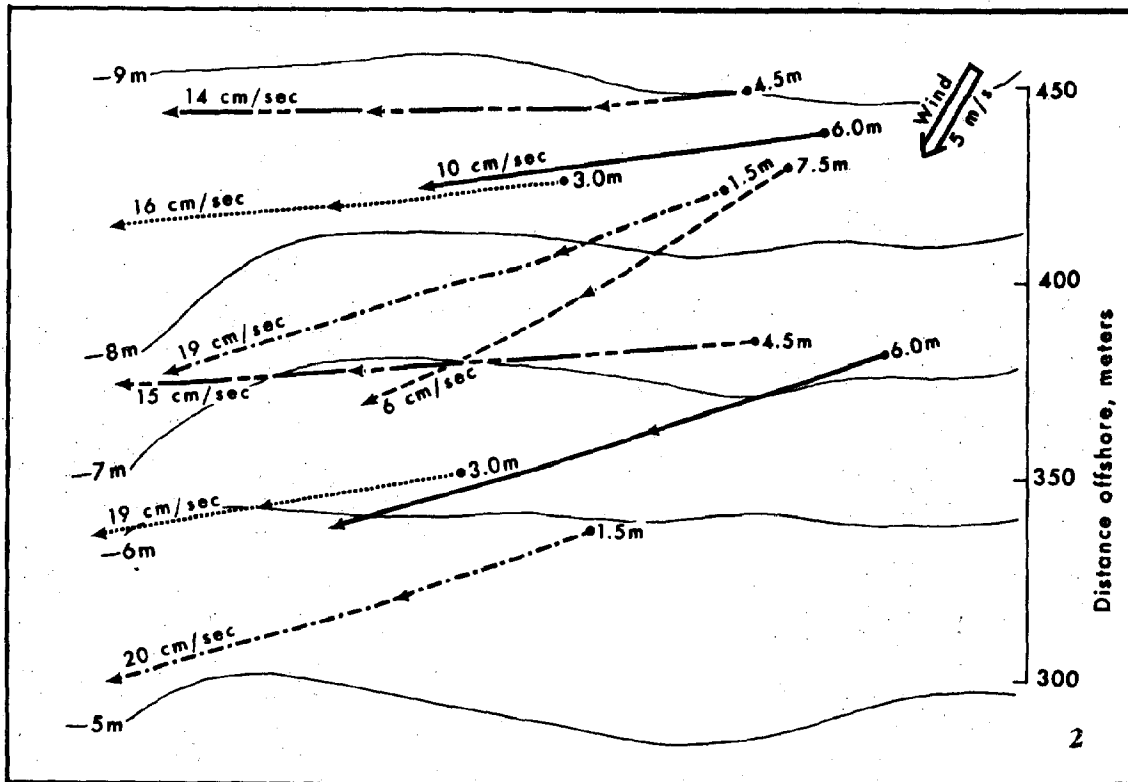


Figure 26. Nearshore currents driven by light local winds along the Florida Panhandle coast 30 km west of Destin Pass. Origin of tracks is labeled with the depth of drogue setting.

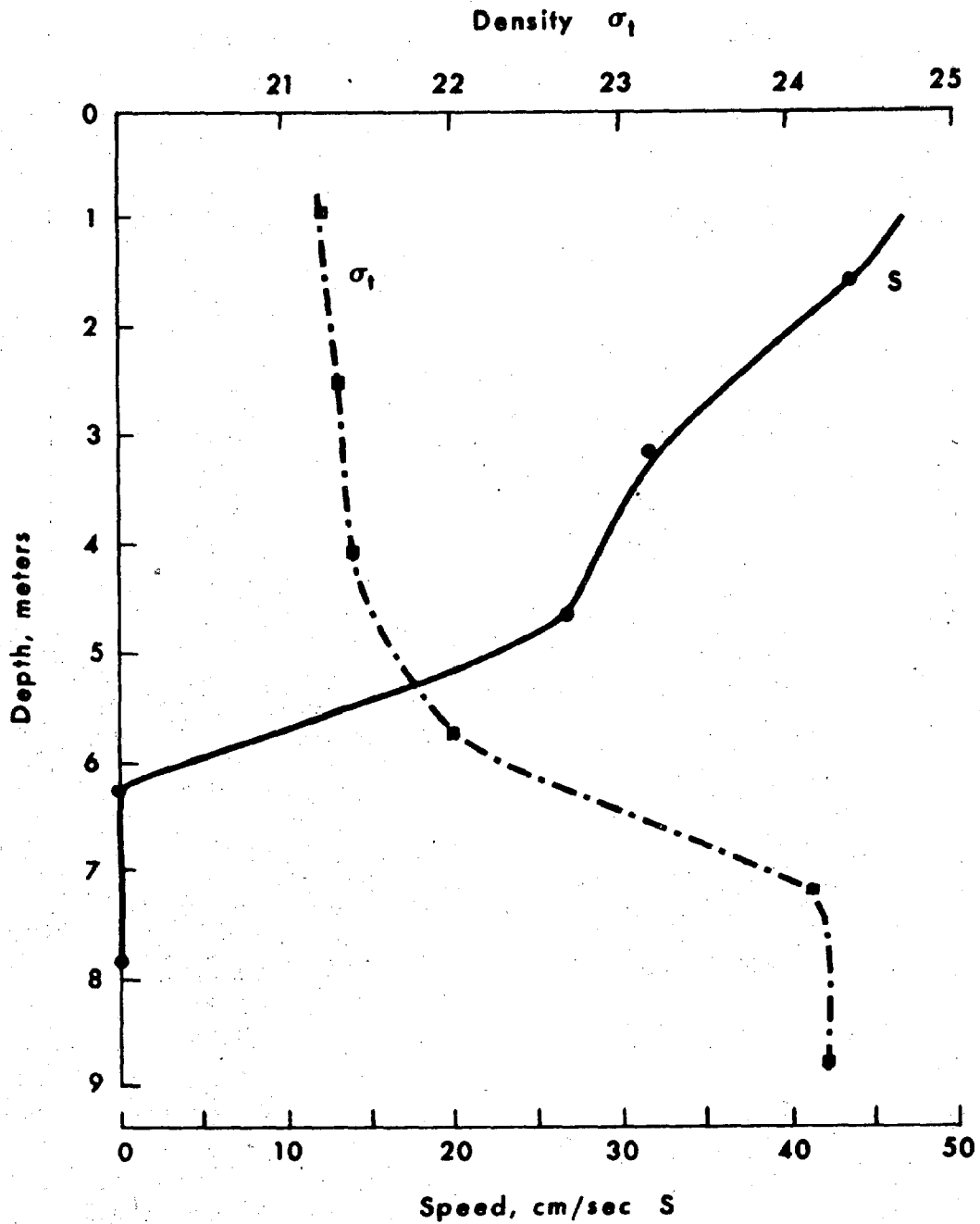


Figure 27. Profile of alongshore current speed illustrating the effect of a density gradient in damping out the downward transfer of momentum necessary to generate currents at the lower levels.

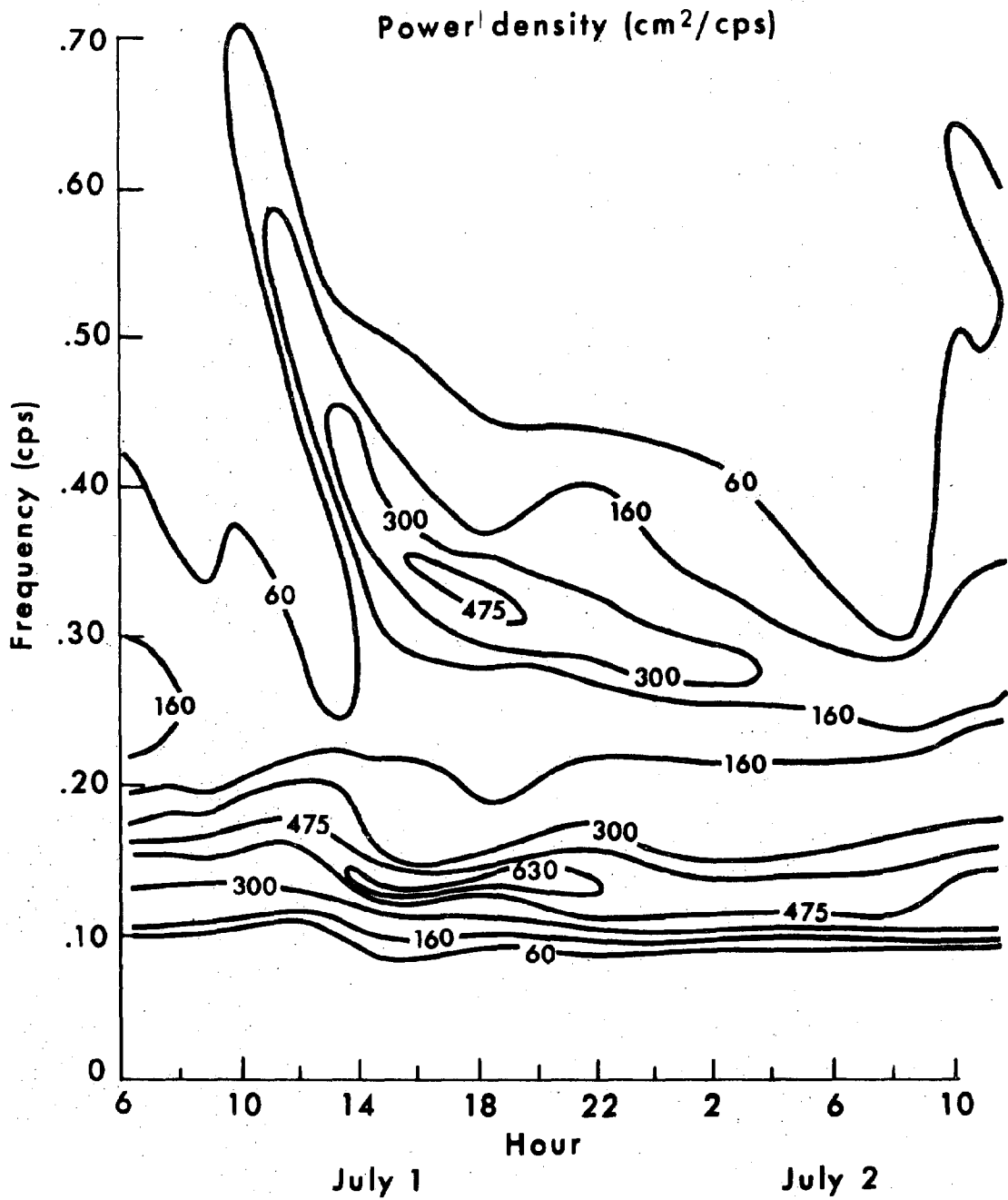


Figure 28. Power spectrum of the nearshore wave field under light coastal winds. Note the generation and growth of high-frequency waves at about 1000 hours as the sea breeze strengthens.

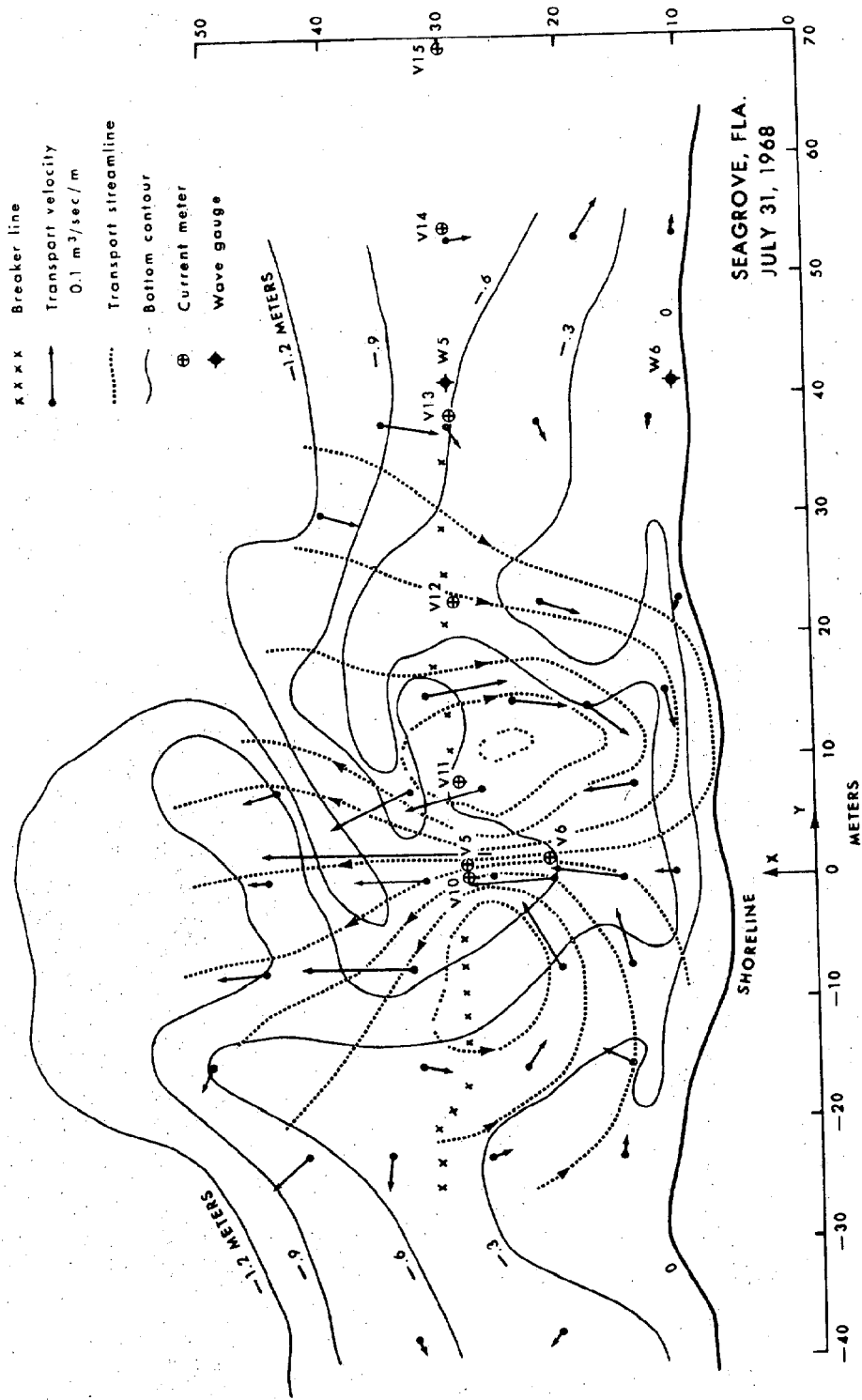


Figure 29. Wave-driven currents in the breaker zone showing onshore flow on both flanks of a strong seaward-directed "rip" current.

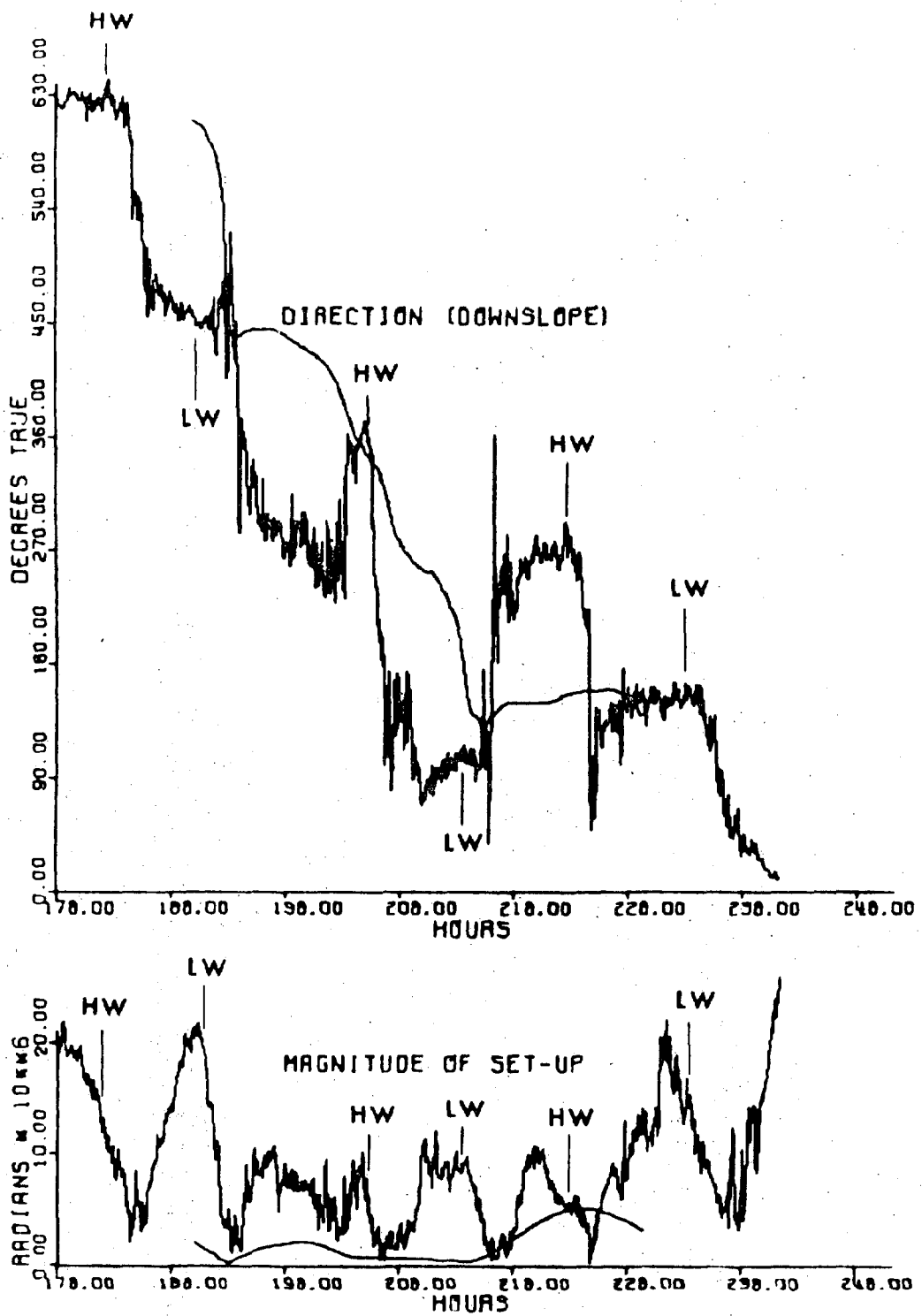


Figure 30. Observations of the direction and magnitude of water surface slopes in Caminada Bay under fair weather conditions.



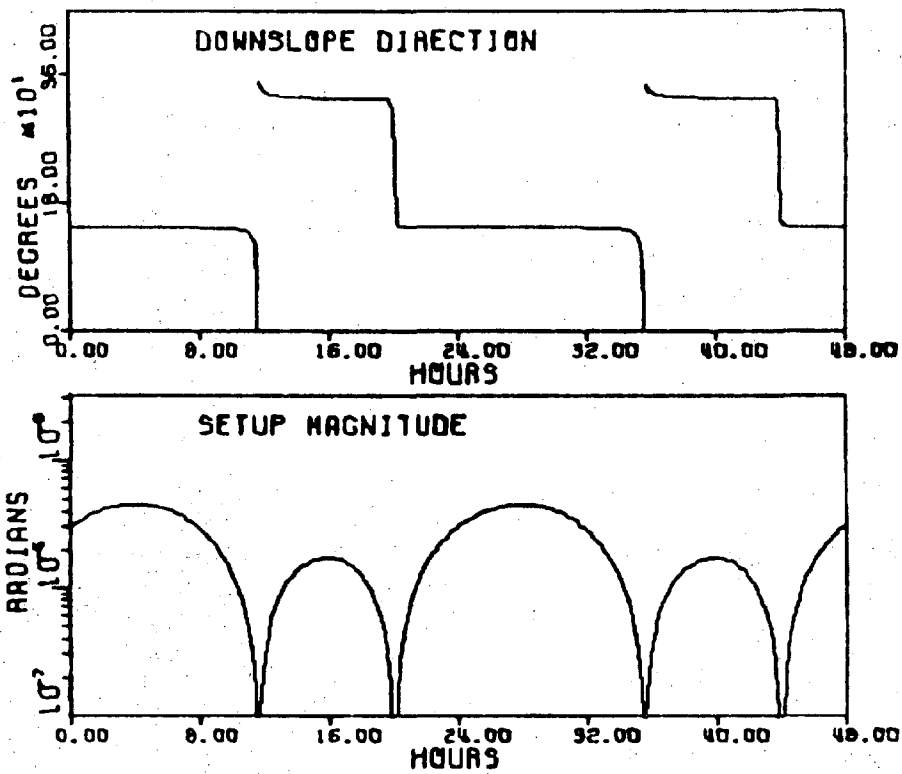


Figure 31. Simulation of direction and magnitude of water surface slopes in Caminada Bay by the analytical model of Kierve (1973).

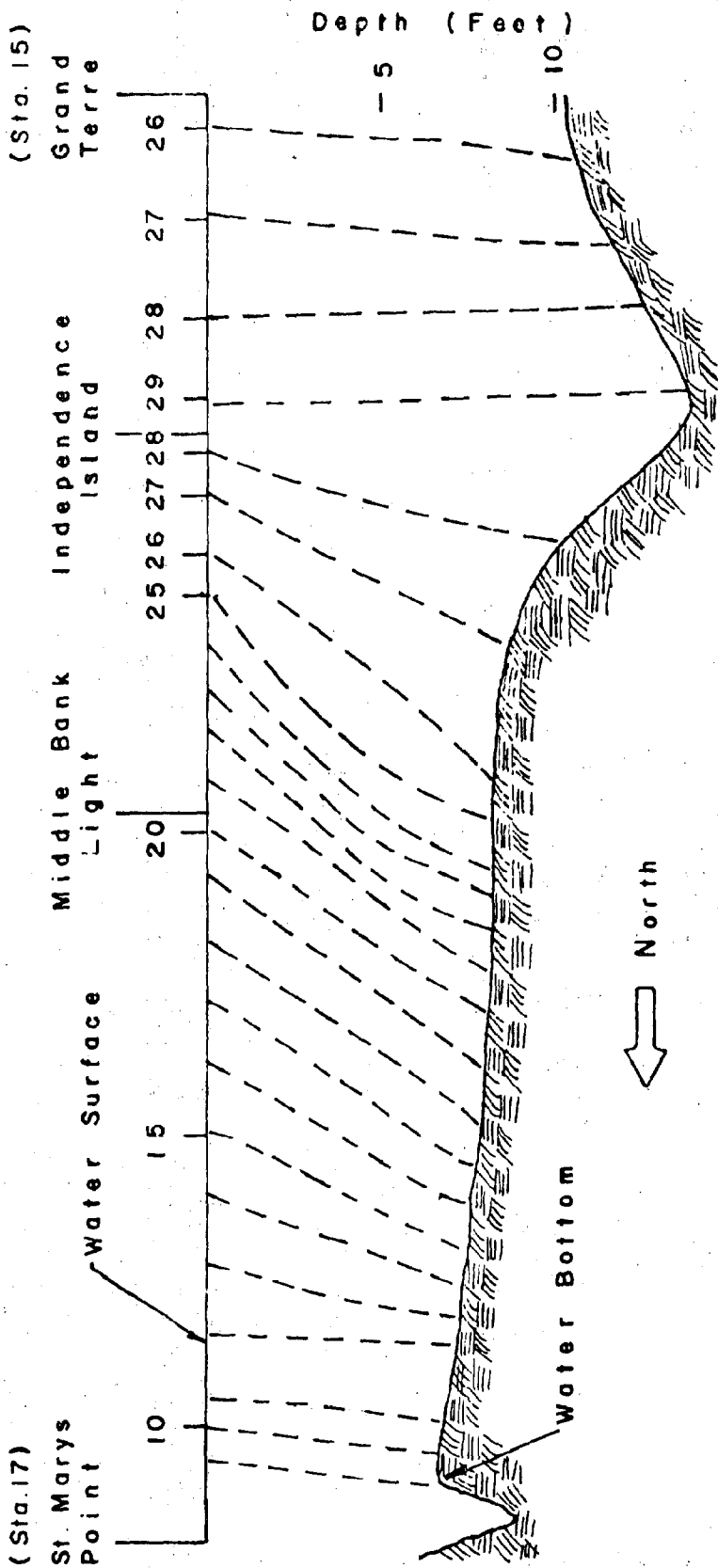


Figure 32. Vertical cross-section of the salinity distribution (ppt) in Barataria Bay (after Barrett, 1971).

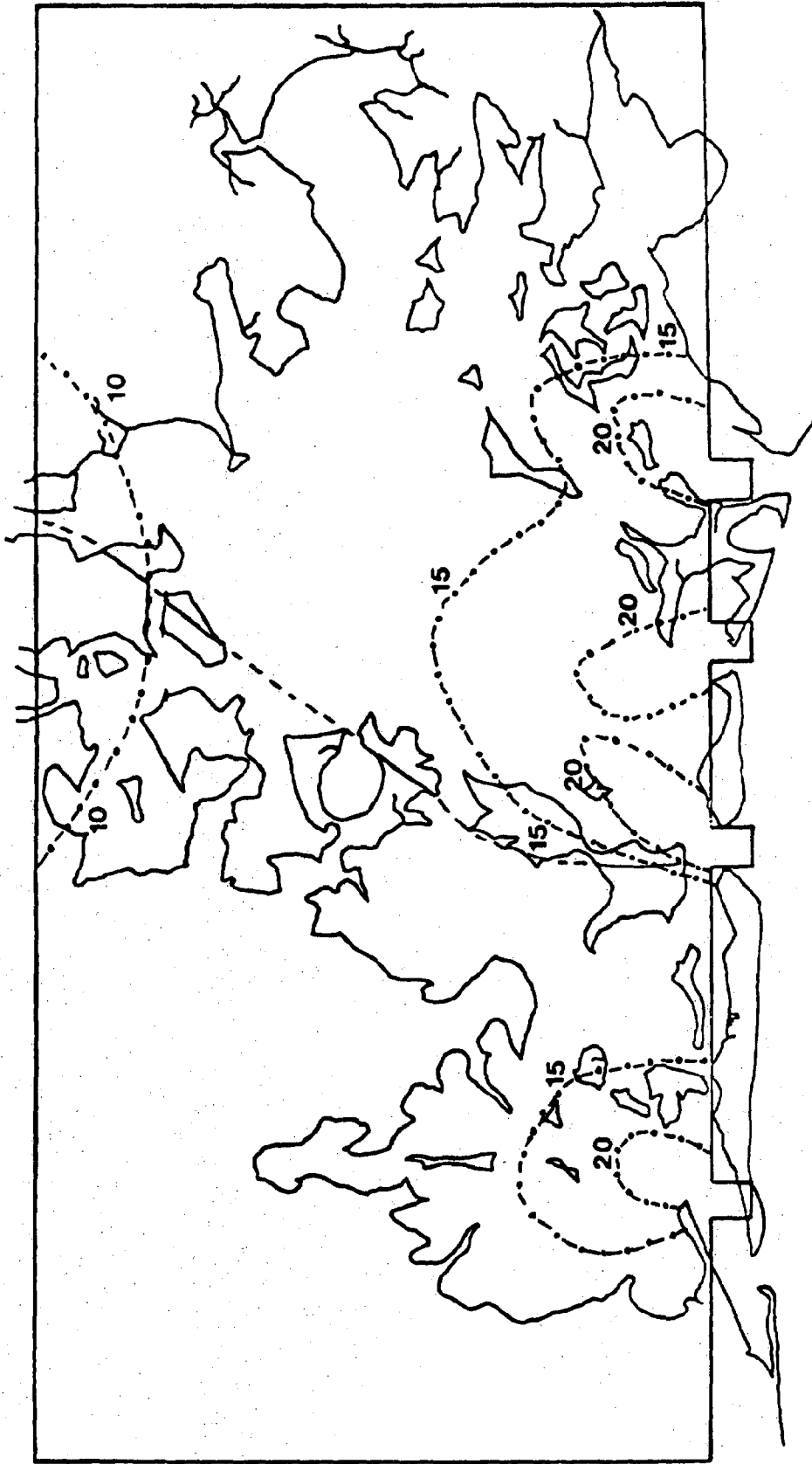


Figure 33. Distribution of isohalines in the Barataria Bay complex predicted by the numerical simulation model of Hacker (1973) under average tidal conditions.

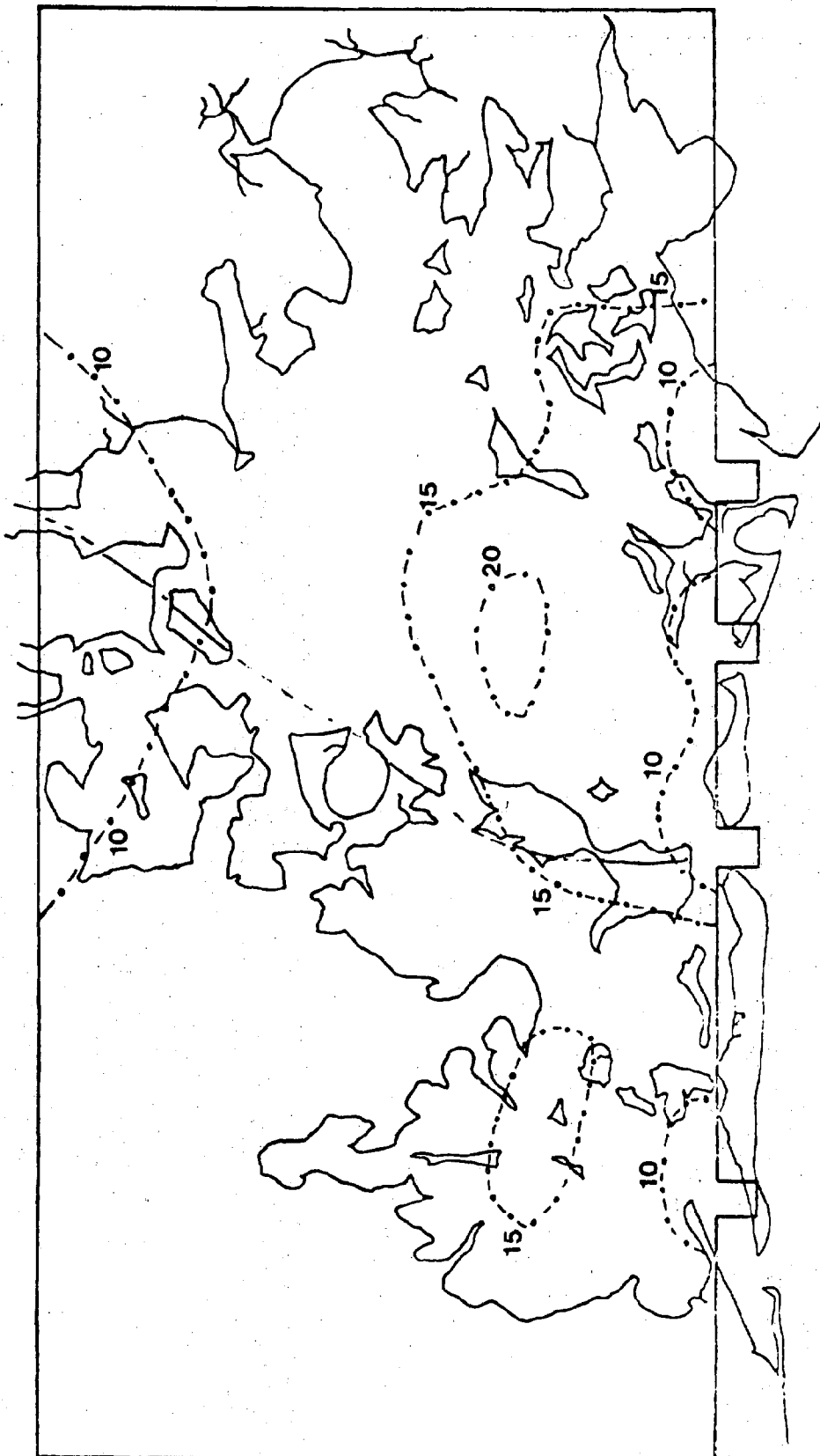


Figure 34. Simulation by Hacker (1973) of the distribution of isohalines in the Barataria Bay complex 3 hours after a 10-ppt drop in salinity at the passes.

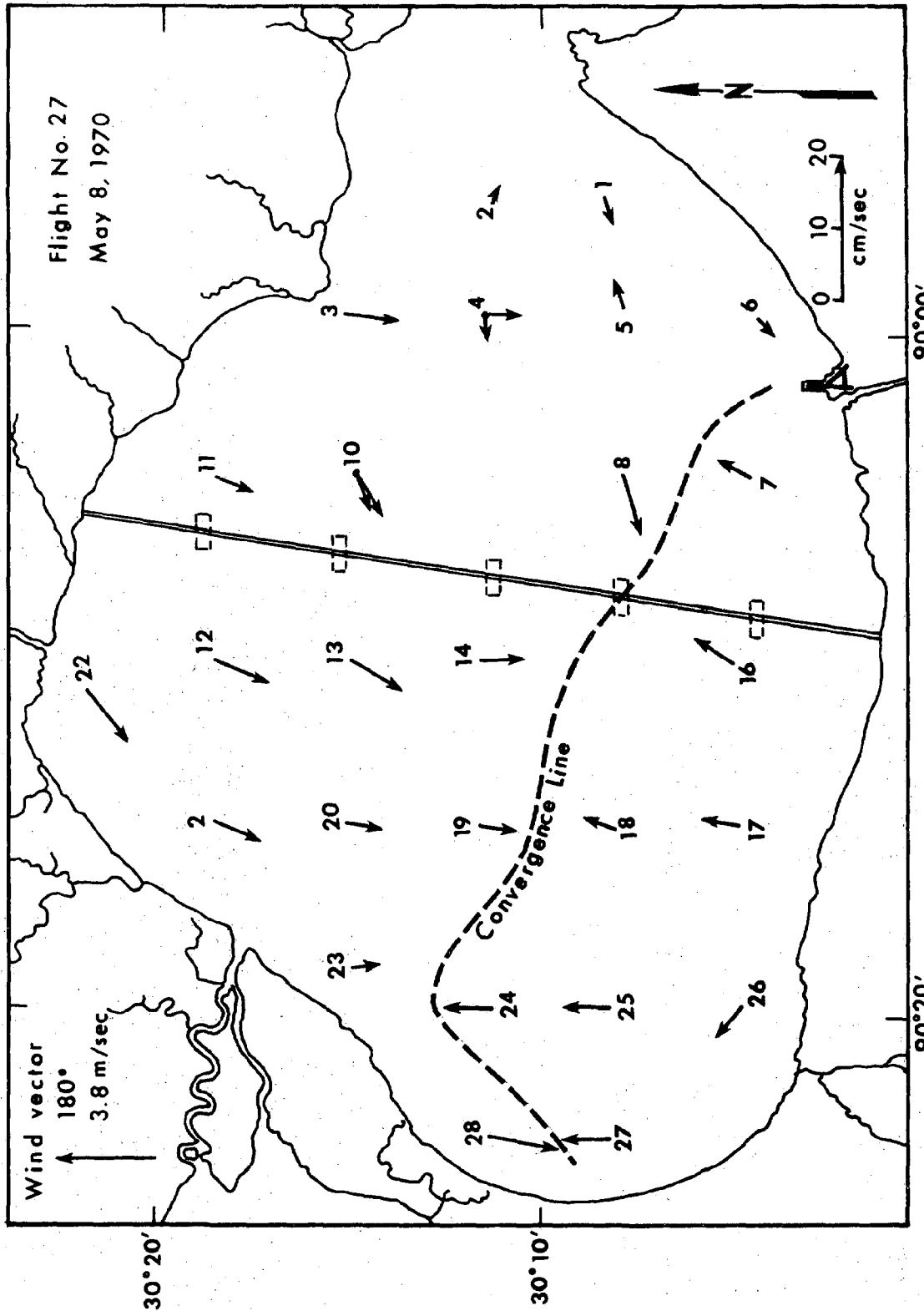


Figure 35. Surface circulation in Lake Pontchartrain under the influence of a southerly wind (after Stone et al., 1972).

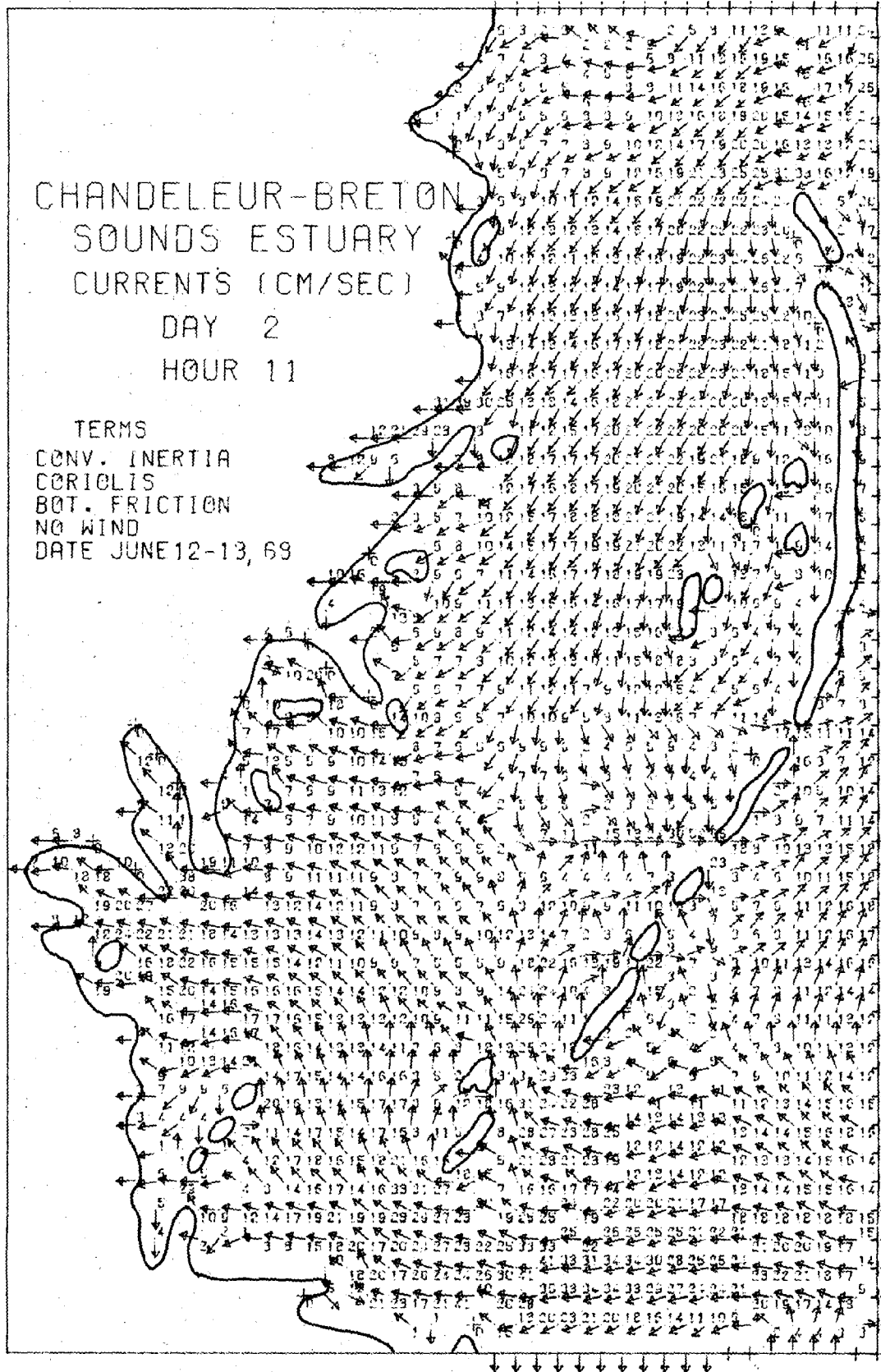


Figure 36. Bathymetry (depths in feet) of Chandeleur-Breton Sound.

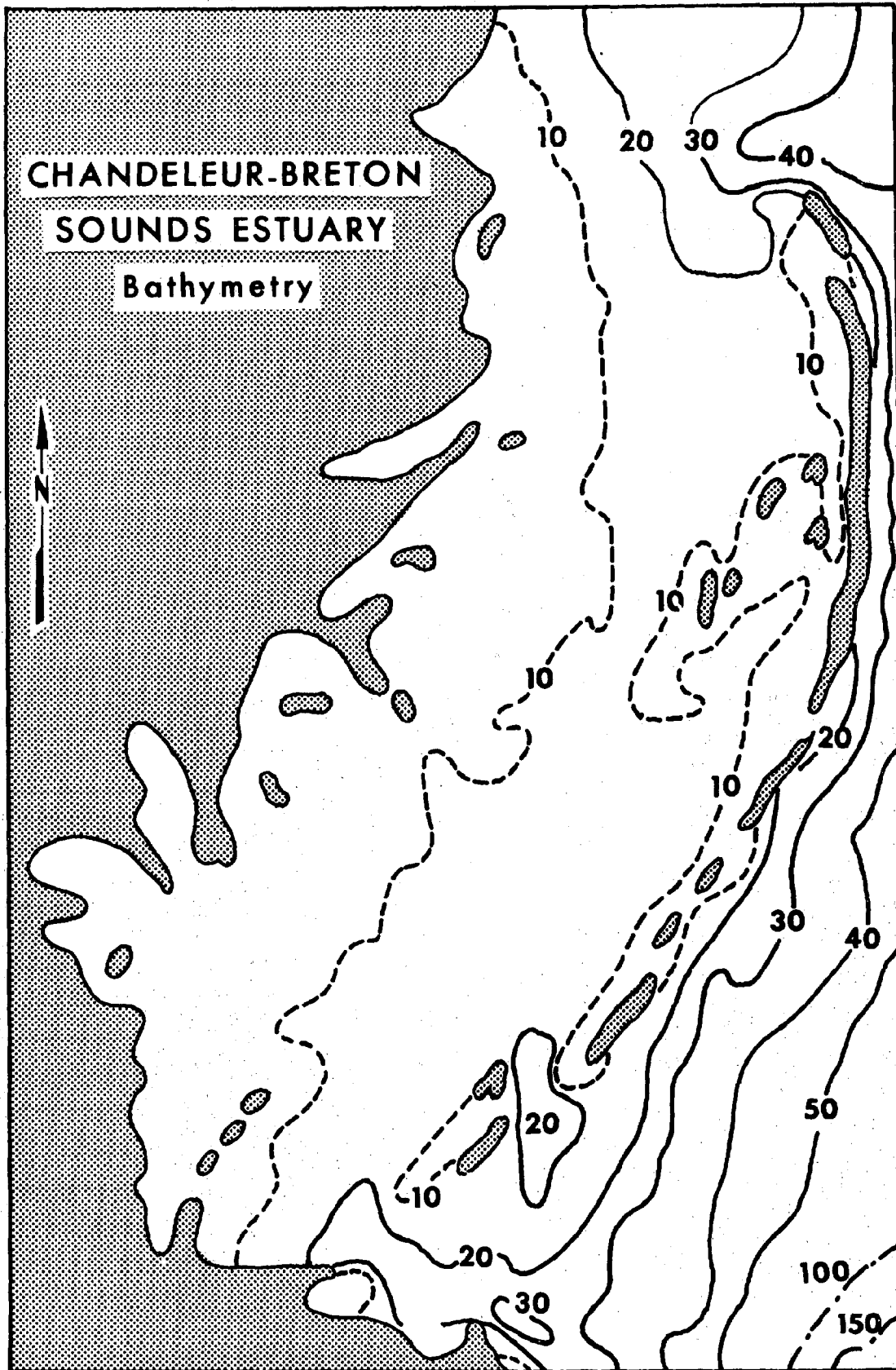


Figure 37. Currents (speeds given in centimeters per second) 3 hours after low tide at the entrances predicted by the two-dimensional numerical model of Hart (1975).

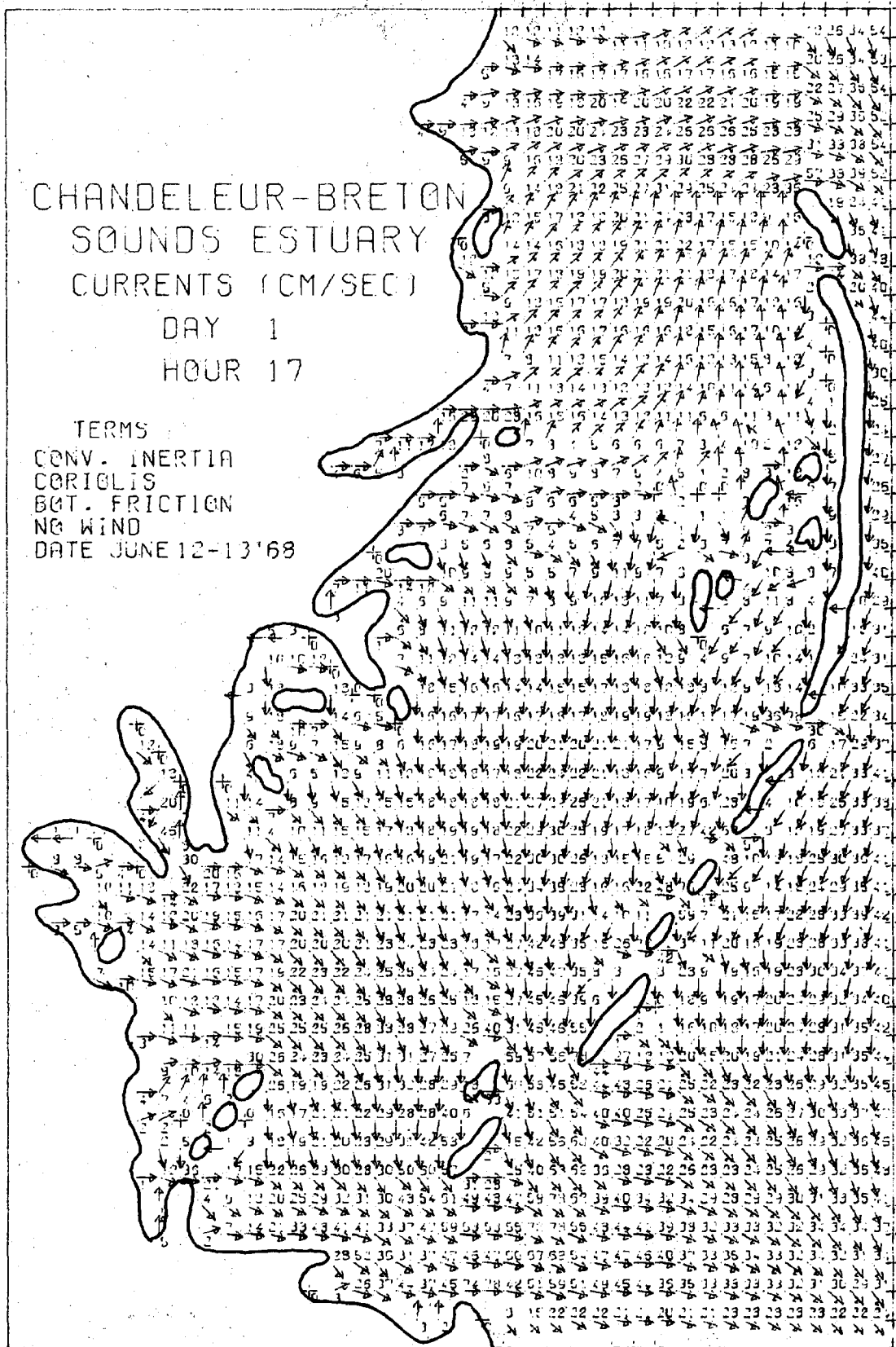


Figure 38. Currents (speeds given in centimeters per second) 1 hour after high water at the entrances predicted by the two-dimensional model of Hart (1975).



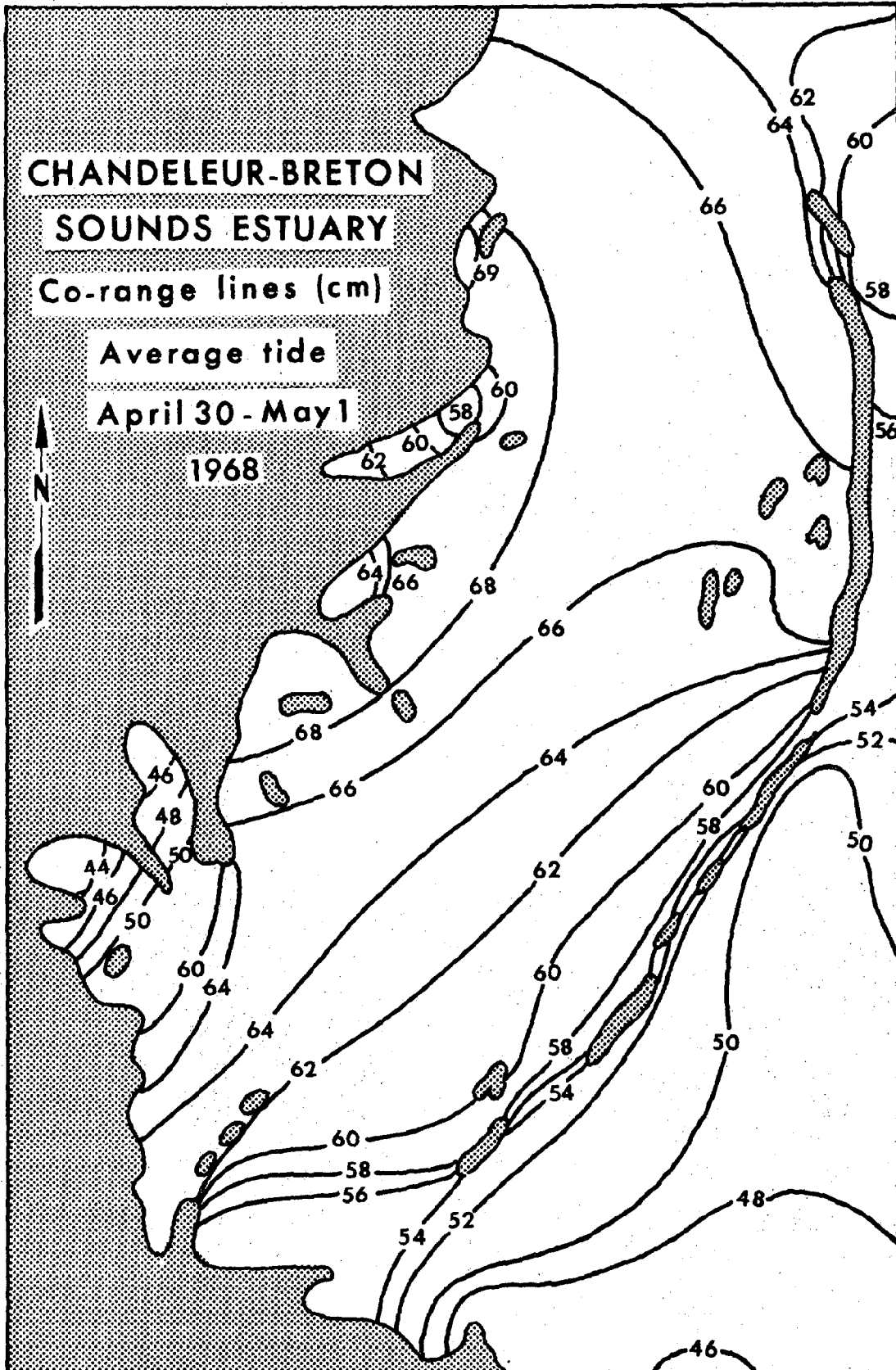


Figure 39. Co-range lines predicted by the two-dimensional numerical model of Hart (1975).

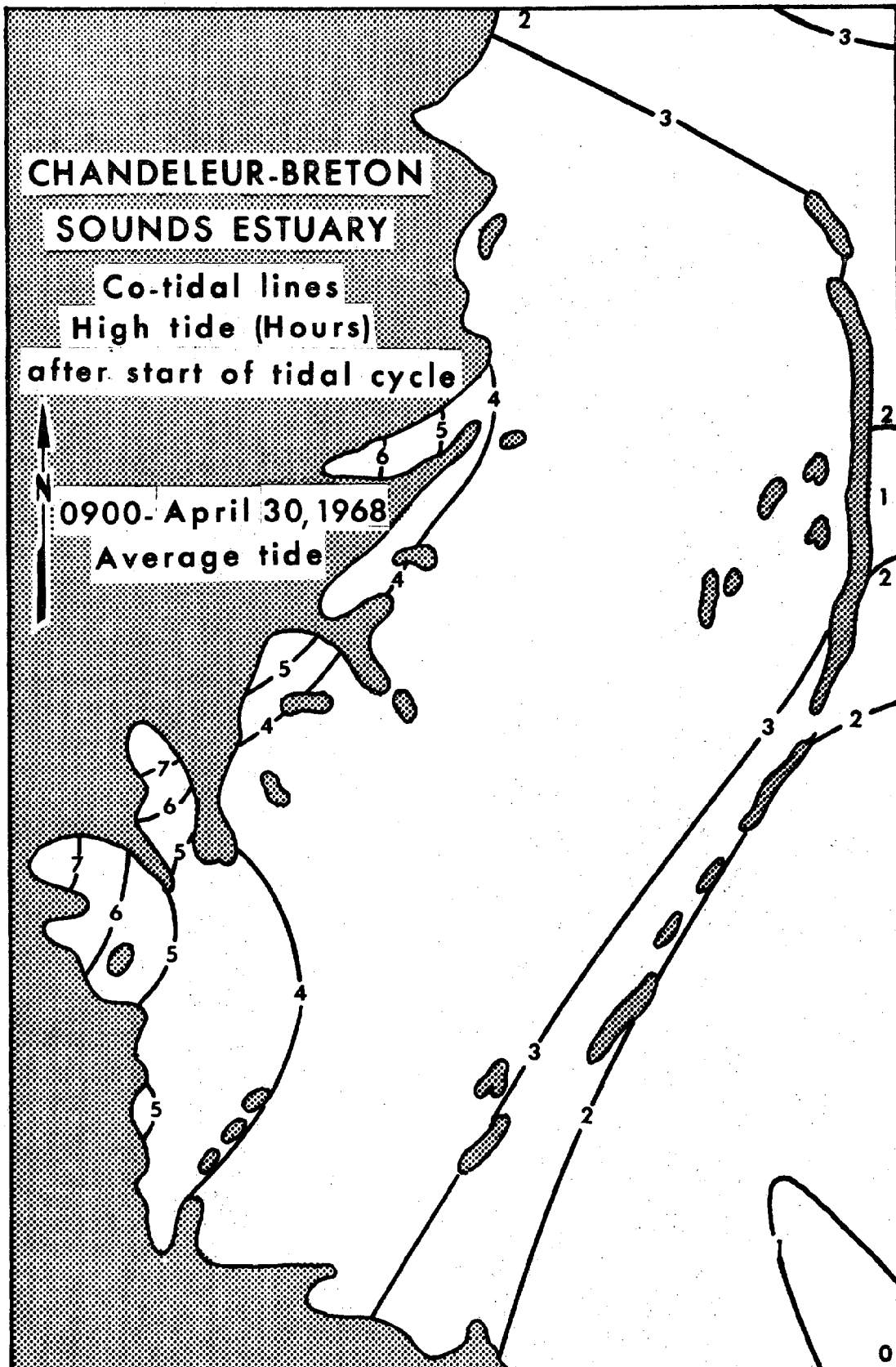


Figure 40. Co-phase lines predicted by the two-dimensional numerical model of Hart (1975).

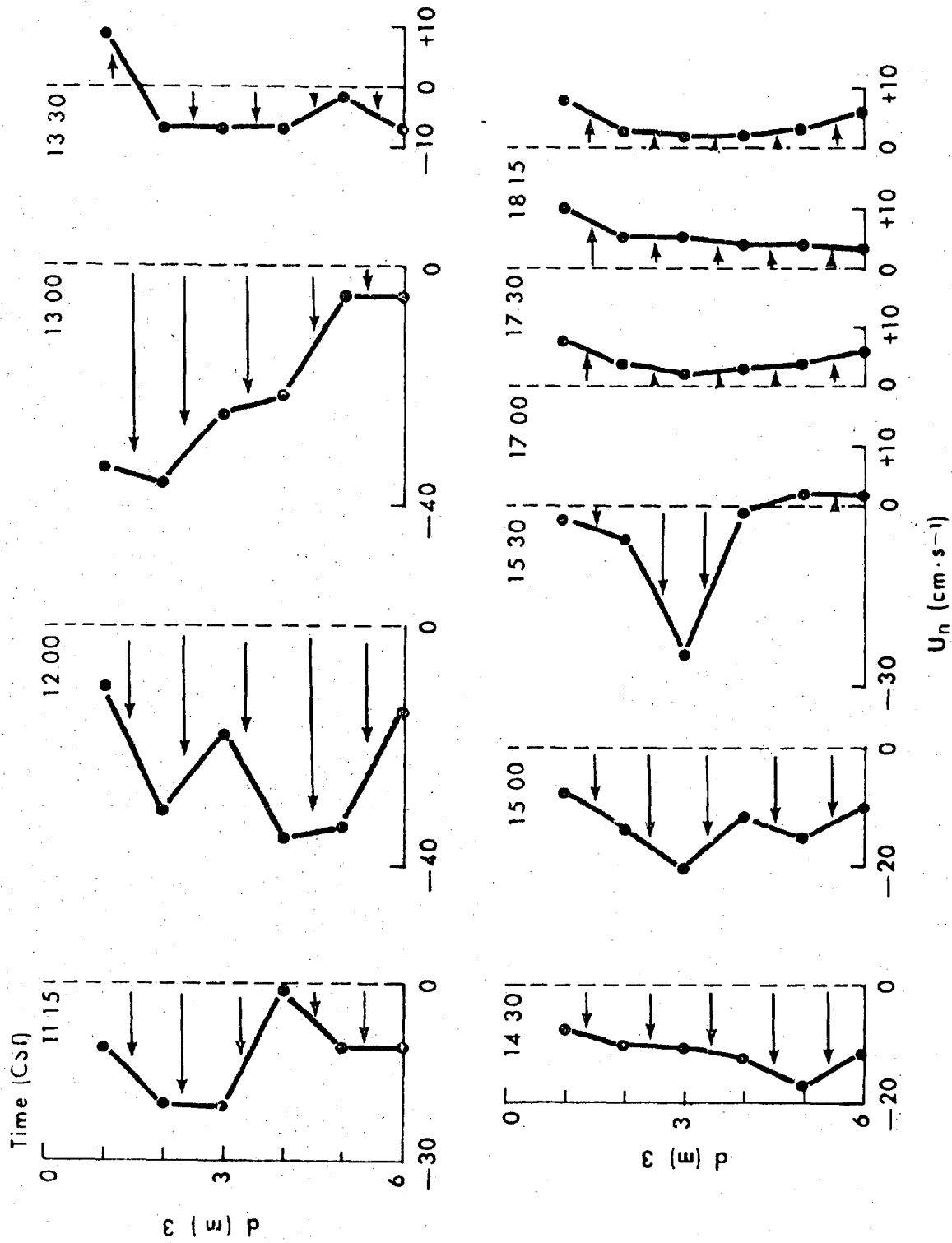


Figure 41. Sequential profiles of current speed in Caminada Pass.

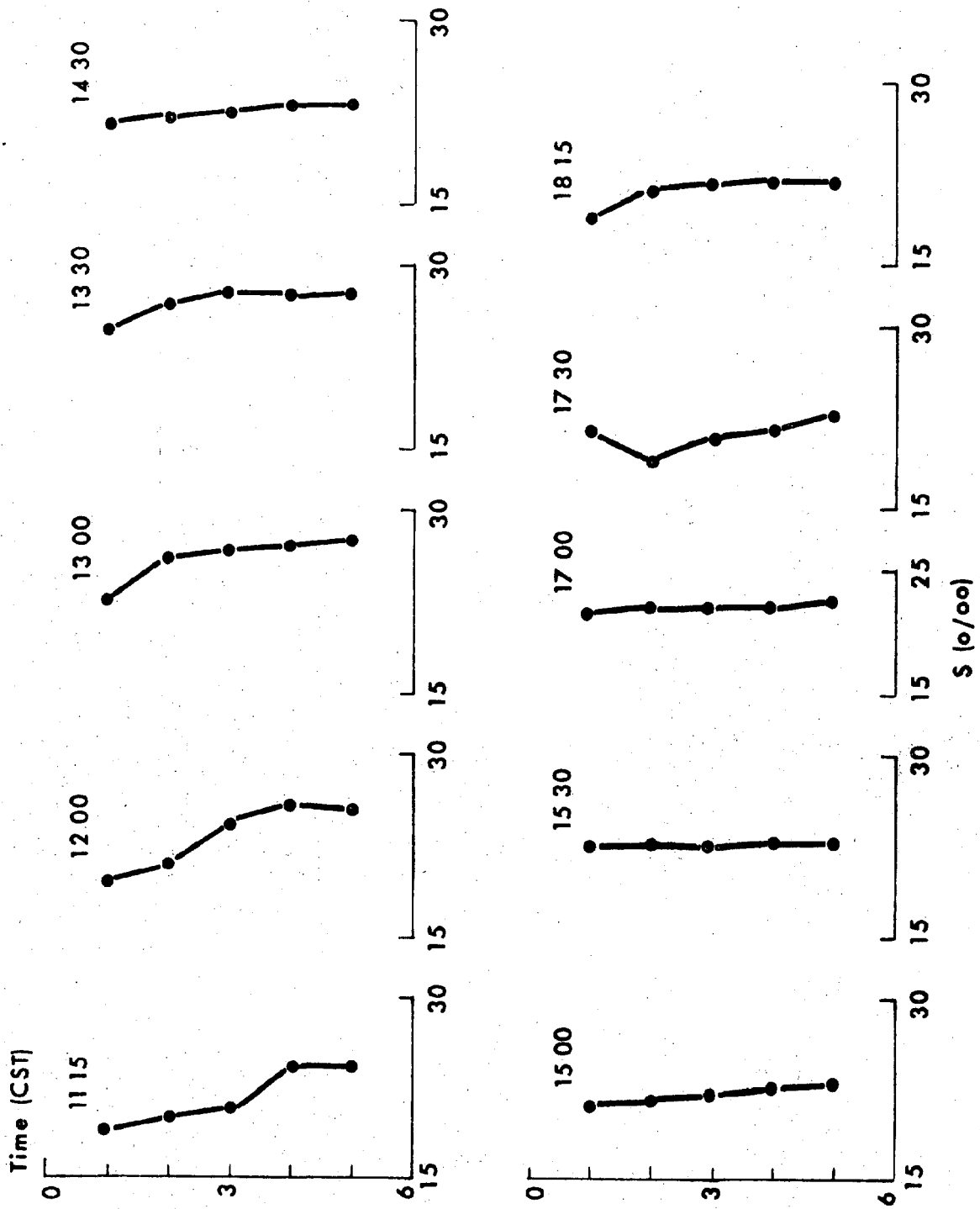


Figure 42. Sequential profiles of salinity in Camisada Pass.

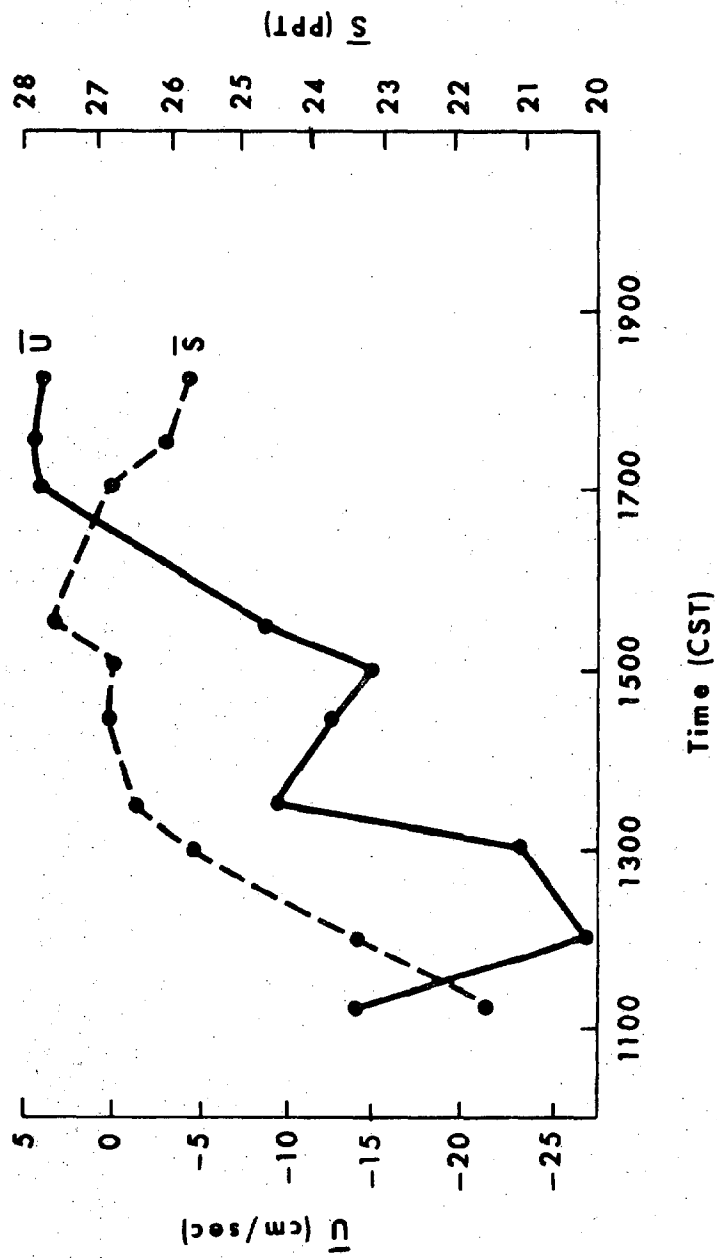


Figure 43. Vertical averages of speed,  $\bar{U}$ , and salinity,  $\bar{S}$ , as a function of time in Caminada Pass.

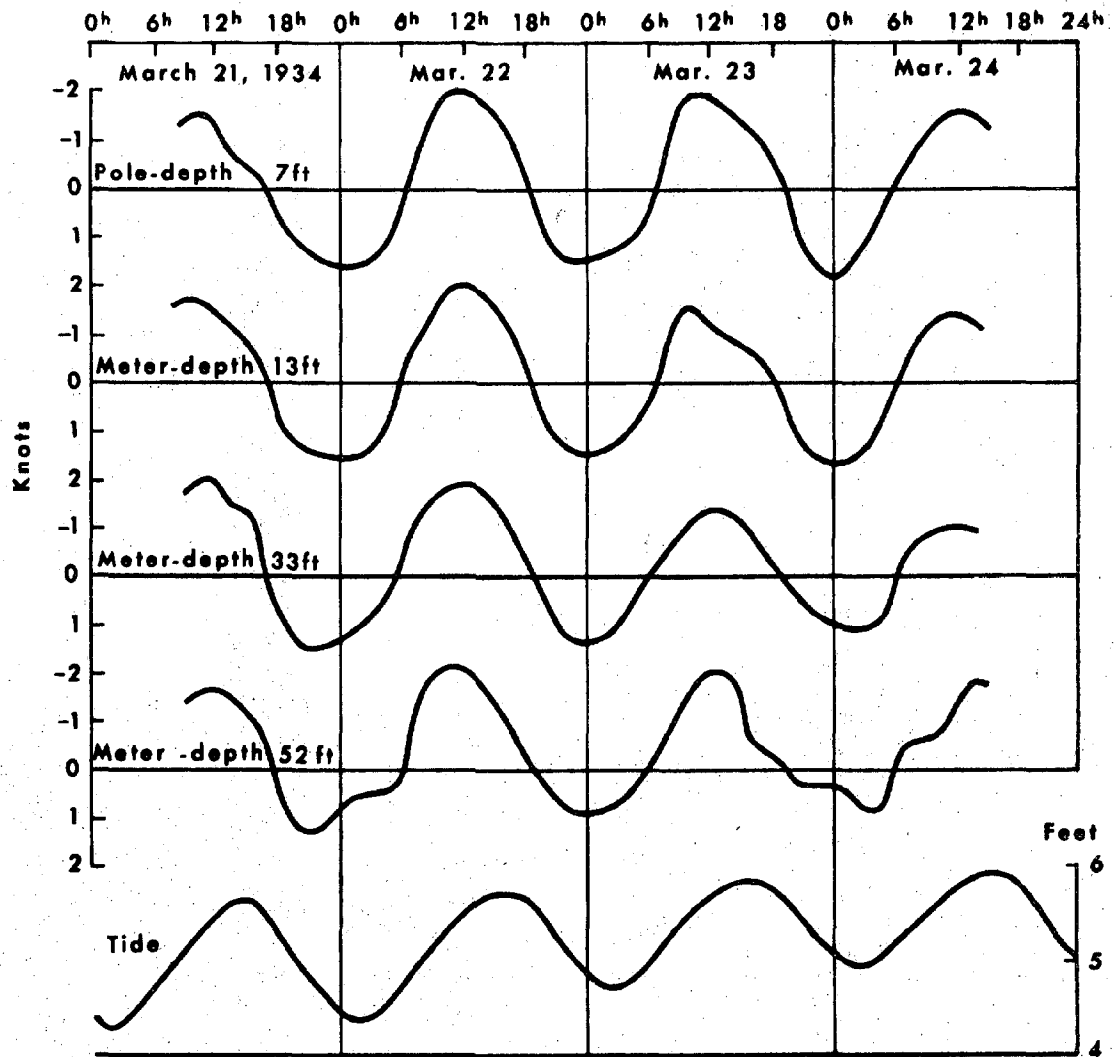


Figure 44. Current at various depth levels in Barataria Pass, 1934. Flood currents have a negative sign, ebb currents have a positive sign.

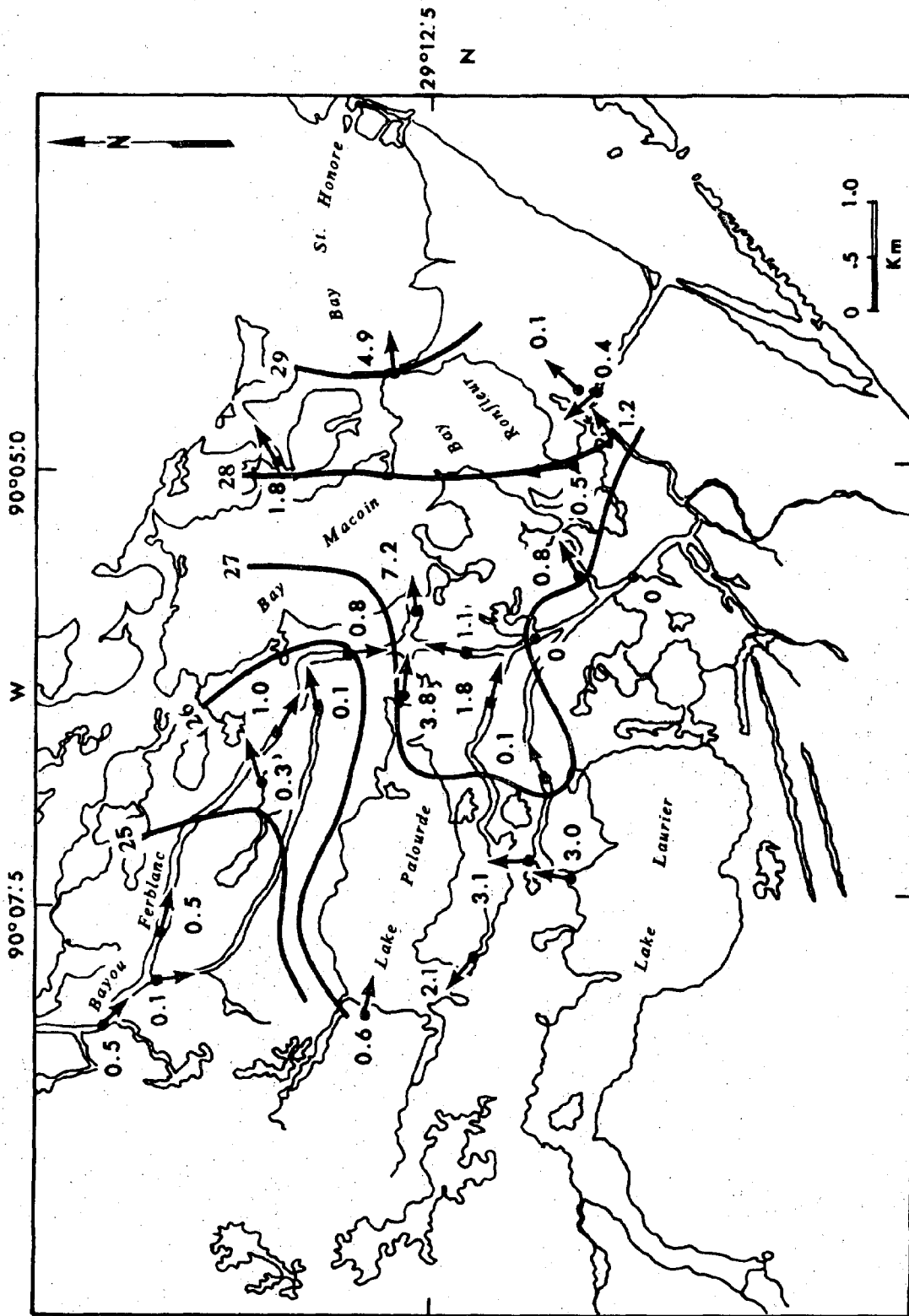


Figure 45. Isohalines (ppt) and values of the time-averaged net discharge (cubic meters per second) in the wetlands west of Caminada Bay determined by Kjerfve (1971).

NOAA COASTAL SERVICES CENTER LIBRARY  
  
3 6668 14103 2203

COASTAL ZONE  
INFORMATION CENTER